



January 2016

## CNTF Potentiates Survival And Sprouting Of Axotomized Magnocellular Neurons

Kathryn E. Erickson

[How does access to this work benefit you? Let us know!](#)

Follow this and additional works at: <https://commons.und.edu/theses>

---

### Recommended Citation

Erickson, Kathryn E., "CNTF Potentiates Survival And Sprouting Of Axotomized Magnocellular Neurons" (2016). *Theses and Dissertations*. 2014.  
<https://commons.und.edu/theses/2014>

This Thesis is brought to you for free and open access by the Theses, Dissertations, and Senior Projects at UND Scholarly Commons. It has been accepted for inclusion in Theses and Dissertations by an authorized administrator of UND Scholarly Commons. For more information, please contact [und.common@library.und.edu](mailto:und.common@library.und.edu).

CNTF POTENTIATES SURVIVAL AND SPROUTING OF AXOTOMIZED  
MAGNOCELLULAR NEURONS

by

Kathryn E. Erickson  
Bachelor of Science, University of North Dakota, 2009

A Thesis

Submitted to the Graduate Faculty

of the

University of North Dakota

in partial fulfilment of the requirements

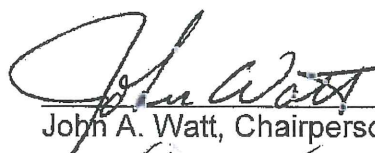
for the degree of

Master of Science


Grand Forks, North Dakota  
December  
2016



This thesis, submitted by Kathryn E. Erickson in partial fulfillment of the requirements for the Degree of Master of Science from the University of North Dakota, has been read by the Faculty Advisory Committee under whom the work has been done and is hereby approved.

  
\_\_\_\_\_  
John A. Watt, Chairperson

  
\_\_\_\_\_  
Patrick A. Carr, PhD

  
\_\_\_\_\_  
Kenneth G. Ruit, PhD

This thesis is being submitted by the appointed advisory committee as having met all of the requirements of the School of Graduate Studies at the University of North Dakota and is hereby approved.

  
\_\_\_\_\_  
Dr. Grant McGimpsey  
Dean, School of Graduate Studies

December 1, 2016  
\_\_\_\_\_  
Date

## PERMISSION

Title: CNTF Potentiates Survival and Sprouting of Axotomized  
Magnocellular Neurons

Department: Anatomy and Cell Biology

Degree: Master of Science

In presenting this thesis in partial fulfillment of the requirements for a graduate degree from the University of North Dakota, I agree that the library of this University shall make it freely available for inspection. I further agree that permission for extensive copying for scholarly purposes may be granted by the professor who supervised my thesis work or, in his absence, by the Chairperson of the department or the dean of the School of Graduate Studies. It is understood that any copying or publication or other use of this thesis or part thereof for financial gain shall not be allowed without my written permission. It is also understood that due recognition shall be given to me and to the University of North Dakota in any scholarly use which may be made of any material in my thesis.

Kathryn E. Erickson  
November 28, 2016

## TABLE OF CONTENTS

LIST OF FIGURES .....	viii
LIST OF TABLES .....	x
ACKNOWLEDGEMENTS.....	xi
ABSTRACT .....	xiii
CHAPTER	
I. INTRODUCTION.....	1
Hypothalamic Magnocellular Neurosecretory System .....	1
Paraventricular Nucleus .....	2
Supraoptic Nucleus .....	3
Accessory Nuclei.....	4
Magnocellular Neurons.....	5
Parvocellular Neurons .....	6
Pars Nervosa.....	7
Oxytocin .....	8
Vasopressin.....	9
Astrocytes.....	10
Magnocellular Neurosecretory System Plasticity.....	16
Ciliary Neurotrophic Factor.....	19
Hypothesis.....	27

II.	MATERIALS AND METHODS .....	29
	Animals.....	29
	Mini-Osmotic Pump Infusions.....	29
	Tissue Homogenate Preparation.....	31
	Primary Astrocyte Cultures.....	33
	Astrocyte Application.....	36
	Coverslip Treatment and Fixation.....	37
	Cell Culture Flask Treatment and Collection .....	38
	Dosage Inhibition of Astrocyte Cultures.....	44
	XTT Cell Viability-Dosage Inhibition .....	44
	Hypothalamic Organotypic Explant Cultures .....	44
	Astrocyte Conditioned Media for Hypothalamic Organotypic Cultures.....	45
	Immunocytochemical Examination .....	47
	Rat Cytokine Antibody Array .....	49
	Enzyme-Linked Immunosorbent Assay .....	50
	Western Blot Examination .....	52
	Real Time Reverse Transcriptase Polymerase Chain Reaction Arrays .....	54
	Real Time Reverse Transcriptase Polymerase Chain Reaction Primers.....	55
	Organotypic Explant Immunohistochemistry .....	56
	Magnocellular Neuronal Counts .....	56
	Data Analysis .....	57

III.	RESULTS .....	60
	Specific Aim I: Determine if CNTF Activates the JAK/STAT Pathway in Astrocytes .....	60
	Specific Aim II: Determine the Functional Response of Astrocytes to CNTF Cytokine Release Analysis.....	68
	Specific Aim III: Determine if Response is a Result of CNTF Activation of the JAK2/STAT3 Pathway by Examining if the Inhibition of JAK2/STAT3 will Alter the CNTF Induced Functional Outcome .....	91
	Specific Aim IV: Determine if the Functional Response Promotes Survival and Sprouting of Neurons Utilizing the Hypothalamic Explants Cultures .....	102
IV.	DISCUSSION.....	106
	Specific Aim I: Determine if CNTF Activates the JAK/STAT Pathway in Astrocytes .....	107
	Specific Aim II: Determine the functional response of astrocytes to CNTF .....	110
	Specific Aim III: Determine if Response is a Result of CNTF Activation of the JAK2/STAT3 Pathway by Examining if the Inhibition of JAK2/STAT3 will Alter the CNTF Induced Functional Outcome.....	116
	Specific Aim IV: Determine if the Functional Response Promotes Survival and Sprouting of Neurons Utilizing the Hypothalamic Explants Cultures .....	119
	Summary .....	121
	REFERENCES.....	124



## LIST OF FIGURES

Figure	Page
1. Anatomy of the Magnocellular Neurosecretory System .....	2
2. Anatomy of the Supraoptic Nucleus (SON).....	5
3. Stereotaxic Placement of Mini-Osmotic Pump Cannula.....	32
4. Hypothalamic Organotypic Explant Culture Section. ....	46
5. 3 Day 100 ng/ul rrCNTF Infusion Elicits an Increase in GFAP .....	61
6. Expression of the Tripartite Receptor Complex in Primary Astrocyte Cell Cultures .....	64
7. Immunofluorescent Staining for tSTAT3 and GFAP .....	66
8. Time-Dependent Activation of Cultured Astrocytes by 25 ng/ml Exogenous rrCNTF in DMEM.....	67
9. Translocation of pSTAT3 following 30-minute, 25 ng/ml rrCNTF incubation followed by isolation of cytoplasmic and nuclear extractions.....	69
10. Preliminary Western Blot Analysis of Nuclear Extraction .....	70
11. RayBio Cytokine Membrane Arrays .....	71
12. R&D Systems VEGF ELISA.....	75
13. R&D Systems IL-6 ELISA .....	77
14. RayBio Fractalkine ELISA.....	78
15. Real-Time Reverse Transcriptase Polymerase Chain Reaction Primers. ....	80

16.	6 Hour Neurotrophins and Receptors RT <sup>2</sup> PCR to 25 ng/ml rrCNTF. ....	81
17.	12 Hour Neurotrophins and Receptors RT <sup>2</sup> PCR.....	83
18.	24 Hour Neurotrophins and Receptors RT <sup>2</sup> PCR.....	84
19.	6 Hour Chemokines and Receptors RT <sup>2</sup> PCR .....	86
20.	12 Hour Chemokines and Receptors RT <sup>2</sup> PCR. ....	87
21.	24 Hour Chemokines and Receptors RT <sup>2</sup> PCR .....	88
22.	6 Hour Jak/STAT Signaling Pathway RT <sup>2</sup> PCR .....	90
23.	12 Hour Jak/STAT Signaling Pathway RT <sup>2</sup> PCR.....	92
24.	24 Hour Signal Transduction Pathway Finder RT <sup>2</sup> PCR .....	93
25.	XTT Cell Viability Dosage Inhibition with AG490. ....	95
26.	Nuclear Extraction Western Blot Analysis of pSTAT3 tyr 705 Translocation Following Dosage Inhibition with AG490 .....	97
27.	XTT Cell Viability Dosage Inhibition with Cucurbitacin.....	98
28.	GFAP Protein Western Blot Analysis.....	99
29.	Cucurbitacin Inhibition of pSTAT3 tyr 705.....	101
30.	Paraventricular Nucleus Oxytocinergic Neuron Counts .....	103
31.	Supraoptic Nucleus Oxytocinergic Neuron Counts .....	105

## LIST OF TABLES

Table	Page
1. Normal Serums, Primary, Secondary and Tertiary Antibodies.....	48
2. RayBio Cytokine Antibody Array 1 .....	72
3. RayBio Cytokine Antibody Array 2 .....	73
4. Percent Change in Cytokine Release .....	74
5. Rat Neurotrophin and Receptors RT <sup>2</sup> PCR.....	85
6. Rate Chemokines and Receptors RT <sup>2</sup> PCR Fold Changes.....	89
7. 6 and 12 Hour Jak/STAT Signaling Pathway RT <sup>2</sup> PCR and the 24 Hour Signal Transduction Pathway Finder RT <sup>2</sup> PCR Fold Changes.....	94

## ACKNOWLEDGEMENTS

Before all else, I would like to thank my advisor, Dr. John Watt for his guidance, patience and encouragement. Your support and guidance throughout my graduate career has been something I will always be grateful for. I am indebted to you for your willingness to share your knowledge, which is something I will always admire. Additionally, I would like to thank my committee members, Dr. Pat Carr and Dr. Ken Ruit. Your continual support is something I will always cherish. Thank you for your willingness and availability to answer my never ending questions.

My appreciation goes to all those who have passed through the Watt lab, especially Dr. Jason Askvig and Laura Burckhard. Jason, you have always been in my corner answering my questions and cheering for me to succeed. Laura, you made all those days of astrocyte collections breeze by.

Thank you to the Anatomy and Cell Biology Department. You were my home away from home and became my extended family. It has truly been an honor to get to know all of you. I would specifically like to thank Bonnie Kee. Without you, none of this would have been possible. You introduced me to the department and lead me through the struggles of being a graduate student including the completion of my degree and thesis.

Lastly, I'd like to thank my family. Mom and Dad, you have always had my best interests at heart. Dustin, you have been there to push me even when I didn't want to. Thank you.

## ABSTRACT

Ciliary neurotrophic factor (CNTF) is believed to promote neuronal sprouting and survival within the magnocellular neurosecretory system (MNS) by means of astrocyte activation following injury. When CNTF binds to its receptor complex, CNTF receptor alpha, located on the extracellular surface of the astrocyte, it initiates the Jak/STAT3 pathway. The activation of this pathway and the translocation of phosphorylated STAT3 (pSTAT3) to the nucleus is believed to lead to the release of multiple factors that act in a paracrine manner to influence survival and sprouting of MNS neurons. To confirm the ability of CNTF to activate the astrocyte, the three receptor components were confirmed to be present by means of immunocytochemistry and/or Western Blotting on in-vitro rat primary astrocyte cell cultures. Next activation of the astrocyte, translocation of pSTAT3 to the nucleus, was measured using Nuclear Extractions of cell cultures that had been incubated in rat recombinant CNTF (rrCNTF) and compared to non-treated cell cultures. Western blotting of the nuclear extractions indicates that rrCNTF activation of the Jak/STAT3 pathway occurs within 30 minutes of application. Using Rat Cytokine Antibody Arrays from RayBio, the comparison of 72 hour rrCNTF treated astrocyte cell cultures supernatants to non-treated, showed an increase release of roughly 20% in several factors; Fractalkine (66.67%), IL-6 (22.22%), LIX (18.42), and VEGF (36.54%). Further

analysis of Fractalkine, IL-6, LIX and VEGF by means an Elisa on the cytosolic portions of nuclear extractions and the corresponding supernatants did not indicate any significant changes in protein production or release. To test levels of RNA multiple real time reverse transcriptase polymerase chain reaction (RT<sup>2</sup> PCR) profiler arrays were performed on RNA collected from both control and rrCNTF treated astrocyte cell cultures after 6, 12 or 24 hour incubations. The gene analysis indicates numerous changes falling beyond a threefold cut off. The inhibition of the Jak/STAT3 pathway within the cultured astrocytes was tested by the application of AG490 to inhibit Jak2 and cucurbitacin to inhibit STAT3. Within the cultured astrocytes, AG490 did not successfully inhibit the CNTF activated pathway, although the inhibition of STAT3 by cucurbitacin arrested the activation process. To test if astrocytes do indeed release neuronal promoting factors, astrocyte conditioned media from a non-treated control, rrCNTF treated, AG490, AG490 plus rrCNTF, cucurbitacin and cucurbitacin plus rrCNTF treatments was applied to hypothalamic organotypic explant cultures and the MNS neurons were counted and compared. The comparison showed a significant increase in neuronal survival for explants exposed to CNTF as well as AG490 plus CNTF. This indicates that AG490 does not inhibit the CNTF activation of cultured astrocytes. The exposure to cucurbitacin does effectively prevent the astrocytes from becoming activated by CNTF, preventing the release of pro-survival neuronal factors. In summary, CNTF potentiates the survival of axotomized magnocellular neurons by means of the resident astrocytes.

## CHAPTER I

### INTRODUCTION

#### Hypothalamic Magnocellular Neurosecretory System

The hypothalamic magnocellular neurosecretory system (MNS) has become a classic model for peptidergic neurons over the last seventy years due to the initial work of Ernst and Berta Scharrer (1954). Thanks to the advances in tissue staining by Gyorgy Gomori (Gomori, 1939, 1941, 1950), the MNS has been shown to consist of two categories of peptide hormone producing neurons (magnocellular and parvocellular neurons) found within the paraventricular nuclei (PVN; magnocellular and parvocellular) and the supraoptic nuclei (SON; magnocellular) as well as some accessory nuclei (Figure 1). The parvocellular neurons have been shown to influence the anterior pituitary through the release of multiple regulatory hormones into the hypophyseal portal system (A. J. Silverman & Zimmerman, 1983). While, the axons of the magnocellular neurons extend through the median eminence and terminate in the posterior pituitary (neural lobe; NL) collectively forming the hypothalamo-neurohypophysial tract (Alvarez-Buylla, Livett, Uttenthal, Hope, & Milton, 1973). Activation of this system can be induced by numerous factors including, but not limited to, blood osmolality (Bourque, Oliet, & Richard, 1994), sexual stimulation (Pedersen & Boccia, 2006), an infant's cry (Leng, Caquineau, & Sabatier, 2005), and invasive surgery (Hatton, 1983).



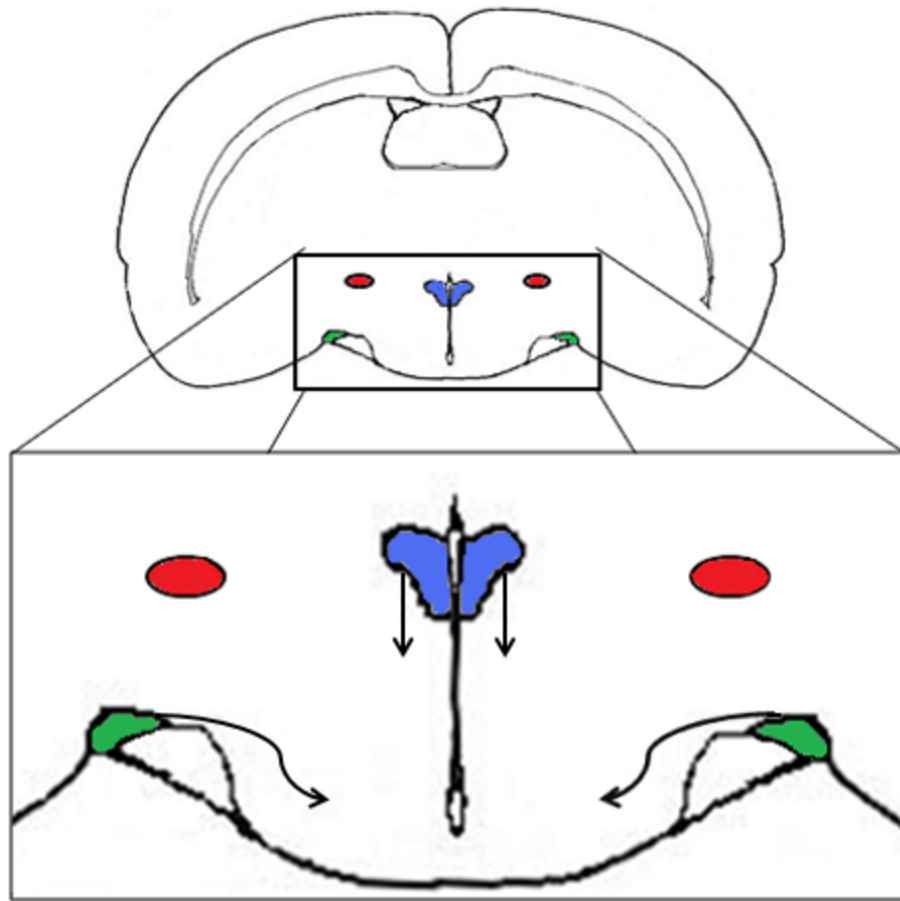


Figure 1. Anatomy of the Magnocellular Neurosecretory System. The somas of the magnocellular neurons lie within the paraventricular nuclei (PVN; blue), supraoptic nuclei (SON; green), and accessory nuclei (ACC; red). The axons (indicated by arrows) of the PVN extend ventrally and caudally meeting up with the SON axons that extend medially and caudally forming the hypothalamo-neurohypophysial tract which passes through the median eminence and terminates in the pars nervosa.

### Paraventricular Nucleus

The PVN are paired triangular shaped neuronal clusters located adjacently to the dorsal sides of the third ventricle and consists of both magnocellular and parvocellular neurons. The PVN can be subdivided into eight distinct subdivisions of neurons, of which three are magnocellular; anterior, medial and posterior magnocellular divisions (Swanson & Kuypers, 1980). The

largest of the magnocellular divisions and the primary one of focus in our studies is the posterior magnocellular portion (Swanson & Sawchenko, 1983).

The axons of the PVN magnocellular neurons extend in one of two destinations; medially to the stria medullaris or laterally bending towards the median eminence and terminating in the peripheral regions of the pars nervosa (Swanson & Sawchenko, 1983). The axons found in the zona externa of the median eminence follow an ipsilateral arc-shaped path (Antunes, Carmel, & Zimmerman, 1977). Those that travel through the internal median eminence terminate in the peripheral regions of the pars nervosa (Alonso & Assenmacher, 1981; Hernandez et al., 2015; Ju, Liu, & Tao, 1986). This tract is also referred to as the tract of Greving.

The five remaining divisions are distinctly parvocellular; periventricular, anterior parvocellular, medial parvocellular, lateral parvocellular, and dorsal parvocellular (Swanson & Kuypers, 1980). The parvocellular neurons found in these five divisions extend their axons through the ventral surface of the external zone of the median eminence and terminate in the proximal infundibulum.

### Supraoptic Nucleus

The SON are also paired nuclear groups located on the lateral boarder of the optic chiasm. The cytoarchitecture of the SON consist of several distinct cell types; the magnocellular neurons, microglia, endothelial cells, and two separate types of astrocytes (a macro-glial cell). The basal aspect of the SON, known as the ventral glial limitans (VGL) serves as a barrier between the menigial pia matter and the SON proper (Salm & Hawrylak, 2004). The VGL consists of tightly

packed protoplasmic astrocytes that extend processes perpendicular from the base of the brain to the dorsal aspects of the SON. The fibrous or stellate astrocytes are found sparsely throughout the SON proper with the magnocellular neuron somas (Bonfanti, Poulain, & Theodosis, 1993). The other glial cells of the central nervous system, oligodendrocytes and microglial are seldom seen; however, microglia will increase in numbers in response to chronic neurosecretory activity (Ayoub & Salm, 2003). The neurons extend their dendrites in a vertical orientation forming the dendritic zone directly dorsal to the VGL (Figure 2). The axons of the SON magnocellular neurons project medially and caudally from the dorsal aspect of the nucleus to the inner zone of the median eminence terminating throughout the pars nervosa with the highest density in the central region (Alonso & Assenmacher, 1981).

#### Accessory Nuclei

There are several accessory nuclei that contain magnocellular neurons; rostral parventricular, anterior fornical, posterior fornical, nucleus circularis, and the nucleus of the medial forebrain bundle. In addition to these nuclei there is a series of individual magnocellular neurons that extend laterally and ventrally from the PVN to the SON (A. J. Silverman & Zimmerman, 1983). The axons from these neurons also extend to the pars nervosa.

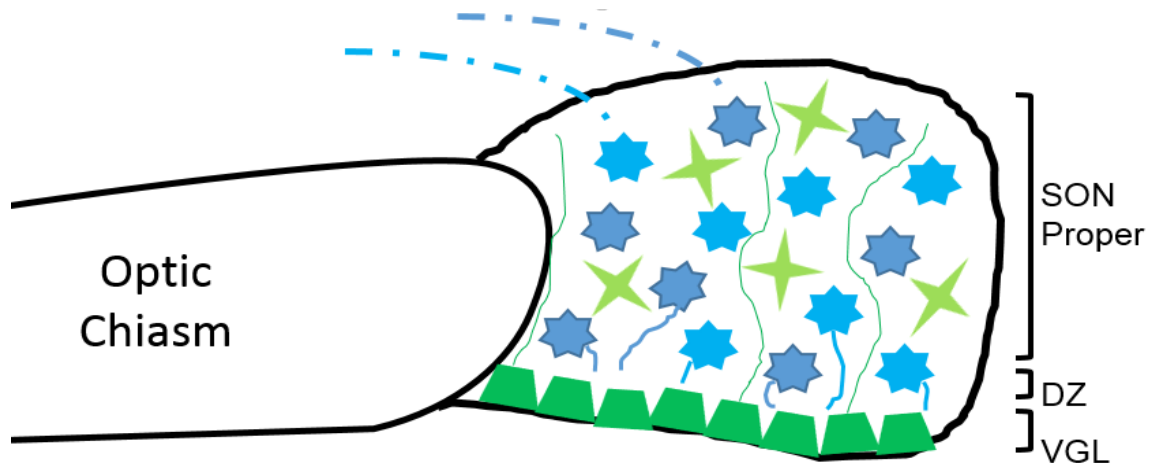


Figure 2. Anatomy of the Supraoptic Nucleus (SON). Protoplasmic astrocytes (green trapezoids) form the ventral glial limitans (VGL) and extend processes (solid green lines) to the dorsal aspect of the SON. Fibrous astrocytes (light green 4-point star) are found sparsely throughout the SON proper. The somas of the two classifications of magnocellular neurons lie within the SON proper (blue and teal 7-point stars). The dendrites (solid blue and teal lines) of both types extend in a vertical fashion forming the dendritic zone (DZ) inferior to the SON proper. SON axons (blue and teal dashed lines) extend medially and caudally, cross in the internal zone of the median eminence and extend to the pars nervosa with a majority of termination being centrally located.

### Magnocellular Neurons

The primary neuron of the hypothalamic neurosecretory system is the magnocellular neuron, also referred to as neuroendocrine or peptidergic neuron for their neurosecretory functions. Immunocytochemical staining indicates that the somas of these neurons are round to oval in appearance with a diameter of 20 to 35  $\mu\text{m}$  (Sofroniew & Glasmann, 1981). These neurons are large modified bipolar neurons with two primary dendrites and the axon extending from one of those dendrites (Hatton, 1986). There are slight phenotypic differences between the SON and PVN (Weiss & Hatton, 1990a, 1990b).

The neurons of the SON have one to five branching dendrites that branch in a ventro-lateral orientation. The ventral dendrites extend toward the ventral glial limitans forming the dendritic zone. The axons of these neurons extend medially and caudally forming the hypothalamoneurohypophysial tract that terminates throughout the pars nervosa with a high central concentration (Felten & Cashner, 1979). SON cell counts indicated a range between 4400 and 7000 magnocellular neurons (Leranth, Zaborszky, Marton, & Palkovits, 1975; Olivecrona, 1957). In comparison, the neurons of the PVN have two to three simple dendrites of which only one is a primary dendrite. The magnocellular neurons of the PVN have been estimate to be between 1300 and 2000 (Bodian & Maren, 1951; Olivecrona, 1957).

There are two types of magnocellular neurons, each of which is named for the specific neuropeptide it is responsible for producing; oxytocinergic neurons are responsible for the production of oxytocin (OT) and vasopressinergic which produces vasopressin (VP) (Cross et al., 1975). The distribution of these neurons has been systematically mapped by Anna Hou-Yu et.al (1986) and C. H. Rhodes et.al. (1981). Using immunocytochemical analysis it was determined that within the SON the VP and OT neurons were mixed with peripheral exemptions. Swanson and Sawchenko (1983) state that this organization allows for the zones to be functionally influenced independently.

#### Parvocellular Neurons

The parvocellular neurons found throughout the five parvocellular divisions of the PVN are bipolar and multipolar simple neurons with two to three short

primary dendrites that have minimal branching. These neurons have been estimated to average 7000 in number when combining the divisions (Sawchenko & Swanson, 1981, 1983). Some axons of the parvocellular neurons extend to make synaptic connections with both magnocellular and parvocellular neurons within other parvocellular divisions (van den Pol, 1982). Other axons are directed through the ventral surface of the external zone of the median eminence and terminate in the proximal infundibulum for secretion of neuropeptides into the primary portal plexus for stimulation of the pars distalis, also known as the anterior pituitary. The neuropeptides produced by these parvocellular neurons include corticotrophin releasing factor (CRF), dopamine (DA), growth hormone-releasing hormone (GHRH), gonadotropin-releasing hormone (GnRH), somatostatin (SS), and thyrotrophin-releasing hormone (TRH) (Flament-Durand, 1980; Markakis, Palmer, Randolph-Moore, Rakic, & Gage, 2004).

#### Pars Nervosa

The pars nervosa comprises the posterior aspect of the pituitary gland. Also known as the posterior pituitary, the neurohypophysis or the neural lobe, it is composed primarily of the axonal projections from the hypothalamic neurosecretory system. The axonal projections from the magnocellular neurons transport the neuropeptides vasopressin and oxytocin to close proximity of the pars nervosa capillaries. The axon terminals take one of three morphological appearances; undilated axon terminal, axon end swellings called Herring bodies, or a dilated terminal called sensu stricto (Nordmann, 1977; Rosso & Mienville, 2009). These terminals are responsible for the release of the neuropeptides into

the hypophyseal circulation through fenestrated capillaries. In addition to the magnocellular axon terminals, there is an astrocyte-like cell, the pituicyte. This pars nervosa cell has been shown to be GFAP immunoreactive (Salm, Hatton, & Nilaver, 1982) and has the ability to engulf numerous axonal endings (Hatton, 1988). The pituicyte contributes to the controlled release of oxytocin and vasopressin into circulation (Hatton, 1988; Rosso & Mienville, 2009).

### Oxytocin

The neuropeptide oxytocin is produced by magnocellular neurons from both the paraventricular and supraoptic nuclei and released into circulation through fenestrated capillaries of the pars nervosa. The production and release of oxytocin can be stimulated by multiple factors, some of which also elicit the release of vasopressin. These factors include, but are not limited to, increased plasma osmotic pressure, parturition, lactation, sexual stimulation and pair-bonding (Russell & Leng, 1998).

Oxytocin plays a role in preventing defensive behaviors allowing for positive social interaction leading to bond-pairing and eventual reproduction (Carter, 1998). The role of oxytocin in parturition was first suggested by G. W. Harris, (Harris, 1947, 1948) after studying pregnant female rabbits with diabetes insipidus. It was later determined that increased levels of oxytocin elicits an augmented production of prostaglandins and leads to heightened contraction of the uterus. Following parturition, the neuropeptide is active in lactation by influencing the contractions of the myoepithelial cells of the mammary glands allowing for milk ejection in response to the cry or suckling of the infant(s) (Miyata

& Hatton, 2002; Neumann, Russell, & Landgraf, 1993; Russell & Leng, 1998). During the act of lactation, oxytocin is released in interval pulses to compensate for the diminished response of the mammary glands to continuous hormone exposure (Leng et al., 2005; Poulain & Wakerley, 1982). Recently, Kruger et. al (2003) demonstrated the possibility of an acute increase of oxytocin levels directly after male orgasm, although these changes were not statistically significant nor consistent. Additionally, oxytocin acts as a positive feedback on the neurons that produce it (Falke, 1991).

### Vasopressin

Vasopressin is also produced by magnocellular neurons of both the PVN and SON. Vasopressin shares multiple types of stimuli with oxytocin but is primarily influenced by blood plasma osmolality. The stimulation of vasopressinergic neurons leads to elevated levels of vasopressin mRNA which is controlled by synaptic activity (Sladek, Fisher, Sidorowicz, & Mathiasen, 1995). Vasopressin, also referred to as arginine vasopressin or antidiuretic hormone (ADH), is released into the circulation through fenestrated capillaries within the pars nervosa following stimulation. Stimulation is elicited by osmotic stress associated with hemorrhaging, dehydration or hypotension (Dunn, Brennan, Nelson, & Robertson, 1973). Osmoreceptors, a specialized osmolality sensing receptor, have direct involvement with vasopressin release and are associated with thirst and salt appetite (Bourque et al., 1994). These receptors are found in the central nervous system as well as peripherally (Robertshaw, 1989). Those that are central are found in areas that lack the blood brain barrier; the



subfornical organ and organum vasculosum lamina terminalis (Bourque et al., 1994). Upon sensing body hyperosmolality by means of blood plasma, these specialized receptors elicit the magnocellular neurons to release the pars nervosa vasopressin stores into the circulation. Accordingly, vasopressin regulates the reabsorption of water by the distal tubules and collecting ducts in the kidney. Increased levels of vasopressin results in increased water reabsorption and vice versa (Bourque et al., 1994). Thus, the physiological role of vasopressin is essential in maintaining a homoeostatic environment through the conservation of body water.

### Astrocytes

The macro-glial astrocyte, first described by Rudolf Virchow in 1860 (Nag, 2011; Somjen, 1988) as a nerve glue-like cell, or neuro-glia. These stellate and spindle-shaped cells, which are confined to the central nervous system (CNS), were described as having numerous processes extending to blood vessels, separating neurons and enveloping neuron synapses. After the discovery that they could not be electrically excited, they were considered trophic, metabolic and structural supporting cells of neurons (Nag, 2011).

### *Astrocyte Classification*

Immunocytochemistry distinguishes astrocytes from neurons and other glial cells by the expression of the astrocyte specific intermediate filament glial fibrillary acid protein (GFAP). This classification of glial cells is divided into two subtypes based on localization and named for appearance; protoplasmic or fibrous. The protoplasmic astrocyte also known as type 1 primary, or stellate,

astrocytes are found throughout the gray matter of the CNS. This subtype develops prior to the fibrous subtype and expresses lower levels of GFAP (Miller & Raff, 1984). The numerous branched processes are responsible for the envelopment of neuronal synapses (Sofroniew & Vinters, 2010). Protoplasmic astrocytes also form the glial limitans that surround the brain forming an astrocyte barrier between the pial matter and the neural parenchyma (Salm & Hawrylak, 2004). The fibrous astrocyte is also called type 2, secondary or spindle-shaped astrocyte. This subtype is found throughout the white matter of the CNS and has higher basal levels of GFAP than its counterpart (Miller & Raff, 1984). In addition to having more GFAP, fibrous astrocytes can be distinguished from protoplasmic astrocytes by the presence of a polysialoganglioside that is immunocytochemically labeled by the antibody A2B5 (Miller & Raff, 1984). The name fibrous was given due to the cell's many long fiber-like processes some of which contact nodes of Ranvier.

Further classification of astrocytes in humans and primates yields four subtypes based on location. The protoplasmic subtype is localized to cortical layer 2 through 6 and includes the interlaminar astrocyte found only in cortical layer 1. The intermaninar astrocytes form the glial limitans and have very long processes that extend to layers 3 and 4 of the cortex (Nag, 2011). The fibrous astrocytes found throughout the white matter are shown to be the only astrocyte to extensively intermingle and function only in the capacity of metabolic support. The last subtype is the polarized astrocyte. This is a unipolar macro-glial cell that is found in very low numbers within cortical layers 5 and 6. The single processes

of the polarized astrocyte can extend up to 1 mm, but the function has yet to be determined (Nag, 2011; Oberheim, Wang, Goldman, & Nedergaard, 2006).

### *Astrocyte Function in Development*

The function of the astrocyte in a healthy central nervous system begins at development. Even though the developmental generation occurs after the initial development of neurons (Magavi, Friedmann, Banks, Stolfi, & Lois, 2012), the astrocytes play an essential role in the development of the central nervous system. Astrocytes are responsible for the extracellular matrix proteins and adhesion molecules both promoting and inhibiting the maturation and migration of neurons (Wiese, Karus, & Faissner, 2012). Multiple growth-promoting molecules have been identified including N-cadherin, laminin, neural cell adhesion molecule (NCAM) and fibronectin (Liesi, Dahl, & Vaheri, 1983; Neugebauer, Tomaselli, Lilien, & Reichardt, 1988; Price & Hynes, 1985). The presence of proteoglycans such as keratin sulfate and chondroitin sulfate, act as growth inhibitors for extending neurons (Snow, Lemmon, Carrino, Caplan, & Silver, 1990). Astrocytes also release factors that promote the maturation and survival of the developing neurons. Included among these are nerve growth factor (NGF), brain-derived growth factor (BDNF) fibroblastic-growth factor (FGF), neurotrophin-3 (NT-3) and ciliary neurotrophic factor (CNTF) (Rudge et al., 1992; Vaca & Wendt, 1992). The astrocytic release of molecular signals such as thrombospondins has recently been indicated as an essential factor in synapse development (Christopherson et al., 2005).

There are several factors either released or displayed by astrocytes during vasculogenesis of the CNS. Studies indicate that prior to blood vessel development, astrocytes form a vascular-like plexus that will be penetrated by the vascular endothelial cells (Gariano, 2003). These astrocytes produce interleukin-6 (IL-6), FGF and vascular endothelial growth factor (VEGF) all of which influence the growth of blood vessels (Bernal & Peterson, 2011). The processes of the astrocytes that form the plexus show high expression levels of VEGF that decreases along with IL-6 after birth (Fee et al., 2000; Gerwins, Skoldenberg, & Claesson-Welsh, 2000; Saito et al., 2011; Seghezzi et al., 1998). Epoxyeicosatrienoic acid is released by astrocytes and acts both as a chemokines and a morphogen for the in-coming endothelial cells (C. Zhang & Harder, 2002). The astrocytes are responsible for the production of the laminin layer found between astrocytic foot processes and the vascular endothelial cells (Lattera, Guerin, & Goldstein, 1990).

#### *Mature Astrocyte Function*

Astrocytes play an essential role in the maintenance of the central nervous system be it a trophic, metabolic, or structural support. As previously stated, astrocytes are found throughout the CNS and play a vital role in its development, but their functions are a never-ending continuous string of events. The astrocytic foot processes that originated for the development of the brain vasculature also play an essential role in the blood brain barrier. The application of astrocyte conditioned media to endothelial cell cultures induced the endothelial cells to increase tight junction formation, reducing the permeability of the blood vessel

walls (Arthur, Shivers, & Bowman, 1987; Raub, Kuentzel, & Sawada, 1992). In addition to functioning in the blood brain barrier, astrocytes help control the blood flow through the production and release of mediators such as prostaglandins (PGS), nitric oxide (NO) arachidonic acid (AA), and prostaglandin 2 (Gordon, Mulligan, & MacVicar, 2007; Iadecola & Nedergaard, 2007; Koehler, Roman, & Harder, 2009).

The aptitude of an astrocyte to contact both a blood vessel and a neuron allows for the astrocyte to aid in controlling the CNS metabolism. The uptake of glucose from the circulation by astrocytes and storage of glycogen within astrocytes is used to furnish neurons with energy. Large accumulations of glycogen in astrocytes provides a sustained neuronal source for activity during hypoglycemia and during periods of high activity (Suh et al., 2007).

Immunocytochemical localization (Pfeiffer-Guglielmi, Fleckenstein, Jung, & Hamprecht, 2003) and electron microscopy (Phelps, 1972) have both shown localization of glycogen and its mobilizing enzyme glycogen phosphorylase to be localized almost exclusively to the astrocyte.

Astrocyte excitability is calcium based. Cytosolic calcium levels fluctuate through outside influences including glutamate and extracellular calcium levels (Nag, 2011). In addition to calcium influences, astrocytes express potassium and sodium channels. Potassium channels allow for a process called potassium spatial buffering; the transportation of extracellular potassium from areas of high concentration to those of lower concentrations (Kimmelberg, 2010).

Each astrocyte is estimated to contact several hundred dendrites and has the potential of enveloping up to 140,000 synapses (Bushong, Martone, Jones, & Ellisman, 2002). Astrocytes provide a healthy environment for the synapse through the maintenance of the synaptic interstitial fluid ions, pH, and transmitter homeostasis. By enveloping a synapse, the astrocyte can directly affect the synaptic function through the release and buffering of glutamate, adenosine triphosphate (ATP) (Halassa, Fellin, & Haydon, 2007) gamma-aminobutyric acid (GABA) (Dani & Smith, 1995), and neuroactive steroids such as estradiol and progesterone (Garcia-Segura & Melcangi, 2006). Long-term influence is also possible with the release of growth factors and cytokines such as tumor necrosis alpha (TNF $\alpha$ ) (Stellwagen & Malenka, 2006). All of the astrocytic reactions influencing the synapses are controlled by the changes of astrocytes intracellular calcium levels (Sofroniew & Vinters, 2010).

Astrocytes influence all aspects of the central nervous system. From development of the vasculature and the migration of neurons to providing a healthy environment for a functional CNS, the astrocyte is vital. Interestingly, the ratio of astrocytes to neurons shows a considerable increase corresponding with advances in evolution; in *Caenorhabditis elegans* the astrocyte to neuron ratio is 1:6, rodents 1:3, cats 1.2:1, and 1.4 astrocytes to every neuron in humans (Nedergaard, Ransom, & Goldman, 2003).

## Magnocellular Neurosecretory System Plasticity

One of the primary reasons for the magnocellular neurosecretory system (MNS) to become a classic model for peptidergic neurons is the plasticity of the system. The MNS has been shown to have predictable and reversible plasticity in response to outside influence. Hyperosmotic stimulation of the system causes the magnocellular neuron somas and axons to increase in size, displacing the astrocyte processes (Hatton, 1986; Kalimo, 1975). Additionally, the dendritic branches of the SON neurons form dendritic bundles allowing for multiple neuron communication including double synapses not seen at basal levels. The double synapses are only found between phenotypically identical neurons and can act as a positive feedback loop; e.g., oxytocin has the ability to stimulate its own production and release (Hatton, 1988).

At a resting state within the pars nervosa, the pituicytes completely surround the axon terminals regulating neuropeptide release. In response to stimulation, the pituicytes retract allowing the axon terminals to make close contact with the fenestrated capillaries permitting release of oxytocin (OT) and vasopressin (VP) into circulation (Hatton, 1988; Prevot et al., 1999; Rosso & Mienville, 2009). These events enable the system to react in an efficient, heightened, and synchronized manner. In addition to hyperosmotic stimulation, these changes are also seen during lactation, parturition and pair-bonding (Russell & Leng, 1998). In the case of hypoosmotic condition the magnocellular neuron somas decrease in size by approximately 60%. The decreased soma size is affiliated with 10-20% down-regulation of the mRNA for both oxytocin and

vasopressin (B. Zhang, Glasgow, Murase, Verbalis, & Gainer, 2001). Removal of physiological stimuli results in the return of the MNS to the basal anatomical organization and cellular relationship (Hatton, 1986).

Trauma to the magnocellular neurosecretory system also elicits a plastic response. Following a unilateral lesion of the MNS severing the hypothalamo-neurohypophysial tract of one hemisphere, the lesion results in the loss of 90% of the magnocellular neurons in the injured SON (Askvig et al., 2013), which results in the subsequent loss of 43% of axons in the NL (Watt et al., 1999; Watt & Paden, 1991). Uninjured magnocellular neurons from the contralateral SON show increased neurosecretory activity that accompanies a collateral sprouting response that reinnervates the NL (Watt et al., 1999; Watt & Paden, 1991). Similar outcomes have been noted following adenohipophysectomy (Bodian & Maren, 1951). The astrocytes transition to a reactive stage that can be shown by increased levels of glial fibrillary acidic protein (GFAP) and nuclear hypertrophy.

Generally, at the site of trauma, astrocytes form a glial scar that is impenetrable by neuron axons and responsible for the release of chemokines that contribute to an inflammatory reaction (Fitch & Silver, 2008; Haas, Neuhuber, Yamagami, Rao, & Fischer, 2012; D. Sun, Lye-Barthel, Masland, & Jakobs, 2010). Although intense trauma prevents the central nervous system from returning to the prior uninjured state, the magnocellular neurosecretory system compensates by axonal projections from the uninjured hypothalamic nuclei (Watt & Paden, 1991).



Astrocytes have become renowned for being a primary responder to brain trauma. Following a CNS injury, astrocytes enter a reactive state known as reactive astrogliosis. The occurrence of astrogliosis was proposed by Sofroniew (2009) to be the integration of four interdependent primary features. The first is that this reaction occurs for all forms and severities of trauma and CNS disease. Secondly, the degree of astrogliosis intensifies with the severity of the CNS complication. Thirdly, this reaction is mediated by specific signaling. And lastly, astrogliosis has the potential to affect the functionality of the astrocytes and therefore impacting all cell types in close proximity either negatively or positively. As the severity of the reactive astrogliosis increase, the levels of GFAP and vimentin correspondingly rise (D. Sun et al., 2010). In addition to increased levels of intermediate filaments, the astrocyte becomes hypertrophic and cell signaling cascades lead to increased levels of adhesion molecules, antigen presenting molecules, calcium binding proteins, and numerous cytokines, chemokines, neurotrophins and growth factors (Eddleston & Mucke, 1993).

In mild to moderate reactive astrogliosis, the cell reactivity is very localized and confined within the astrocyte with minimal increases in astrocyte interaction (Sofroniew, 2005). Proliferation and glial scar formation is rare in these cases allowing for a return to a comparably healthy state. Examples of mild to moderate reactive astrogliosis include but are not limited to regions distant from a CNS laceration, concussions and immunological responses to viral or bacterial infections (Wilhelmsson et al., 2006). More severe reactive astrogliosis results in proliferation and increased astrocyte interaction. These changes are more

pronounced and longer lasting than the mild to moderate situation (Sofroniew & Vinters, 2010). The change in the cytoarchitecture commonly expands beyond the site of injury decreasing the probability of returning to the healthy non-injured state. In instances of very severe astrogliosis, a glial scar will form. The glial scar is found at the site of severe injury and consists of densely packed, overlapping astrocytes and fibroblast lineage cells (Sofroniew, 2009). Localized to the site of injury is an immediate and robust inflammatory response brought about by the astrocytic release of pro-inflammatory cytokines (Sofroniew, 2005). The inability of glial scar formation to occur results in; prolonged increased levels of leukocytes, the failure of the blood-brain barrier to repair, spread of tissue damage, increased neuronal loss and demyelination, increased neurite outgrowth and the decreased likelihood of function recovery (Bush et al., 1999; Faulkner et al., 2004). The overall response of reactive astrogliosis in any CNS trauma promotes CNS repair by the reformation of the various barriers and neuronal protection leading to reestablishment of the homeostatic environment.

### Ciliary Neurotrophic Factor

#### *Ciliary Neurotrophic Factor Identification and Properties*

In the late 1970's research was being done to determine the trophic factors associated with survival mediation of developing parasympathetic, sympathetic and sensory neurons of the chick ciliary ganglia. In addition to the known Nerve Growth Factor (NGF), a second agent was thought to assist in the survival and growth of the cultured ciliary neurons (Helfand, Riopelle, & Wessells, 1978; Helfand, Smith, & Wessells, 1976). Analysis indicated a putative factor was

produced in high amounts by the ciliary body, iris and choroid layers of the developing chick eye that differed from NGF. The absence of this factor in cultured ciliary neurons resulted in cell death. For its properties this factor was named cholinergic neuronotrophic factor (Adler, Landa, Manthorpe, & Varon, 1979; Ebendal, Olson, Seiger, & Hedlund, 1980; Varon, Manthorpe, & Adler, 1979). This trophic factor later became known as ciliary neuronotrophic factor and eventually ciliary neurotrophic factor (CNTF).

Analysis and purification of CNTF from the chick eye yielded a 20.5 kDa monomer (Barbin, Manthorpe, & Varon, 1984; Manthorpe, Barbin, & Varon, 1982). Purification of CNTF from the adult rat sciatic nerve extract yielded a 24 kDa monomer (Manthorpe, Skaper, Williams, & Varon, 1986). Comparison of the CNTF extracts of both species showed numerous similarities. The application of either extract to cultures demonstrated the ability of the trophic factor to promote survival of dorsal root, sympathetic and ciliary ganglion as well as an insensitivity to anti-NGF antibodies (Manthorpe et al., 1986). Advances in the purification process from the rat sciatic nerve in addition to cDNA cloning of RNA collected from rat brain cells known to produce CNTF allowed for a more precise analysis of the protein. These studies yielded a 200 amino acid protein with a short 5' untranslated 77 base pair region and a long untranslated 436 base pair 3' region ending with a poly-A tail that has a relative molecular mass of 23 kDa (Stockli et al., 1989). This protein is folded into a helical structure with four anti-parallel alpha-helices (Bazan, 1991; McDonald, Panayotatos, & Hendrickson, 1995; Panayotatos et al., 1995). The cloning of human CNTF showed an 83%

homology to rat CNTF (Lam et al., 1991; Sendtner, Carroll, Holtmann, Hughes, & Thoenen, 1994).

In addition to CNTF's role in dorsal root, sympathetic and ciliary ganglion development and survival, this neurotrophin has been indicated in the survival of multiple neuronal phenotypes of both the central and peripheral nervous systems. The application of CNTF to CNS spinal motor neuron cultures showed at least a 60% survival of the developing neurons. In comparison, the application of trophic factors NGF or BDNF did not alter survival levels from the control cultures (Arakawa, Sendtner, & Thoenen, 1990). When applied to human spinal cord neuron cultures, the combination of CNTF with NT-3 (neurotrophin-3) and BDNF elicits a 4-fold increase in choline acetyltransferase activity. The application of any one of these trophic factors resulted in only a 2-fold increase in activity and the combination of CNTF plus BDNF or NT-3 plus BDNF increase activity by 3-fold. Increases in cholinergic function measured by the levels of choline acetyltransferase correlated with increased survival and differentiation of the spinal cholinergic neurons (Kato & Lindsay, 1994). CNTF has also been shown to promote survival of embryonic hippocampal neurons including GABAergic (2-fold), cholinergic (28-fold) and calbindin-immunopositive (3-fold) (Ip et al., 1991). Additionally, the local application of CNTF to axotomized motor neurons prevents lesion-induced death (Sendtner, Kreutzberg, & Thoenen, 1990). Within the supraoptic nucleus astrocytes are the source of CNTF (Rusnak, House, Arima, & Gainer, 2002; Watt, Bone, Pressler, Cranston, & Paden, 2006) and CNTF has been found to contribute to magnocellular neuronal

survival and axonal sprouting. For example, the application of CNTF to the hypothalamic organotypic in vitro culture model, which allows for the cytoarchitecture of the PVN and SON to remain intact, shows increased survival of vasopressin and oxytocin producing magnocellular neurons (Askvig et al., 2013; House, Li, Yue, & Gainer, 2009; Rusnak et al., 2002; Rusnak, House, & Gainer, 2003; Vutskits, Bartanusz, Schulz, & Kiss, 1998). Our lab has evidence suggesting a role for CNTF in promoting the collateral sprouting of neurosecretory axons following unilateral lesion of the hypothalamoneurohypophyseal tract. In response to the unilateral transection of the hypothalamoneurohypophysial tract, CNTF protein levels increased in the contralateral SON from which the axonal sprouting originates (Askvig, Leiphon, & Watt, 2012; Watt et al., 2006). Moreover, our lab has also demonstrated that CNTF promotes magnocellular neuron process outgrowth in hypothalamic organotypic cultures (Askvig & Watt, 2015).

#### *CNTF Secretion*

It has been proposed that the lack of a signal sequence targeting CNTF to the Golgi system restricts CNTF to the cytosol of the synthesizing cell preventing release of CNTF through the classical secretory pathways (Lin et al., 1989; Stockli et al., 1989). Paradoxically, in order for CNTF to fully function, it must be released into the extracellular matrix to act on its target cells. It's been hypothesized that CNTF is released following a rupture of the astrocyte (Richardson, 1994). However, Kamiguchi et.al. (1995) demonstrated release of CNTF from cultured astrocytes following treatment with IL-1 and tumor necrosis

factor alpha (TNF- $\alpha$ ) in the absence of astrocyte cell lysis. These results suggest that CNTF can be released through non-classical secretory mechanisms. Within the magnocellular neurosecretory system, the presence of IL-1 $\beta$  has been demonstrated within the oxytocin and vasopressin neurons (Watt & Hobbs, 2000) and the levels of the cytokine secretion from the dendrites are increased following osmotic stimulation (Summy-Long, Hu, Long, & Phillips, 2008; Watt & Hobbs, 2000). Therefore, the method of secretion in vivo is thought to be paracrine in which the release of IL-1 $\beta$  from neuronal dendrites influences the activated astrocytes to release CNTF into the extra cellular matrix where it can act in either an autocrine or a paracrine manner (Richardson, 1994).

#### *The Tripartite CNTF Receptor Complex*

Structurally and functionally, CNTF is related to the interleukin-6 cytokine family. This family of cytokines is based on the helical structure of the cytokine and the receptor subunit makeup. Cytokines included in this family are leukemia inhibitory factor (LIF), IL-6, interleukin-11 (IL-11), oncostatin M (OSM), cardiotrophin-1 (CT-1), and cardiotrophin-like cytokine (CLC). The typical receptor complex for any member of the IL-6 cytokine family requires the dimerization of the beta subunits in association with an alpha subunit (Hibi, Nakajima, & Hirano, 1996; Hirano, Matsuda, & Nakajima, 1994). Each alpha subunit confers a high-affinity specific binding region for the specific cytokine in contrast to the beta units which can be utilized in conjunction with multiple alpha subunits allowing for signal transduction (Frank & Greenberg, 1996).

In order for CNTF to activate the target cell, it must first bind to the receptor complex alpha subunit CNTF receptor- alpha (CNTFR- $\alpha$ ). Unlike the IL-6 receptor, the CNTFR- $\alpha$  component lacks both transmembrane and cytosolic domains and is instead anchored to the extracellular matrix by a glycosyl phosphatidylinositol (GPI) linkage (Davis et al., 1991). The lack of a transmembrane and cytosolic domain on the CNTFR- $\alpha$  lead to the identification of two beta subunits in association with CNTF cell activation; glycoprotein-130 (GP-130) (Ip et al., 1992) and leukemia inhibitory factor beta (LIF- $\beta$ ) (Ip & Yancopoulos, 1992; Stahl et al., 1993). Collectively these three components constitute the tripartite CNTF receptor complex. In order for CNTF to generate a functional response, all three components must be present (Davis, Aldrich, Ip, et al., 1993; Davis, Aldrich, Stahl, et al., 1993; Gearing et al., 1994; Stahl & Yancopoulos, 1994).

The binding of CNTF to CNTFR- $\alpha$  induces the association and heterodimerization of the beta subunits leading to cellular signaling activation (Ip & Yancopoulos, 1996). The three components are found throughout the central nervous system, and all three have been identified on astrocytes (Rudge et al., 1994). Within the SON, the only cell that contains all of the CNTF receptor components is astrocytes (Watt et al., 2009; Askvig and Watt, 2012). Thus, CNTF will function in the SON in an autocrine mechanism.

#### *CNTF Signal Transduction*

Signal transduction following the binding of CNTF to CNTFR- $\alpha$  initiates the activation of multiple pathways. The most commonly known pathway is the

Jak-STAT (Janus kinas-signal transducers and activators of transcription) pathway (Justicia, Gabriel, & Planas, 2000). The heterodimerization of gp-130 to LIFR- $\beta$  is immediately followed by the phosphorylation of the tyrosine residues on both beta subunits. Subsequently, the beta subunits' associated Jak proteins are transphosphorylated on the tyrosine residues (Wilks et al., 1991). The phosphorylation of the Jak proteins recruits two STAT proteins which bind to the beta subunits, are phosphorylated, released and dimerize with each other. Following dimerization of the phosphorylated STAT proteins, they translocate from the cytosol to the nucleus where they bind to DNA and activate transcription (Bonni, Frank, Schindler, & Greenberg, 1993). Slight variations to this pathway are noted within the families of either the Janus kinas or STAT proteins. Of the four known members of the Janus kinas family, only two have been observed as phosphorylated following CNTF stimulation, Jak1 and Jak2 (Montmayeur & Borrelli, 1994; Stahl et al., 1994). The STAT molecules that are recruited in the activation sequence include STAT1 and two isoforms of STAT3. The primary isoform is the phosphorylated STAT3 tyrosine-705 (STAT3-Tyr-705). Once the two STAT molecules have been phosphorylated and released from gp130 and LIFR- $\beta$ , they have the ability to heterodimerize or homodimerize. The translocation of the STAT molecules to the nucleus is a rapid and transient reaction that can be maintained while in the continual presence of CNTF. Studies indicate that removal of CNTF leads to decreased levels of phosphorylated STAT in the nucleus within 60 minutes (Frank & Greenberg, 1996; Liu, Gaffen, & Goldsmith, 1998; Wishingrad, Koshlukova, & Halvorsen, 1997). Askvig et. al.



(2013) demonstrated that not only was tSTAT3-immunoreactivity highly localized to the SON specifying a specific localization of the Jak-STAT pathway, but that the inhibition of this pathway abolishes the pro-survival response elicited by CNTF.

In addition to the Jak-STAT pathway, multiple other pathways have been indicated following CNTF cell activation. Alonzi et.al. (2001) showed that the activation of STAT also can lead to the phosphatidylinositol-3'-phosphatase-kinase (PI3K)/ Akt pathway and the MEK/MAK pathway (mitogen-activated protein kinase kinase/mitogen-activated protein kinase). Both of these pathways have been shown in connection with sensory and motor neuron survival (Alonzi et al., 2001; Dolcet et al., 2001). Additionally the MAPK-ERK pathway helps to facilitate oxytocinergic neuron survival and the PI3K-AKT pathway has influence on neuronal process outgrowth in stationary organotypic cultures of the hypothalamus containing the SON and PVN (Askvig & Watt, 2015).

#### *CNTF Activation of Astrocytes*

In regard to astrocytes, CNTF has a very intimate role. CNTF is found endogenously within the cytosol of astrocytes following injury (Dobrea, Unnerstall, & Rao, 1992; Lee, Deller, Kirsch, Frotscher, & Hofmann, 1997; Stockli et al., 1991) and other related glial cells such as the peripheral Schwann cell (Friedman et al., 1992). This coincides with studies indicating that the expression of CNTF messenger RNA is restricted to such non-neuronal cells (Rudge et al., 1992). The production of CNTF within the central nervous system occurs in type-1 astrocytes (Lillien, Sendtner, Rohrer, Hughes, & Raff, 1988) and

immunoreactivity is restricted to GFAP containing astrocytes (Stockli et al., 1991). Synthesis appears to be regulated by direct or indirect signals from axons (Dobrea et al., 1992; Stockli et al., 1989) and expression varies by location, developmental stage, and presence of injury. During development of the CNS, in addition to the prior stated effects on various neuron phenotype development, the production and release of CNTF from type-1 astrocytes induces the differentiation of type-2 astrocytes from O2-A (oligodendrocyte-type-2-astrocyte) progenitor cells in cooperation with extracellular matrix associated molecules (Hughes, Lillien, Raff, Rohrer, & Sendtner, 1988; Lillien, Sendtner, & Raff, 1990). Following injury, CNTF mRNA levels increase in activated astrocytes directly adjacent to the site of injury and these CNTF expressing astrocytes migrate into the wound zone (Seniuk, Henderson, Tatton, & Roder, 1994). The increased expression is a rapid and compounding reaction that can be noted for an extended period of time following initial trauma (Ip, Wiegand, Morse, & Rudge, 1993; Kang, Keasey, Cai, & Hagg, 2012). The reactive gliosis astrocytes undergo in response to trauma can also be initiated by the exogenous application of CNTF (Escartin et al., 2007; Kahn, Ellison, Speight, & de Vellis, 1995; Levison, Ducceschi, Young, & Wood, 1996; Winter, Saotome, Levison, & Hirsh, 1995).

### Hypothesis

Numerous studies have shown an effect of CNTF on astrocytes. It has been shown that this glial cell is responsible for the endogenous production of CNTF and can be influenced to release its product by IL-1 and TNF. In addition to synthesizing CNTF, astrocytes have recently been shown to have all the

necessary receptor components for autocrine CNTF cellular activation. The inhibition of the Jak2 pathway prior to CNTF exposure prevents the astrocytes from entering a reactive gliosis state (Sarafian et al., 2010) leading to the question, what is the astrocytes role in neuronal protection?

The following study was undertaken to test the hypothesis that “CNTF potentiates survival and sprouting of axotomized magnocellular neurons through activation of astrocyte-specific signal transduction pathways leading to increased expression levels of factors which mediate the neuronal response” with the following specific aims:

**Specific Aim I:** Determine if CNTF activates the JAK/STAT pathway in astrocytes.

**Specific Aim II:** Determine the functional response of astrocytes to CNTF.

**Specific Aim III:** Determine if response is a result of CNTF activation of the JAK2/STAT3 pathway by examining if the inhibition of JAK2/STAT3 will alter the CNTF induced functional outcome.

**Specific Aim IV:** Determine if the functional response promotes survival and sprouting of neurons utilizing the hypothalamic explants cultures.

CHAPTER II  
MATERIALS AND METHODS

Animals

Male and pregnant female (E15) Sprague-Dawley rats, purchased from Harlan Laboratories (Minneapolis, MN), were housed in the Biomedical Research Facility on the campus of the University of North Dakota, an AAALAC accredited facility, with a 12-hour light: 12-hour dark cycle. The rats were allowed continual access to lab chow and tap water. All of the following experimental investigations adhered to the standards in the NIH Guide for the Care and Use of Laboratory Animals and were approved by the UND Institutional Animal Care and Use Committee approval #0704-2C.

Mini-Osmotic Pump Infusions

*Assembly of Mini-Osmotic Pumps*

To maintain a sterile environment, the mini-osmotic pumps (ALZET, model #1007D, DURECT Corporation; Cupertino, CA) were assembled in a Nuair Biological Safety Cabinet (Plymouth, MN) following the manufacturer's instructions. After removal of the plastic flange that was attached to the stainless steel pump flow moderator, a 3.0 cm polyethylene tube was connected to the moderator. The pumps were then filled with 100  $\mu$ l of either a 0.1 mg/ml rat recombinant ciliary neurotrophic factor (rrCNTF; R&D Systems; Minneapolis, MN;

catalog #557-NT/CF) in 290 milliosmolar artificial cerebral spinal fluid (aCSF; 0.87% NaCl, 0.02% KCl, 0.02% CaCl<sub>2</sub> dihydrate, 0.017% MgCl<sub>2</sub> hexahydrate, 0.02% Na<sub>2</sub>HPO<sub>4</sub> heptahydrate, 0.003% NaH<sub>2</sub>PO<sub>4</sub> monohydrate; Sigma-Aldrich; St. Louis, MO) or aCSF. Following the reattachment of the moderator, an 8.5 mm cannula (Plastics One Inc.; Roanoke, VA) was connected to the free end of the polyethylene tube and the entire apparatus was placed in a petri dish filled with aCSF and incubated for 12 hours at 37°C/5.0% CO<sub>2</sub> to allow for priming of the tubing and cannula prior to implantation.

#### *Stereotaxic Surgery, Mini-Osmotic Pump Placement*

Utilizing the adolescent male Sprague-Dawley rats, weighing 250-350 grams, each rat was anesthetized with isoflurane (Butler Animal Health Supply; Dublin, OH) until unresponsive to a tail pinch. The fur on the superior surface of the head was shaved off and the rat was placed in a stereotaxic apparatus (Stoelting; Wood Dale, IL) with a nose cone providing a constant flow of isoflurane/O<sub>2</sub> (2.5%; Abbott Laboratories; Abbott Park, IL) by means of a table top anesthesia apparatus in combination with a vaporizer (Matrix Quantiflex Low Flow V.M.C. and VIP 3000; Orchard Park, NY). Using a scalpel, a small incision was made parallel to the axial alignment, the incision was held open using a retractor and the fascia was gently displaced exposing the skull. The prepared cannula was inserted into a custom holder (Stoelting) on the stereotaxic apparatus and the bregma and lambda fissures were measured and adjusted to be equal to insure a level skull for precise cannula placement. Using bregma as stereotaxic zero, the coordinate was marked; anterior/posterior -0.9 mm,

medial/lateral -1.9 mm. Using a dremel drill, a small hole through the skull was made on the marked coordinate along with two shallow holes to either side which dental screws were fastened into. The cannula was slowly lowered to a depth of - 8.5 mm dorsal/ventral, placing the cannula tip directly into the dorsal supraoptic nuclei (Figure 3). Dental cement was then prepared and applied to the base of the cannula and out to the dental screws, securing the cannula in place. Once the cement was dry, the cannula was released from the stereotaxic apparatus and the top portion of the cannula was removed after which the pump was placed under the skin between the scapulae and additional cement was applied to the cannula and screws ensuring a smooth surface. When the cement was stiff to the touch, the scalp was sutured and the animal was removed from the stereotaxic apparatus, weighed and placed back into its cage on top of a heating pad until it recovered from anesthesia.

#### Tissue Homogenate Preparation

Following the 72-hour infusion from the mini-osmotic pumps, the animals were anesthetized using isoflurane and decapitated with a small animal guillotine (Kent Scientific Corporation; Torrington, CT). After removal of both the skin and the top of the cranium, the intact brain was extricated and blocked to isolate the tissue directly rostral to the optic chiasm and caudal to the median eminence which was then placed in a petri dish filled with RIPA lysis buffer (0.24% trizma base, 0.877% sodium chloride, 1% nonidet P-40, 0.5% sodium-deoxycholate, 1% 100mM EDTA, 0.1% SDS, 1% phosphate inhibitor, 0.5 % protease inhibitor, 1% phenylmethanesulfonylfluoride, pH 7.5). Using an Olympus

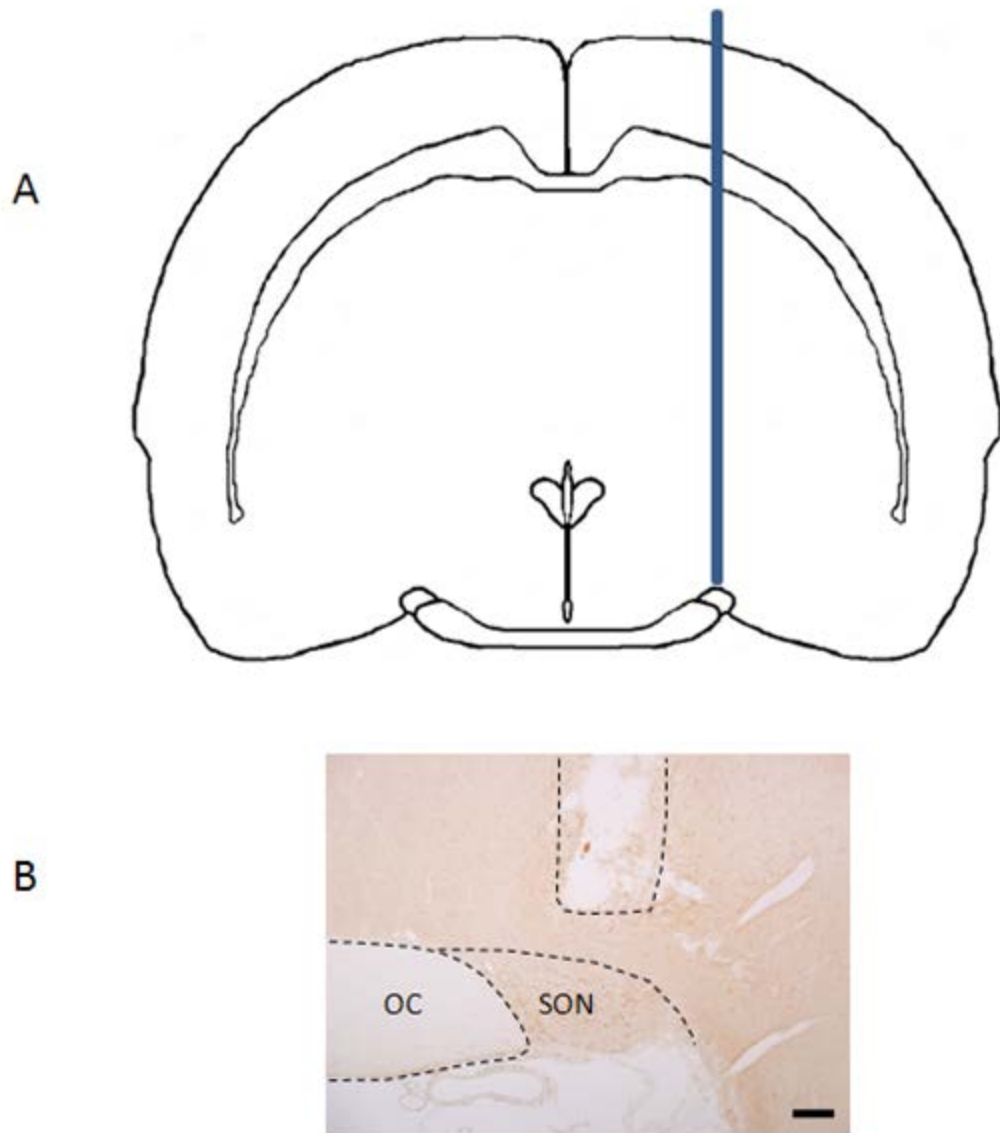


Figure 3. Stereotaxic Placement of Mini-Osmotic Pump Cannula. A) Diagram demonstrating the placement of the cannula (the blue cylinder) directly above the supraoptic nucleus. B) Cannula placement was confirmed by immunohistochemistry. The cannula tract, represented by the dotted line is seen dorsal to the labeled supraoptic nucleus. The scale bar equal 100  $\mu\text{m}$ .

stereomicroscope, the visible meninges were removed and the tissue was further dissected leaving two small regions containing the SONs which were then placed into labeled centrifuge tubes containing RIPA lysis buffer. The tissues were then sonicated (Misonix; Famingdale, NY) and centrifuged at 10,000 x g for 10

minutes after which the supernatant was transferred to a new centrifuge tube. The protein concentration was calculated using a BCA standard protein kit (Thermo Scientific; Rockford, IL) and the supernatant was stored at -80°C.

### Primary Astrocyte Cultures

#### *Astrocyte Collection*

To maintain a sterile environment, all possible steps were performed within a cell-culture hood (Nuaire Biological Safety Cabinets; Plymouth, MN). A minimum of 3 postnatal day two (P2) rat pups born at the Biomedical Research Facility were utilized per cell culture preparation using a modification of the protocol first described by Ken D. McCarthy and Jean DeVellis (1980). The rat pups were sprayed with 70% EtOH and the body was removed with a large sterilized scissors. The skin was then removed from the dorsal side of the head from neck to snout followed by the removal of the skull in the same manner using a sterile small curved-tip scissors. After removal of the skull the brain was carefully extracted, keeping the cerebellum attached, and placed into a petri dish containing sterile cold Calcium/Magnesium Free buffer (CMF; 20 mM HEPES, 1 mM sodium pyruvate, 4.2 mM sodium bicarbonate, 3 mg/ml bovine albumin serum, 10% 10X HBSS, pH 7.3). Using a fine tipped forceps and tweezers, the meninges and visible blood vessels were removed followed by the division of the brain into two hemispheres. The midbrain was removed along with the diencephalon leaving the two cortices in the appearance of a small bowl. Any remaining blood vessels were carefully removed and the resulting cortices were transferred to a second petri dish containing sterile CMF. The remaining pups



were prepared in the same manner. All cortices were then finely chopped using a sterile one-sided razor and transferred to a sterile centrifuge tube along with the CMF. The cortical tissue was triturated slowly with a 10 ml pipette then placed in the pre-warmed water bath (37° C) for ten minutes with careful agitation every two minutes. Next, the tube was centrifuged at room temperature for 5 minutes at 1500 rpm. After careful removal of the supernatant, two to four mls of Dulbecco's Modified Eagle Media/F12 (DMEM/F12, Gibco, Grand Island, NY; 10 mM HEPES, 0.5 mM sodium pyruvate, 14.4 mM sodium bicarbonate, 10% pen step, 10% fungizone, pH 7.4) with 15% fetal bovine serum (FBS, Gibco) was added and the pellet was dislodged by means of trituration with sterile flame-constricted siliconized glass pipettes of varying diameters while avoiding frothing of the cells. This process created a homogenous mixture of the 15% FBS/DMEM/F12 and cortical cells. The volume was then increased with additional 15% FBS/DMEM/F12 to accommodate the prepared flasks. The homogenous mixture was then divided into T-25 cell culture flasks (Corning polystyrene tissue culture flasks) that had been coated in 0.1 mg/ml Poly-L-Lysine (PLL, Sigma) and equilibrated in the cell culture incubator at 37° C/5.0% CO<sub>2</sub> (VWR). The ratio of pups to T-25 flask is 1:1.5. The volume of each flask was then brought to 5 ml with 15% FBS/ DMEM/F12 and placed in the cell culture incubator. After 24 hours each flask was washed twice using a volume equivalent to one third the original with warm DMED/F12 serum free, feed with warm 10% FBS/DMEM/F12, and placed in the incubator. The previous step is repeated every third day until the cells reached approximately 80% confluence.

### *Purification and Splitting of the Cells*

All washes and trypsin incubations performed used one third of the total feeding volume; 24-well plate (0.5 ml total volume per well), T-25 (5 ml total volume), T-75 (15 ml total volume), T-175 (35 ml total volume). Once cells reached 80% confluence, the cultures were purified to remove oligodendrocytes, macrophages, and type II astrocytes. Before purification, the cells were washed three times with warm DMEM/F12 followed by a feeding of 10% FBS/DMEM/F12 and allowed to equilibrate in the cell culture incubator for one hour. After equilibration, the flask caps were tightly sealed and the flasks taped together. Next the flasks were vacuum sealed in two separate plastic bags and the bagged flasks were taped securely to the base of a warmed shaking incubator. The shaking incubator was set at 37° C and 250 rotations per minute (rpm) for at least 18 hours. After shaking the flasks, the supernatant was removed and the adhered cells were washed three times with warm CMF to remove the 10% FBS/DMEM/F12. 1x trypsin in CMF was then used to release the astrocytes from the culture flasks. Once the cells released, FBS was added at a 1:1 ratio to the trypsin in each flask, neutralizing the trypsin. The mixture of trypsin, FBS, and cells was then collected in sterile centrifuge tubes and centrifuged at 1500 rpm for five minutes at room temperature. The supernatant was discarded and the cell pellet re-suspended in two-four mL 10% FBS/DMEM/F12. The cell pellet was broken up by means of trituration with sterile flame-constricted siliconized glass pipettes of decreasing tip diameters while avoiding frothing of the cells. The cell slurry volume was increased to accommodate one T-75 PLL coated flask to each

of the original T-25 culture flasks allowing for a re-plating at a one-third of the original density. Each T-75 flasks was filled with 15 mL of the cell slurry, loosely capped and placed in the incubator for 48 hours. At this time the purification steps were repeated resulting in a  $\geq 98\%$  primary astrocyte culture. After trituration of the cells, a cell count was done using a Bright-Line hemacytometer (Hausser Scientific; Horsham, PA). The cell count enabled the proper cell number plating for the chosen experiments.

#### Astrocyte Application

##### *Coverslip Application*

Prior to astrocyte application to the 12 mm diameter coverslips, (Carolina Biological Supply, thickness of 0.13-0.17mm) were washed twice in 100% EtOH and exposed to germicidal UV light in the culture hood for 15 minutes while in a third EtOH wash. The EtOH was removed and the coverslips were rinsed 3 times with sterile water followed by 0.1mg/ml PLL incubation overnight at 4°C in a closed petri-dish. After removal of the PLL, the coverslips were washed 3 times in sterile water to remove any remaining PLL and transferred into the wells of a sterile 24-well plate and placed into the culture incubator for equilibration. Cells were prepared as previously stated at a concentration of 20 cells per micro-liter (500 astrocytes per well) in 10% FBS/DMEM/F12 and administered into the 24-well plate with coverslips and returned to in the culture incubator. The cells were washed with DMEM/F12 and fed with 10% FBS/DMEM/F12 every third day.

### *Cell Culture Flask Application*

Astrocytes were seeded at a concentration of 200 cells per microliter in 10% FBS/DMEM/F12 into PLL treated T-25, T-75 or T-175 cell culture flasks. The flasks were washed 2 times using DMEM/F12 and fed 10% FBS/DMEM/F12 every third day until the astrocytes were at least 80% confluent. Upon reaching confluence, the flasks were washed 2 times with CMF followed by a DMEM/F12 wash and were subject to treatment.

### *Astrocyte Treatment*

For all methods of astrocyte application unless otherwise noted, once confluence reached  $\geq 80\%$ , the cells were washed 2 times with CMF followed by a DMEM/F12 rinse removing any dead/non-adhered cells and residual FBS. The cells were then subject to treatment; DMEM/F12 (control), 25 ng/ml rat recombinant ciliary neurotrophic factor (rrCNTF; Sigma) or 25ng/ml reverse sequence CNTF (rsCNTF; JW reverse, NeoGroup, Cambridge MA) in DMEM/F12 at various time points.

### *Coverslip Treatment and Fixation*

Astrocytes adhered to coverslips were treated for 10, 20, 30, 60 or 90 minutes with rrCNTF and the corresponding timed controls. Following treatment, the cells were once again washed 2 times in CMF and allowed to sit in paraformaldehyde-lysine-periodate extra fixative (PLP extra; 3.2% paraformaldehyde, 2.2% lysine-HCL, 0.33% sodium-meta-periodate) at room temperature for at least 30 minutes. After removal of the PLP extra, the

coverslips were rinsed three times for a minimum of 20 minutes with phosphate buffered saline (PBS; .02 M phosphate buffer, 8.5% sodium chloride).

#### Cell Culture Flask Treatment and Collection

##### *Astrocyte Culture Homogenates*

Astrocytes were grown up in either T-25 or T-75 culture flasks and treated for 24, 48 or 72 hours with rrCNTF and the corresponding control. Following treatment, the flasks were washed 2 times with CMF and then incubated in a 1X trypsin for 5 minutes. FBS was added at a 1:1 ratio with the 1X trypsin, neutralizing its effects. Keeping each flask as a separate experiment, the astrocyte/trypsin/FBS mixture was transferred to sterile conical tubes and centrifuged for 5 minutes at 1500 rpm at room temperature. The conical tubes were then aspirated leaving the cell pellet which was then washed with 10 ml sterile cold PBS using sterile flame-constricted siliconized glass pipettes with small openings and centrifuged for 5 minutes, 1500 rpm, at room temperature. The conical tube was aspirated again and the pellet was washed in the same manner using 1.5 ml of cold PBS. After breaking up and washing the astrocyte cell pellet, the PBS/astrocyte mixture was transferred to a 2 ml centrifuge tube and centrifuged for 5 minutes at 3000 rpm and 4° C. The supernatant was then aspirated and 100-750 microliters of RIPA lysis buffer was added followed by ultrasonication (Misonic, Farmingdale, NY). The samples were then centrifuged for 15 minutes at 14,000 rpm at 4° C. The supernatant was then transferred to a pre-labeled tube and protein levels were measured using a Thermo Scientific BCA protein assay kit (Rockford, IL).

### *Astrocyte Nuclear Extraction*

Nuclear extraction was performed using a kit from Chemicon International (Millipore; Billerica, MA) with several modifications. Astrocytes were grown in T-75 or T-175 culture flasks and were treated for 0.5, 1, 3, 24, 48, or 72-hours with rrCNTF, rsCNTF or the corresponding aCSF control. Astrocytes used at the 24, 48, and 72-hour time points were treated in a DMEM/F12 phenol red free media for supernatant analytical purposes. Upon completion of the treatment, the supernatant was removed; discarded at the 0.5, 1, and 3-hour time points, the 24, 48 and 72-hour time points were aliquoted and stored at -80° C. The flasks were then washed 2 times with sterile PBS and incubated in a 1X trypsin/PBS solution until the cells released. Keeping all flasks as separate experiments, the astrocyte/trypsin mixture was then transferred to conical tubes. The flasks were then rinsed with 2/3 the total volume using ice cold sterile PBS, and the rinses were transferred to the appropriate conical tubes. The conical tubes were then centrifuged for 5 minutes at 300 g and 4° C. After aspirating the conical tubes, the cell pellets were washed in 10 ml of ice cold PBS using sterile small diameter flame-constricted siliconized glass pipettes and centrifuged for 5 minutes, 300 g, 4° C. This aspiration, wash and centrifugation was repeated 2 more times with the third wash having a volume of 1.5 ml and transfer of astrocyte/PBS to a 2 ml centrifuge tube before centrifugation. After the third centrifugation, the astrocyte cell pellets were measured by comparison to a known amount of water in a separate centrifuge tube; the pellet size was used as the standard for the amount of buffers to be added. 1X cytoplasmic lysis buffer (0.5mM dithiothreitol,

.1% protease inhibitor cocktail) was added to each pellet at 5 times the pellet size. The pellets were resuspended by inversion and incubated on ice for 15 minutes and centrifuged at 5 minutes, 300 g, 4° C. The tubes were then aspirated and 2 times the pellet volume of cytoplasmic lysis buffer was added. The pellet was then triturated at least 5 times using sterile 27 gauge needles and syringes and centrifuged for 20 minutes, 8000 g, 4° C. The supernatant containing the cytosolic portion of the astrocytes was collected and set on ice for later protein analysis. Nuclear extraction buffer (0.5mM Dithiothreitol, .1% protease inhibitor cocktail) was added to the remaining pellet at a volume equivalent to the pellet size and triturated 5 times with sterile 27 gauge needles and syringes resulting in a homogenized lysate. The samples were placed on ice on a slow rotating shaker at 4° C for 1 hour. Next the samples containing the nuclear portion of the astrocytes were centrifuged for 5 minutes, 14000 g, at 4° C and placed on ice with the cytosolic portion during protein analysis. All cytosolic and nuclear samples protein levels were analyzed using a Thermo Scientific BCA protein assay kit (Rockford, IL). Samples were stored at -80°C.

#### *Supernatant Collection*

Supernatants from the astrocyte culture flasks were transferred to 50 ml conical tubes, centrifuged for 5 minutes, 1500 rpm, at room temperature and placed in a -80° C freezer. Supernatants for which a known amount of protein was needed (from nuclear extraction 24, 48, and 72 hour samples) were thawed and a 3 ml sample was taken for dialysis. Using hydrated Slide-A-Lyzer Dialysis Cassettes (Thermo Scientific, Rockford, IL) with a 7 kDA molecular weight cut

off, samples were dialyzed in 600 ml of 2.0 M Tris (Sigma) buffer, pH 7.4 overnight at 4° C on a rotating shaker with 1 buffer change. Samples were removed from the cassettes and protein levels were measured using a Bradford Standard (Bio Rad; Hercules, CA) microassay for microtiter plates procedure.

#### *Astrocyte Ribonucleic Acid Collection*

Ribonucleic acid (RNA) from astrocytes was collected using an RNeasy Mini Kit from Qiagen (Valencia, CA) with several modifications to the Purification of Total RNA from Animal Cells Using Spin Technology protocol. Astrocytes were grown up in T-75 or T-175 cell culture flasks and upon reaching confluence were treated for 6, 12, or 24 hours with rrCNTF and the appropriate timed control. At the conclusion of treatment, the supernatant was removed, aliquoted and stored at -80°C. The cells were then washed with sterile PBS, removing any remnants of the treatment along with any dead or non-adhered cells. The astrocytes were detached using a 1X trypsin in PBS and 10% FBS/DMEM/F12 was added at a 1:1 ration to neutralize the trypsin. Keeping each flask as a separate experiment, the astrocyte/trypsin/media mixture was transferred to 50 ml conical tubes. Using sterile flame-constricted siliconized glass pipettes of small diameter, cell pellets were disrupted and a cell count was performed using a Bright-Line hemacytometer (Hausser Scientific; Horsham, PA), the mixture was then centrifuged at 300 g for 5 minutes at room temperature. After aspiration of the remaining supernatant, buffer RLT was added and the cell slurry then transferred to a 2 ml RNase free centrifuge tube with the cell pellet; 350 ul for  $< 5 \times 10^6$  and 600 ul for  $5 \times 10^6 - 1 \times 10^7$ . The cell pellet was then homogenized with the lysate



using a 20-gauge needle and syringe by triturating the sample 5-10 times. A volume equivalent to the buffer RLT of 70% EtOH was added to the samples and mixed by pipetting. 700 ul of the samples were transferred to an RNeasy spin column, placed in 2 ml collection tubes and centrifuged for 15 seconds at 10,000 rpm. The flow-through was discarded and any leftover samples were transferred to the spin columns, centrifuged, and flow-through was discarded. To remove any genomic DNA contaminants, a DNase digestion was performed at this time using an RNase-Free DNase Set (Qiagen; Valencia, CA). 350 ul of buffer RW1 was added to the spin columns and centrifuged for 15 seconds, 10,000 rpm, and the flow-through was discarded. 80 ul of DNase I incubation mix (10 ul DNase stock and 70 ul buffer RDD) was applied directly to the spin column membranes and allowed to incubate at room temperature for 15 minutes with the tubes closed. 350 ul of buffer RW1 was added to the spin columns and centrifuged for 15 seconds, 10,000 rpm, and the flow-through was discarded. The spin column membranes were then washed using 500 ul of buffer RPE and then centrifuging the spin columns for 15 seconds at 10,000 rpm and discarding the flow-through. This membrane wash step was repeated with a 2 minute, 10,000 rpm centrifugation and the collection tube was discarded and replaced with a new 2 ml collection tube. The spin column was then centrifuged for 1 minute at 14,000 rpm to remove any possible buffer RPE carryover and the collection tube was then replaced with a 1.5 ml collection tube with a lid. 50 ul of RNase-free water was added directly to the membrane and allowed to incubate at room temperature for 10 minutes after which the spin columns were centrifuged for 1

minute at 10,000 rpm. 50 ul more of RNase-free water was added to the membrane and centrifuged, resulting in roughly 100 ul of flow-through containing the astrocyte RNA. The RNA was then cleaned-up further and concentrated using a RNeasy MinElute Cleanup Kit (Qiagen; Valencia, CA). 350 ul of Buffer RLT and 250 ul of 100% EtOH was added to the RNA flow-through and mixed by pipetting. The samples were then transferred to RNeasy MinElute spin columns and centrifuged for 15 seconds, 10,000 rpm and the flow-through and collection tubes were discarded. Using a new 2 ml collection tube, 500 ul of buffer RPE was added to each spin column and they were centrifuged for 15 seconds, 10,000 rpm and the flow-through was discarded. Next, 500 ul of 80% EtOH was added to the spin columns and they were centrifuged for 2 minutes at 10,000 rpm and the collection tubes containing the flow through were discarded. After placing the spin columns in new 2 ml collection tubes, they were centrifuged with the lids open for 5 minutes at 14,000 rpm after which the collection tubes and flow-through were discarded. The spin columns were then placed in 1.5 ml lidded collection tubes and 20 ul of RNase-free water was added directly to the spin column membranes and was then eluted with the RNA by a 1 minute, 14,000 rpm centrifugation. To calculate RNA purity and concentration, each sample was run in triplicates at a dilution of 1:100 with 10 mM Tris-HCL, pH 8.0 which was also used as a background standard. Using a Spectra Max Plus 384 (Molecular Devices; Sunnyvale, CA) dual readings were taken at 260nm and 280nm. After finding the average absorbance of each sample at both absorbencies, purity was calculated by  $A_{260}/A_{280}$ ; pure RNA will have an evaluation of 1.9-2.1. Each  $A_{260}$

absorbance is equivalent to 40 µg/ml of RNA, for this reason the concentration of RNA was calculated with the following formula,  $(40 \text{ ug/ml}) \times (A_{260}) \times (\text{dilution factor})$ , for which the dilution factor was 100.

#### Dosage Inhibition of Astrocyte Cultures

Astrocytes were prepared as previously described. Upon reaching confluency the cultures were incubated with fresh DMEM plus 10% FBS for 24 hours. After removal of the supernatant, the cultures were washed two times with CMF followed by one wash of DMEM no FBS. Cultures were then introduced to the inhibitor in DMEM no FBS for 1 hour. After the conclusion of the hour, cultures were spiked with rrCNTF for 30 minutes prior to analysis or collection.

#### XTT Cell Viability-Dosage Inhibition

Astrocytes were seeded in a 96 well plate treated with PLL at 5000 cells per well and allowed to mature for 4 days. After four days, the cells were treated as previously mentioned in dosage inhibition of astrocyte cultures. XTT (Biotium; Fremont, CA) was prepared by mixing 5 ml of XTT solution and 25 µl activation reagent. 25 µl of XTT mixture was added to each well giving a total volume of 100 µl per well. Cell viability was determined every 2-hours over a 12-hour period using a Spectra Max Plus 384 (Molecular Devices; Sunnyvale, CA). Dual readings were taken at 475 nm and 675 nm for nonspecific absorption.

#### Hypothalamic Organotypic Explant Cultures

All steps were performed in either a Purifier Clean Bench (Labconco, Kansas City, MO) or a cell culture hood for sterility purposes. Using a modification of techniques described previously (House, et al., 2009, House, et

al., 2006, House, et al., 1998, Rusnak, et al., 2003, Rusnak, et al., 2002, Vutskits, et al., 1998), 6-day-old Sprague Dawley rat pups were immersed briefly in 70% EtOH, decapitated, the brain carefully removed and placed in chilled Gey's Balanced Salt Solution (Gibco) enhanced with glucose (5 mg/ml; Sigma). The brains were then trimmed to remove exterior cortical material and 350 um coronal sections were obtained using a McIlwain Tissue Chopper (Stoelting, Wood Dale, IL). The coronal sections were then sorted, transferring the sections containing the magnocellular neurosecretory system nuclei to a petri dish containing the Grey's/glucose solution. The sections were then trimmed dorsal to the third ventricle and lateral to the SON under a dissecting microscope (Figure 4). All sections from the same rat pup were transferred on to a single MilliCell-CM filter insert (pore size 0.4 um, 30 mm diameter; Millipore, Bedford, MA) which was placed in a labeled 35X10 mm Petri dish containing 1.2 ml of astrocyte conditioned media (ACM) which was changed every third day for a 7-day experimental period.

#### Astrocyte Conditioned Media for Hypothalamic Organotypic Cultures

Astrocytes were collected as previously described with several modifications. Following the first purification the astrocyte media was changed to a standard culture media consisting of Eagle's Basal Medium with Earle's salts (50%; Gibco), heat inactivated horse serum (25%; Gibco), Hank's Balanced Salt Solution (25%; Gibco), glucose (0.5%; Sigma), penicillin/streptomycin (25 units/ml; Gibco), and glutamine (1.0 mM; Gibco) and cells were split into 10 T-75 PLL treated culture flasks which were divided into 3 groups; one group of 4 and

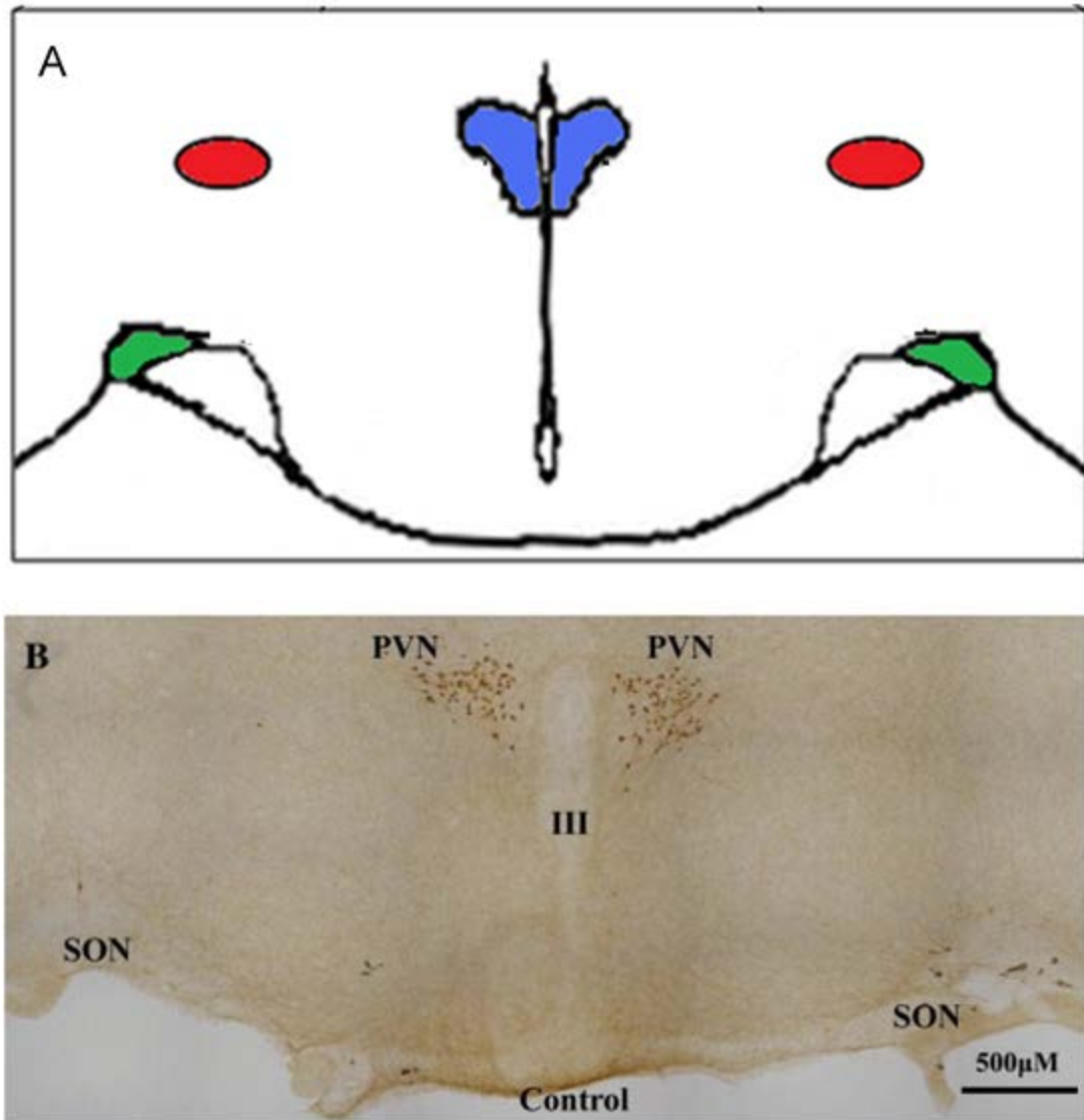


Figure 4. Hypothalamic Organotypic Explant Culture Section.  
 A) Diagram representing the dissected brain sections. The paraventricular nuclei (PVN; blue) surrounding the third ventricle, supraoptic nuclei (SON; green), and accessory nuclei (ACC; red).  
 B) Control treated explant section (Askvig et al. 2013).

two other groups of either 2 or 3 flasks, respectively. Each group was purified, treated and media collected every 2 days for cell consistency and for application to explant cultures. Following the second purification the flasks were fed 24 hours before treatment (roughly 48 hours after seeding). Prior to treatment, each flask

was rinsed 2 times with CMF and one time with media, removing any dead and/or non-adhered cells. Cells were treated for 24 hours, after which the wash steps were repeated and media was added as a standard feed. The media was then collected after 48 hours as the astrocyte conditioned media and applied to the hypothalamic organotypic explant cultures. Treatments consisted of 25 ng/ml rrCNTF, media control, 50  $\mu$ /ml AG490, and 50  $\mu$ m/ml AG490 plus 25 ng.ml rrCNTF. A pretreatment of 50  $\mu$ /ml AG490 was performed for 1 hour directly before application of the 50  $\mu$ /ml AG490 plus 25 ng/ml rrCNTF.

#### Immunocytochemical Examination

All antibodies used for immunocytochemistry are listed in Table 1. All immunocytochemistry was performed on PLP-extra fixed (paraformaldehyde/lysine/periodate fixative) astrocytes. All succeeding incubations were followed by a minimum of three 15 minute washes in PBS. To prevent non-specific staining, the cells were incubated in the appropriate blocking buffer containing 4% normal serum (Jackson ImmunoResearch Laboratories, West Grove, PA) in 1% bovine serum albumin (Sigma) PBS for 1 hour. The primary antibody prepared in the blocking buffer was then administered overnight at 4°C. The cells were then incubated in a biotinylated species-specific secondary antibody at room temperature for 2 hours. For dual staining a second primary antibody was applied and incubated overnight at 4°C. After removal of the second primary antibody, a cocktail containing both an Alexa Fluor streptavidin (Invitrogen) and the appropriate florescent dye-conjugated Affinipure IgG (Jackson ImmunoResearch) were applied for 1 hour at room temperate in

Table 1. Normal Serums, Primary, Secondary and Tertiary Antibodies.

Target	Species	Dilution for ICC	Dilution for Western	Source Company
<i>Normal Serums</i>				
Normal Goat Serum	Goat	1:25	N/A	Jackson Labs
Normal Horse Serum	Horse	1:25	N/A	Jackson Labs
Normal Donkey Serum	Donkey	1:25	N/A	Jackson Labs
<i>Primary Antibodies</i>				
Beta-Actin	Mouse	N/A	1:50,000	AbD Serotec
CNTFR $\alpha$	Mouse	N/ A	1:20,000	BD Pharmingen
CNTFR $\alpha$	Goat	1:20	N/A	R&D Systems
GFAP	Mouse	1:1000	N/A	Sigma
GFAP	Goat	1:1000	1:10,000	Sigma
gp130	Rabbit	N/A	1:5000	Santa Cruz
LIFR $\beta$	Rabbit	N/A	1:5000	Santa Cruz
Ox-42/CD11b	Mouse	1:2000	N/A	AbD Serotec
pJAK 2	Rabbit	N/A	1:2000	AbCam
pSTAT3 Ser 727	Rabbit	N/A	1:2000	Cell Signaling
pSTAT3 Tyr 705	Rabbit	1:300	1:2000	Cell Signaling
tJAK2	Rabbit	N/A	1:2000	Cell Signaling
Tomato Lectin	N/A	1:1000	N/A	Vector
tSTAT3	Rabbit	1:500	1:6000	Cell Signaling
<i>Secondary Antibodies</i>				
Goat Anti-Rabbit	Goat	1:500	N/A	Vector
Horse Anti-Mouse	Horse	1:500	N/A	Vector
Fluorescein Anti Mouse	Donkey	1:500	N/A	Jackson Labs
Fluorescein Anti-Goat	Donkey	1:500	N/A	Jackson Labs
Fluorescein Anti-Mouse	Goat	1:500	N/A/	Jackson Labs
Fluorescein Anti-Rabbit	Goat	1:500	N/A	Jackson Labs
Donkey Anti-Rabbit-HRP	Donkey	N/A	1:200,000	Santa Cruz
Goat Anti-Rabbit-HRP	Goat	N/A	1:200,000	Santa Cruz
Rabbit Anti-Goat-HRP	Rabbit	N/A	1:200,000	Santa Cruz
<i>Tertiary Antibodies</i>				
Streptavidin Alexa 488	N/A	1:1000	N/A	Invitrogen
Streptavidin Alexa 594	N/A	1:1000	N/A	Invitrogen

the absence of light. The coverslips were then removed from the 24-well plate and placed upside down on pre-labeled gelatin subbed slides with the mounting medium for fluorescence Vectasheild plus dapi (Vector) and sealed with a clear fingernail polish. Cells were viewed using either an Olympus BX-51 fluorescent

microscope with DP-71 color camera utilizing Cell Sens capture software (Olympus; Center Valley, PA) or an Olympus Fluoview 300 Confocal Microscope mounted on an Olympus IX70 inverted microscope.

The specificity of each primary antibody was verified by either a primary antibody omission, a biotinylated secondary antibody omission, or by utilizing a direct fluorochrom in place of the biotinylated secondary antibody while maintaining all other steps. The later of the controls also verified that the secondary antibodies biotinylated or flurochrome recognition was due to the primary antibody and not specific recognition of a cellular type.

#### Rat Cytokine Antibody Array

Cytokine expression was detected using the Rat Cytokine Antibody Arrays 1 and 2 (RayBiotech, Inc., Norcross, GA). Using the provided eight-well trays, each membrane was incubated at room temperature in 2 ml of the 1X blocking buffer for 30 minutes. After removal of the blocking buffer, 1 ml of supernatant from 72-hour control/non-treated or 25 ng/ml rrCNTF treated astrocytes was applied to the membranes and allowed to incubate on a rotating shaker at 4°C for 24 hours after which the supernatant was collected and stored at -80° C. Excess supernatant was removed with four 10 minute rinses in wash buffer followed for two 10 minute rinses in wash buffer II. All, but the primary omission membranes, were allowed to incubate in 1 ml of primary antibody on a rotating shaker at room temperature for 2.5 hours followed by three 10 minute rinses in wash buffer I and three 10 minute rinses in wash buffer II. Next, 2 ml of the horseradish peroxidase-conjugated streptavidin was added to each and allowed to incubate



at room temperature on a rotating shaker for 2 hours followed by three 10-minute rinses in wash buffer I and buffer II. Finally, 500  $\mu$ l of a 1:1 dilution of detection buffer C and detection buffer D was applied to each membrane for 2 minutes at room temperature after which each membrane was gently blotted with a kimwipe and sandwiched between two pieces of plastic and taped in place in a Kodak BioMax Cassette (Kodak; Rochester, NY) for x-ray film exposure. The film (Kodak) was exposed for 30 seconds and developed using an AGFA CP1000 film processor (DMS Health Group; Fargo, ND).

#### Enzyme-Linked Immunosorbent Assay

Reagents for all the enzyme-linked immunosorbent assays (ELISA) were allowed to warm to room temperature before use. A standard dilution series was prepared as indicated by each kit; three-fold dilution for lipopolysaccharide induced C-X-C chemokines (LIX, RayBiotech) and Fractalkine (RayBiotech) and a two-fold dilution for vascular endothelial growth factor (VEGF R&D Systems; Minneapolis MN) and interleukin-6 (IL-6, R&D Systems). For the VEGF ELISA a total volume of 50  $\mu$ l of supernatant was added with an unknown amount of protein. For analysis performed using a known amount of protein (cytosolic and supernatant for all ELISAs and SON tissue homogenates for IL-6), samples were diluted using the appropriate diluent; Calibrator Diluent RD5-16 for IL-6, Calibrator Diluent RD5-18 for VEGF, Assay Diluent B for LIX and fractalkine. For each R&D Systems ELISA, the appropriate assay diluent (50  $\mu$ l each RD1-41 for VEGF and RD1-54 for IL-6, 100  $\mu$ l RD1-43 for FGF basic) was pipetted into each well of the microplate using a multichannel pipetter followed by an equal volume

of standard, control or sample which were run in either duplicates or triplicates, covered with an adhesive cover strip and incubated for 2 hours at room temperature. The VEGF plate was placed on a horizontal orbital shaker (IKA Works, Inc; Wilmington, NC) set at 450 rpm, the IL-6 ELISAs were left stationary on the laboratory bench. 100  $\mu$ l of standard, control or sample were added to the RayBiotech ELISA microplates in either duplicates or triplicates, covered with adhesive cover strips, and placed on the orbital shaker for 2.5 hours at room temperature. Next the microplate wells were washed using a squirt bottle with the provided wash buffers diluted with Milli-Q water; 4 washes each for the RayBiotech plates and 5 washes each for the R&D Systems plates. To ensure complete removal of each wash, the microplates were inverted and blotted on filter paper. To the R&D Systems microplates, 100  $\mu$ l conjugate rat VEGF or rat IL-6 basic conjugate were added to each well, covered with a new adhesive cover strip and incubated at room temperature; VEGF plate for 1 hour on the orbital shaker and 2 hours on the bench for the IL-6 ELISA. To the RayBiotech plates, 100  $\mu$ L of the provided biotinylated antibody that had been diluted with Diluent B, was added, the microplates were covered and allowed to incubate on the bench for 1 hour. At this point the prior specified wash steps were repeated. To the R&D Systems microplates, a 1:1 mixture of the color reagents A and B were added making the Substrate Solution, which was added to each well; 100  $\mu$ l for both the VEGF and IL-6 ELISAs. A stationary incubation at room temperature for 30 minutes in the absence of light was followed by the addition of Stop Solution; 100  $\mu$ l to both VEGF and IL-6. To the RayBiotech microplates a 100  $\mu$ l

of the provided Streptavidin solution was added and incubated on the orbital shaker for 45 minutes while covered with an adhesive cover strip followed by the appropriate wash steps. Next 100  $\mu$ l of a TMB One-Step Substrate Reagent was administered to each RayBiotech microplate well; the plates were covered with cover strips, placed on the orbital shaker and protected from light for 30 minutes after which 50  $\mu$ l of stop solution was added to each well. The optical density of each plate was analyzed immediately following the addition of the stop solution using a Bio-Rad Model 680 Microplate reader with Microplate Manager 5.2 software (Bio-Rad) at 450 with a wavelength correction of 570 nm and plotted using a parameter logistic (4-PL) standard curve. Protein concentrations were generated in pg/ml.

#### Western Blot Examination

All samples (nuclear extractions and tissue homogenates) for Western blot analysis were allowed to thaw on ice along with sample buffer (5%  $\beta$ -mercaptoethanol, 2X stock sodium dodecyl sulfate) and molecular weight markers (Fermentas Life Sciences; Glen Burnie, MD). The determined amount of protein was diluted 1:1 with the sample buffer and placed on a 95 $^{\circ}$  C preheated AccuBlock Digital Dry Bath (Labnet International; Woodbridge, NJ) for 2-5 minutes depending on volume and centrifuged for one minute at 10,000 rpm. After positioning the 10 well, 12% precise protein gel (Thermo Scientific) in a SDS-PAGE apparatus (Bio-Rad) the wells were loaded with the samples or 5  $\mu$ l of the molecular weight marker, any unused well was loaded with 5  $\mu$ l of sample buffer ensuring that samples proceed straight during the one hour, 90 volts, room

temperature run in running buffer (12.1% Trizma base, 23.8 % HEPES, 1% sodium dodecyl sulfate). Following a 1-minute methanol equilibration of the Immuno-Blot PVDF membrane (Bio-Rad), the PVDF membrane, gel, filter paper, and fiber pads were incubated in chilled transfer buffer (10% methanol, 1.42% glycine, 0.3% Trizma base) for at least 20 minutes. Following incubation, the fiber pad, filter paper, gel, PVDF membrane, filter paper, fiber pad transfer sandwich was incased in the transfer cassette and inserted into the transfer apparatus. The transfer apparatus was then placed in a large tupperware container, surrounded by ice, then filled with chilled transfer buffer and transferred for two hours at 70 volts while stirring. Upon completion of the transfer, the membrane was removed, submerged in the transfer buffer, and trimmed.

All antibodies utilized are listed on Table 1. For antibodies obtained from Cell Signaling, all washes used either Tris buffered saline (TBS; 2.42% Trizma base, 8% NaCl, pH 7.6) or 0.05% Tween-20 TBS (TBS-Tween) and the blocking buffer was 5% bovine serum albumin (BSA; Sigma) TBS-Tween. Washes for all other antibodies used PBS and 0.05% Tween-20 PBS (PBS-Tween) and the blocking buffers was 5% nonfat dry milk PBS-Tween. All washes and incubations were performed on a rocking platform (VWR) unless otherwise noted. Following trimming, the membranes were washed twice in TBS/PBS followed by two washes in TBS-Tween/PBS-Tween each roughly 10 minutes and subsequently placed in blocking buffer for one hour followed by the primary antibody overnight at 4° C. After removal of the primary antibody, the membranes were washed for two hours in TBS-Tween/PBS-Tween with at least three wash changes and the

secondary biotinylated-HRP antibody conjugate was administered at room temperature for two hours followed by a two-hour wash in TBS/PBS with at least three wash changes. Each membrane was lightly blotted and placed inverted on 1000  $\mu$ l of the 1:1 mixture of the SuperSignal West Femto kit's (Thermo Scientific) solutions for 5 minutes then sandwiched in a transparent cover sheet and taped in place within the Kodak BioMax Cassette for x-ray film exposure. Exposure time for each membrane varied by the strength of the primary antibody, and the film was developed with the AGFA CP1000 film processor. Following exposure, the membranes were stripped using a recipe from Abcam (15% glycine, 1% sodium dodecyl sulfate, 10% Tween-20, pH 2.2) two times for 7 minutes each and all steps following the trimming of the membrane were repeated.

#### Real Time Reverse Transcriptase Polymerase Chain Reaction Arrays

Ribonucleic acid (RNA) levels were measured using real time reverse transcriptase polymerase chain reaction (RT<sup>2</sup> PCR) following the manufacturer's protocol (Qiagen RT<sup>2</sup> Profiler PCR Array Handbook). Using the RT<sup>2</sup> First Strand Kit (Qiagen) 1  $\mu$ g of RNA was added to 2  $\mu$ l of Buffer GE and the volume was brought up to 10  $\mu$ l with RNase-free water in a RNase-free 2 ml capped tube and incubate for 5 minute at 42° C on a heat block then immediately placed on ice for one minute eliminating any remaining DNA. 10  $\mu$ l of the reverse-transcription mix (4% 5x Buffer BC3, 1% Control P2, 2% RE3 Reverse Transcriptase Mix) was added and mixed by pipetting. The mixture was incubated at 42° C for 15 minutes, then 5 minutes at 95°C resulting in the RNA conversion to

complementary deoxyribonucleic acid (cDNA) to which 91  $\mu$ l of RNase-free water was added, mixed by pipetting and placed on ice. The PCR components mix (3.8% cDNA synthesis reaction, 50% 2x RT<sup>2</sup> SYBR Green Mastermix; Qiagen) was prepared in a 15 ml RNase-free conical tube and 25  $\mu$ l aliquots were distributed with a multi-channel pipetter into the RT<sup>2</sup> Profiler PCR array; Rat JAK/STAT Signaling Pathway (PARN-039A), Rat Chemokines & Receptors (PARN-022A), Rat Signal Transduction Pathway Finder (PARN-014A), or Rat Neurotrophin and Receptors (PARN-031A; SABiosciences, a Qiagen company) The array was subsequently capped with the provided strips, centrifuged for one minute and placed in the iCycler iQ5 PCR Thermal Cycler (Bio-Rad) with the attached computer and iQ5 software. The following cycling conditions were used: 1-10-minute cycle at 95<sup>o</sup> C, 40 cycles of 15 seconds at 95<sup>o</sup> C and 1 minute at 60<sup>o</sup> C followed by a default melting curve.

#### Real Time Reverse Transcriptase Polymerase Chain Reaction Primers

Glial fibrillary acidic protein (GFAP) and  $\beta$ -actin RNA levels were measured using RT<sup>2</sup> PCR primers from SABiosciences. Following the RT<sup>2</sup> qPCR Primer Assay Handbook (Qiagen) the samples were prepared in a similar manner as those for the RT<sup>2</sup> Profiler PCR Arrays with the following changes; the PCR components mix (4% cDNA synthesis reaction, 4% RT<sup>2</sup>qPCR Primer Assay, 50% RT<sup>2</sup> SYBR Green Mastermix) was aliquoted into 0.2 ml PCR tubes with attached flat caps (VWR).

## Organotypic Explant Immunohistochemistry

At the conclusion of the 7-day experimental period, the organotypic hypothalamic explants were removed from the ACM, fixed in 4% paraformaldehyde (sigma) in 0.1 M phosphate buffer for 1.5 hours and washed in PBS-Triton (PBS-T; 0.01% triton X-100) for three 10 minute intervals, this wash was repeated before and after all incubations. To prevent any endogenous peroxidase activity and non-specific staining, the explants were placed in a 0.3% H<sub>2</sub>O<sub>2</sub> treatment for 20 minutes and incubated in blocking buffer (10% normal horse serum, 0.3% Triton X-100) for 1 hour. Immediately following the blocking buffer step, the explants were incubated in the primary antibody with monoclonal mouse anti Oxytocin-neurophysin (PS 38, 1:500; a gift from Dr. Harold Gainer) for 36 hours at 4° C on a rotating shaker. Next the explants were incubated in horse anti-mouse biotinylated secondary antibody (1:500; Vector), and subsequently incubated in avidin-biotin complex (ABC; 10 µl/ml in PBS; Vector ABC *Elite* kit) for one hour at room temperature followed by a 0.05% diaminobenzidine (DAB, Sigma) in PBS using the glucose-oxidase method for antibody visualization. Carefully, the hypothalamic organotypic explant slices were removed from the filter inserts and placed on gelatin coated slides for alcohol dehydration followed by a Xylene rinse and coverslipped with Permount (Fisher, Pittsburgh, PA).

## Magnocellular Neuronal Counts

The immunoreactive explant culture slides were coded by a third party and a double-blind count of oxytocinergic neurons was performed using a drawing

table attached to an Olympus BX51 microscope. The neurons were categorized by location of paraventricular nucleus, supraoptic nucleus, or accessory neurons for each slide representing one animal. The mean of the double-blind count was used for the statistical analysis.

## Data Analysis

### *Rat Cytokine Antibody Array Analysis*

The exposed film was photographed using a Kaiser RSI Precision Illuminator (Northern Light) with an attached Scion camera with QICAM software (Q imaging; Surrey, BC, Canada). The digitized film was then analyzed using MCID 7.0 core software (MICD; Cambridge, MA) by collecting the relative optical density (ROD) of each dot. The ROD values were saved as a Microsoft Excel file and imported to the RayBio Rat Cytokine Antibody Array Analysis Tool software (RayBio).

### *Enzyme-Linked Immunosorbent Assay Analysis*

Statistical analysis of the protein was performed using a one-way ANOVA followed by a Dunn's Multiple Comparison Test using GraphPad Prism 5.0 (GraphPad Software; La Jolle, CA) and the results were graphed.

### *Western Blot Analysis*

The Western blot exposed film was digitized using an Epson Perfection V750 PRO (Epson; Long Beach, CA) scanner and Silver Fast (Ai) Launcher (LaserSoft Imaging, Inc.; Sarasote, FL) imaging software. The digitized film was then imported to MCID 7.0 for analysis using the following measurement parameters: relative optical density and density x area. The numerical values



calculated were exported to Microsoft Excel and were normalized with the values given by either total STAT3 or  $\beta$ -actin. The normalized values were analyzed using either a one-way ANOVA with a Tukey post hoc test or a student's t-test on GraphPad Prism 5 with the statistical significance set at  $p \leq 0.05$ . The results were then graphed.

*Real Time Reverse Transcriptase Polymerase Chain  
Reaction Array Analysis*

Following completion of the PCR cycling program, the results were transported from the iQ5 software program and saved as a Microsoft Excel spreadsheet. The spreadsheet was converted to the format laid out by SABiosciences for each standard RT<sup>2</sup> PCR array; the first column indicating well identification and all sequential columns for each array containing the threshold cycles obtained from the iQ5 software placed in line with the appropriate well identification and saved as a xls file. Using the data analysis tool *Web-based software for Cataloged and Custom arrays, RT<sup>2</sup> Profiler PCR Array Data Analysis version 3.5* on the SABiosciences webpage, the Standard RT<sup>2</sup> PCR array was selected and the xls spreadsheet was uploaded. The housekeeping genes (HKG) were selected using the Automatic Selection of HKG Panel, which selects the HKG with the least amount of variance with the maximum amount of variation set at 1.5 cycles. Using the Scatter Plott option, the normalized expression of every gene was compared at a 3-fold regulation cut off.

### *Real Time Reverse Transcriptase Polymerase Chain Reaction Primer Analysis*

The RT<sup>2</sup> qPCR Primer analysis was performed similarly to that of the RT<sup>2</sup> PCR array analysis with the following differences. The Excel spreadsheet was set up with the first column indicating the well identification, the second column indicating the primer gene symbol, and all sequential columns containing the cycle thresholds given by the iQ5 Software program. The Excel spreadsheet was uploaded to the SABiosciences data analysis webpage using the *Single or Multi-Gene qPCR Assays* analysis option. With the absence of housekeeping genes, all other sets were done as indicated in the Real Time Reverse Transcriptase Polymerase Chain Reaction Array Analysis section.

### *Hypothalamic Organotypic Explant Statistical Analysis*

The group mean obtained by the double-blind count was analyzed using Graph Pad Prism Software. The Kolmogorov-Smirnov test indicated that the population was normally distributed allowing parametric statistical analysis to be conducted. Both a one-way ANOVA followed by a Tuckey post hoc test with the statistical significance set at  $p \leq 0.05$  and a Student's t-test was performed and graphed.

## CHAPTER III

### RESULTS

#### Specific Aim I: Determine if CNTF Activates the JAK/STAT Pathway in Astrocytes

##### *Mini-Osmotic Pump Placement and Efficiency*

Correct cannula placement and mean pump out-flow was determined previously by Adam Sudbeck. The placement of the mini-osmotic pump cannula was visually confirmed by DAB immunoreactive staining and found to be in the proper position at an occurrence of 75%. The pump out-flow was calculated to be approximately 68  $\mu$ l based on the remaining volume with an infusion rate of 0.94  $\mu$ l per hour over the 72-hour time period.

##### *CNTF-Induced Activation of Astrocytes*

Activation of astrocytes due to trauma has been shown to elicit a hypertrophic response as well as an increase in the astrocyte specific intermediate filament marker glial fibrillary acidic protein (GFAP). These responses can also be induced by exogenous application of CNTF both in vivo and in vitro (Hudgins & Levison, 1998; Levison, Hudgins, & Crawford, 1998). Our lab confirmed activation within the infused SON by quantifying GFAP protein levels via Western blot analysis (A. Sudbeck, unpublished observation). Figure 5, courtesy of Adam Sudbeck, represents the GFAP protein levels of corresponding

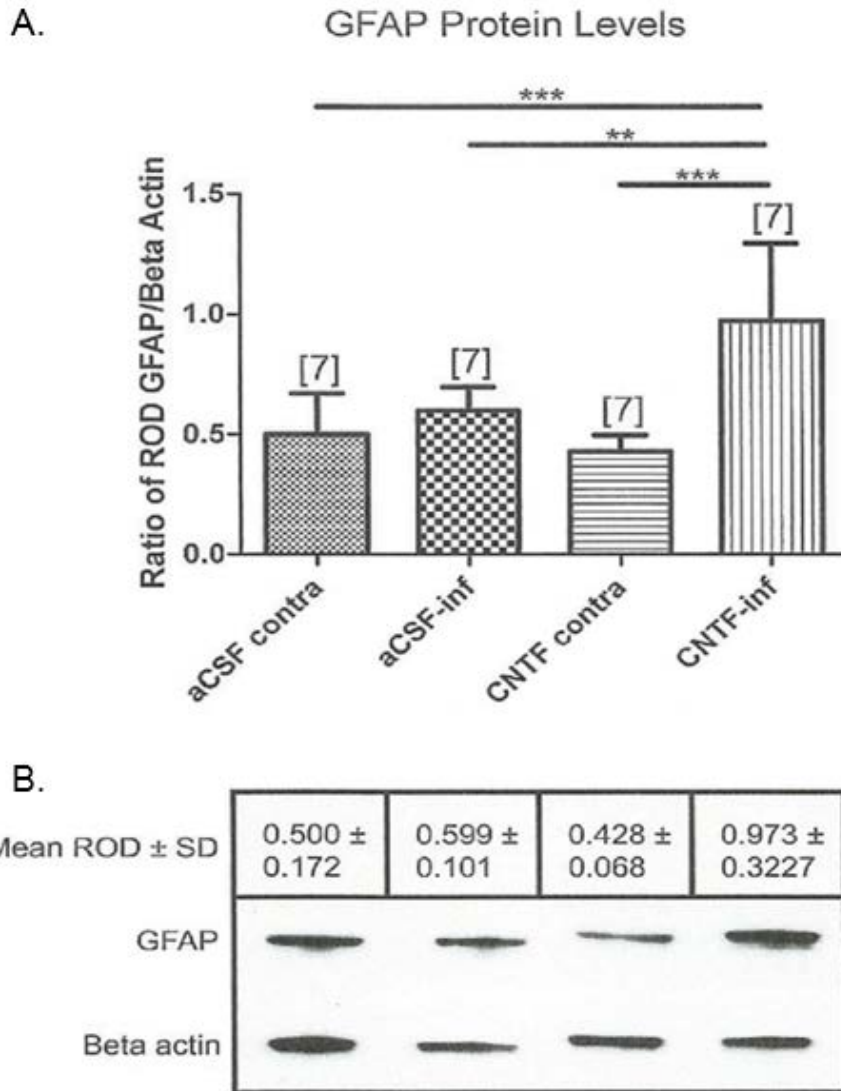


Figure 5. 3 Day 100 ng/ul rrCNTF Infusion Elicits an Increase in GFAP. A) The GFAP Protein ratio for aCSF contralateral (n=7), aCSF infusion (n=7), CNFT contralateral (n=7), and CNTF infusion (n=7) Son analyzed by a one wat ANOVA showed that CNTF-infused SON GFAP protein levels were significantly increased from the CNTF contralateral SON (\*\**p* < 0.0001), aCSF-infused SON (\*\**p* < 0.01) and aCSF-infused contralateral SON (\*\**p* < 0.0001). The Ratio of relative optical density (ROD) ± standard deviation (SD) for each groups are shown in (B). The GFAP (55 kDa) Western blots for the aCSF contralateral, aCSF infusion, CNTF contralateral, and CNTF infusion groups were normalized to beta actin (42 kDa). The Western blot error bars represent the means ± SD. [n]=number of experimental animals. Figure courtesy of Adam Sudbeck, M.S.

SON of seven 3-day CNTF infused animals and seven 3-day artificial cerebral spinal fluid (aCSF) animals. It was determined that the GFAP protein levels of the CNTF-infused SON showed an increase of 62% when compared to the control aCSF-infused SON. Additionally, it was determined that there was a significant increase in GFAP protein levels of the corresponding contralateral SON. The results of a one-way ANOVA of the CNTF-infused SON compared to the contralateral SON demonstrated a significant increase ( $p \leq 0.0001$ ) in GFAP protein levels equivalent to a 127% increase.

#### *Confirmation of Primary Astrocyte Cultures*

Prior to the first purification, a stratification of cell types can be noted within the culture flask. Found adhered to the base of the flask are the astrocytes, suspended directly above the astrocytes are oligodendrocytes and microglia. There is little to no cell interaction between the stratified layers. The purification process results in the disruption of any interaction between the stratified layers allowing for a purer culture following the splitting. The removal of the supernatant and washing steps dislodges any viable oligodendrocytes and microglia. Additionally, astrocytes mitotically divided at a faster rate (McCarthy and de Vellis 1980, Giulian and Baker 1986, Saura, Tusell et al. 2003, Wang, Shi et al. 2012). The ability for astrocytes to proliferate at a quicker rate along with the frequent washing steps allows for preparation of a 95-98% pure primary astrocyte culture.

Throughout the primary astrocyte culture studies, the cultures were subject to cell type confirmation using florescent immunocytochemistry of

prepared cover slips. The presence of astrocytes was confirmed with the astrocyte specific cell marker, GFAP. Culture purity was confirmed by the absence of microglia using microglia cell markers anti-CD11b (OX-42) or Tomato Lectin. As a positive control for microglia staining, both the OX-42 and Tomato Lectin were applied to rat neural lobes. Microglia cells were never observed in the primary astrocyte cultures and according to McCarthy and De Vellis (1980) the removal of oligodendrocytes in the purification and splitting process inhibits the reappearance of the cell type, for this reason no immunocytochemistry was performed testing the presence of oligodendrocytes in the final cultures. The immunocytochemistry analysis of the cultures indicated a  $\geq 98\%$  purity of primary astrocytes.

#### *Tripartite CNTF Receptor Complex Presence on Primary Astrocytes*

As first indicated by Samuel Davis and Neil Stahl (1993; 1993), the ability of CNTF to initiate a cellular reaction is dependent on the presence and availability of three components; LIFR- $\beta$ , gp130, and CNTFR- $\alpha$ . Our lab (Askvig, Leiphon, et al., 2012) previously showed that all aspects of the tripartite CNTF receptor complex is present within the rat supraoptic nucleus. To confirm the presence of CNTFR $\alpha$  on primary astrocytes, dual fluorescent immunocytochemical labeling was performed (Figure 6 A-C). The presence of gp130 and LIFR- $\beta$  was confirmed using Western blot analysis (Figure 6 D). The tissue homogenates of two non-treated primary astrocyte culture with a protein concentrations of 100  $\mu\text{g}$  each were loaded and compared to a 10-day post unilateral lesion SON tissue

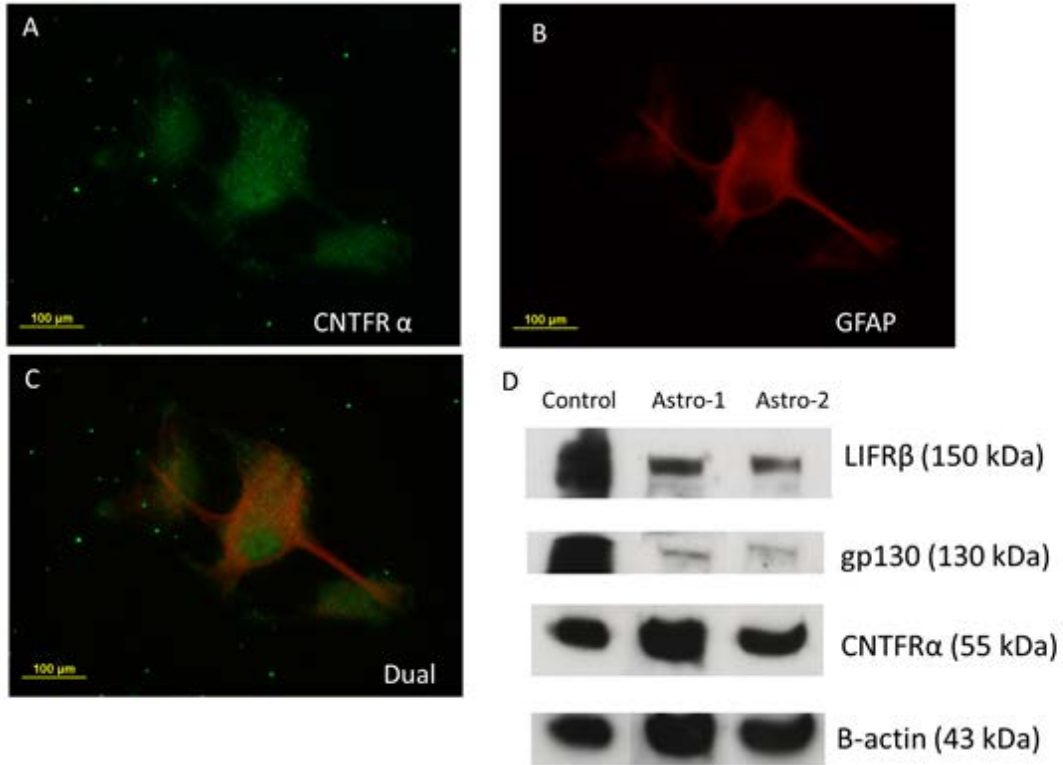


Figure 6. Expression of the Tripartite Receptor Complex in Primary Astrocyte Cell Cultures. Dual fluorescent immunocytochemistry demonstrates astrocyte reactivity for A.) CNTFR $\alpha$  (green) and B.) GFAP (red) the cell marker for astrocytes. C.) The merged image reveals the co-localization of the CNTFR $\alpha$  with the GFAP positive astrocytes. D.) Western blot analysis of two primary cortical rat astrocyte culture tissue homogenates demonstrates that LIFR $\beta$  (150 kDa), gp130 (130 kDa), and CNTFR $\alpha$  (55kDa) are present in total protein concentrations of 100  $\mu$ g when comparing to a control 10-day post unilateral lesion SON tissue homogenate at a 70  $\mu$ g protein concentration. Scale bar equals 100  $\mu$ m.

homogenate control known to have all of the receptor components loaded at a 70  $\mu$ g concentration (Figure 6 D).

Analysis of the blots revealed the presence of LIFR- $\beta$  (150 kDa), gp130 (130 kDa), and CNTFR $\alpha$  (55kDa) in the astrocytes cultures. Neither primary omission nor preabsorption controls (not shown) showed cellular

immunoreactivity with immunocytochemistry. This data, the 10-day lesion tissue homogenate and immunocytochemistry controls, provided evidence that cultured astrocytes maintain the tripartite CNTF receptor complex outside of the in vivo environment. The presence of all receptor components on the cultured primary astrocytes indicates the ability of CNTF to bind and initiate a cellular reaction.

#### *Activation of Primary Astrocyte by Exogenous CNTF Exposure*

##### *Phosphorylation of STAT*

To confirm the presences and activation of CNTF within the cultured astrocytes, fluorescent immunocytochemical staining was performed. Total STAT (tSTAT) was observed in astrocyte control cultures (Figure 7). A time dependent application of exogenous rat recombinant CNTF (rrCNTF) at a concentration of 25 ng/ml in DMEM was applied prior to fixation of the cultured coverslips with PLP extra (Figure 8). Cultures were exposed to rrCNTF for 10 minutes (Figure 8. A), 20 minutes (Figure 8.B), 30 minutes (Figure 8.C), 60 minutes (Figure 8.D) and 90 minutes (Figure 8. E). To insure that activation was influenced by the exogenous rrCNTF, an omission of rrCNTF was performed as a control for 90 minutes (Figure 8. F). Following fixation, the cultured coverslips were dual-stained for GFAP (Texas-Red) and phospho-STAT (pSTAT; FITC). The immunocytochemistry shows co localization of pSTAT with the GFAP in all but the rrCNTF omission control. Omission and preabsorption controls for both antibodies was also performed and resulted in the complete absence of immunoreactivity within the cultured astrocytes.



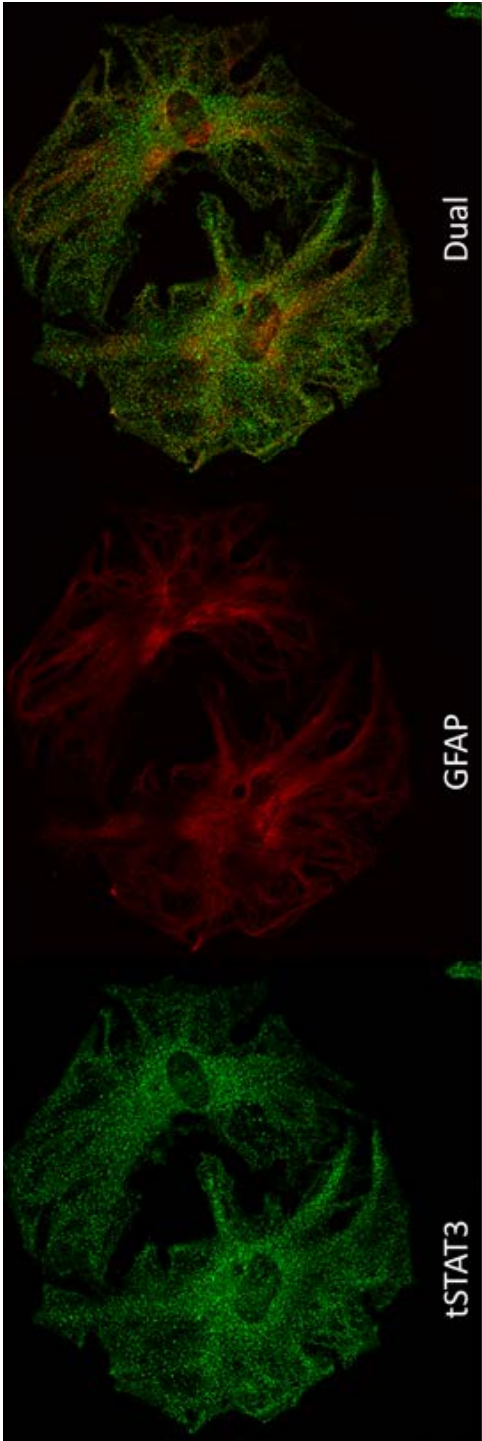


Figure 7. Immunofluorescent Staining for tSTAT3 and GFAP. Staining indicates co-localization of the tSTAT3 protein and GFAP in cultured astrocytes.

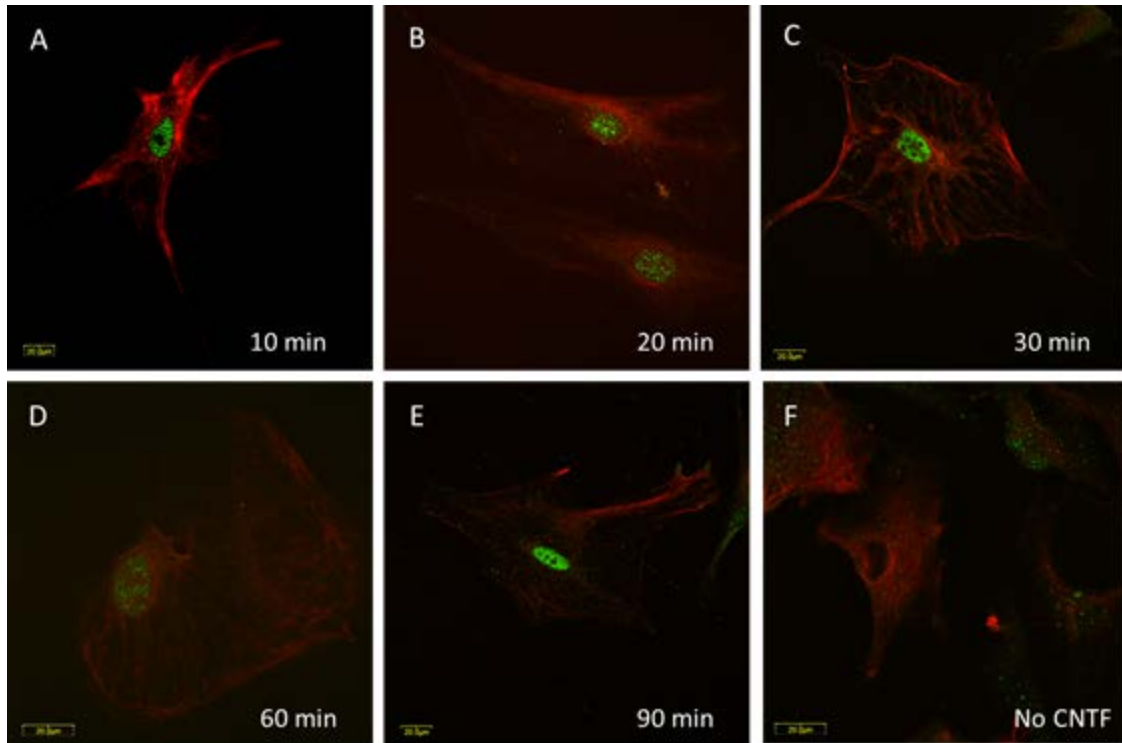


Figure 8. Time-Dependent Activation of Cultured Astrocytes by 25 ng/ml Exogenous rrCNTF in DMEM. Dual fluorescent co-localization staining for GFAP (Texas-red) and pSTAT (FITC).  
 A) 10-minute exposure,  
 B) 20-minute exposure,  
 C) 30-minute exposure,  
 D) 60-minute exposure,  
 E) 90-minute exposure,  
 F) 90-minute rrCNTF omission control. Figures A-E demonstrate activation of pSTAT by the application of rrCNTF which is not present in the omission control.

### *Translocation of pSTAT3*

The activation of the cultured astrocytes was also determined by observation of the translocation of pSTAT 3 tyrosine 705 by means of western blot analysis on nuclear extraction components. Second passage (P2) astrocytes were allowed to reach confluency in 25 cm<sup>3</sup> flasks after which they were washed and the media replaced with DMEM without FBS for 24 hours. Following the

FBS-free incubation period, the cultures were subject to a 10 minute (Figure 10 A), 20 minute (Figure 10 B), 30-minute (Figure 9.) or 40 minute (Figure 10 C) incubation with 25 ng/ml rrCNTF in 0.1% BSA in PBS. The nuclear extraction procedure was performed on the cultures providing a cytoplasmic lysis buffer (CLB) portion containing the cytosolic contents and a nuclear extraction buffer (NEB) portion containing the nuclear contents. rrCNTF omission control cultures were performed in parallel with the rrCNTF treated cultures.

Following the nuclear extraction protocol, the protein levels were calculated and western blot analysis of was performed on a protein concentration of 20 µg of each treated and control samples. The blots were then stained for pSTAT3 tyrosine 705 (tyr 705) and normalized using total STAT3 (tSTAT3) (Figure 9 A and B). Figure 9 C shows a western blot stained for pSTAT3 Serine 727 (ser 727) in addition tSTAT and pSTAT3 tyr 705.

#### Specific Aim II: Determine the Functional Response of Astrocytes to CNTF Cytokine Release Analysis

Since it was demonstrated that there is activation of the Jak/STAT pathway following exposure to exogenous rrCNTF in cultured astrocytes it was our working hypothesis that the astrocytes were releasing potential neuroprotective factors in response to exogenous rrCNTF.

#### *Cytokine Membrane Arrays*

Upon reaching confluency in 6 well plates, the astrocytes were rinsed five times with DMEM in the absence of FBS and subject to a spike application of 25 ng/ml rrCNTF in DMEM FBS free for an incubation of 72 hours. The control received a spike of 0.1% BSA in PBS. The supernatant from three treated and one control

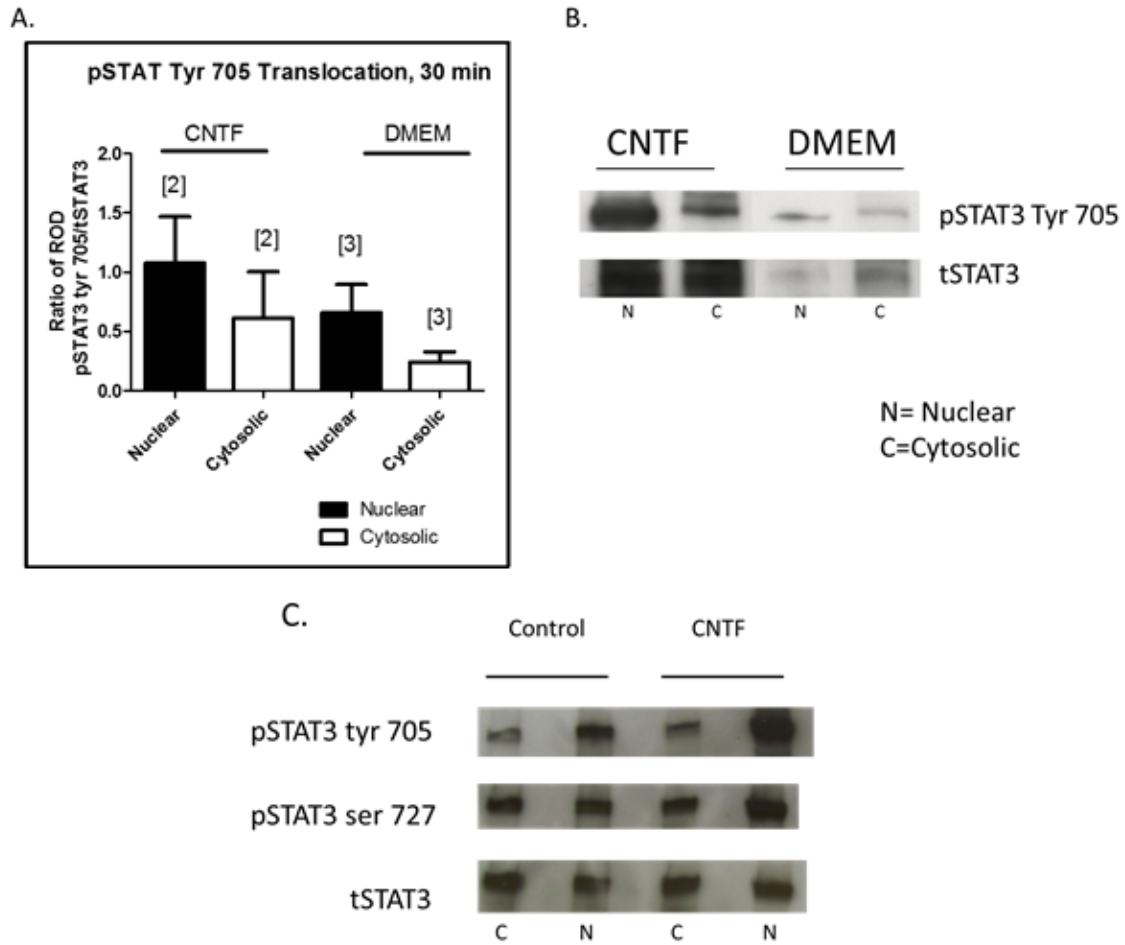


Figure 9. Translocation of pSTAT3 following 30-minute, 25 ng/ml rrCNTF incubation followed by isolation of cytoplasmic and nuclear extractions.

A) Calculation of the ratio of optical density (ROD) of pSTAT3 tyr 705 normalized by tSTAT. Nuclear extraction samples of cultures treated by rrCNTF (n=2) had a ROD of 1.08. Cytosolic extraction samples of treated cultures (n=2) had a ROD of 0.61. Nuclear extraction samples of control nontreated (n=3) had a ROD of 0.65. Cytosolic extraction samples of control nontreated (n=3) had a ROD of 0.28.

B) The ROD of the pSTAT3 tyr 705 (86 kDa) Western blot was normalized to that of tSTAT (79 kDa).

C) Western blot analysis of pSTAT3 tyr 705, pSTAT3 serine 727, and tSTAT3 determined that the phosphorylation of tyrosine 705 was translocating factor to proceed with. The error bars are the mean  $\pm$  SD. [n] = number of experimental samples.

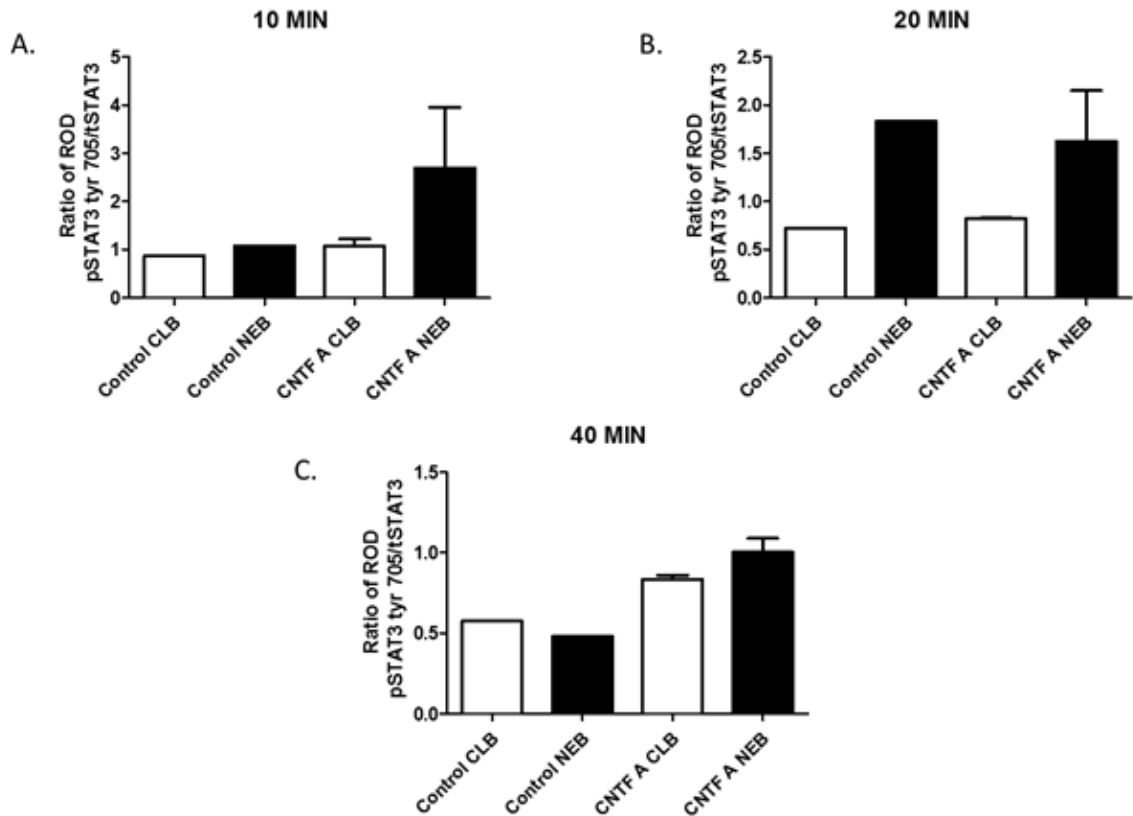


Figure 10. Preliminary Western Blot Analysis of Nuclear Extraction. Time dependent exogenous incubation in 25 ng/ml rrCNTF showing translocation of pSTAT3 tyr 705 and their parallel controls. All samples were normalized using tSTAT3. A.) 10-minute incubation control cytosolic lysis buffer (CLB; n = 1), control nuclear extraction buffer (NEB; n = 1), treated CLB (n=2), treated NEB (n = 2). B.) 20-minute incubation control CLB (n = 1), control NEB (n = 1), treated CLB (n = 2), and treated NEB (n = 2). C.) 40-minute incubation control CLB (n = 1), control NEB (n = 1), treated CLB (n = 2), and treated NED (n = 2). The error bars are the mean  $\pm$  SD. [n] = number of experimental samples.

culture was collected and used following the procedure described by the manufacturer (RayBiotech) (Figure 11). The membranes were allowed to incubate in the supernatant for 24 hours to allow for optimal adhesion to the arrays.

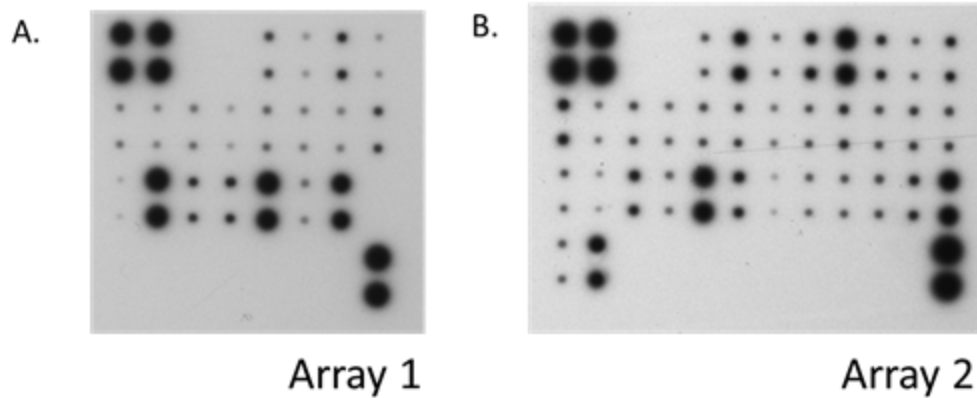


Figure 11. RayBio Cytokine Membrane Arrays.  
 A.) Array one analyzes 19 cytokines.  
 B.) Array 2 analyzes 34 cytokines.

Analysis of the array's provided a comparison of the increase in cytokine levels by performing a normalization with background subtraction (Tables 2 and 3). The average of each cytokine from treated samples was used to calculate the percent change in comparison to the average control samples (Table 4). From the top six cytokines of interest three were investigated further by means of ELISA; IL-6 (22.22% increase), fractalkine (66.67% increase) and VEGF (36.54% increase).

### *ELISA*

In the course of development, astrocytes release both vascular endothelial growth factor (VEGF) and interleukin-6 (IL-6) among other factors during the vasculogenesis of the CNS. (Bernal & Peterson, 2011). These levels decrease following birth (Fee et al., 2000; Gerwins et al., 2000; Saito et al., 2011; Seghezzi et al., 1998). Additionally, fractalkine, IL-6 and VEGF release have been shown to increase in neurodegenerative disorders such as amyotrophic lateral sclerosis (H. Sun et al., 2013).

Table 2. RayBio Cytokine Antibody Array 1. Analysis of supernatants from three 72-hour 25ng/ml rrCNTF treated astrocyte cultures and one 72-hour control astrocyte culture. Normalization with background subtraction. Preliminary cytokines of interest shown in red.

RayBio® Cytokine Antibody Arrays — Rat Cytokine Antibody Array 1					
Normalization (with Background Subtraction)					
	.1%BSA	72 hr rrCNTF a	72 hr rrCNTF b	72 hr rrCNTF c	Average
POS	0.8	0.8	0.8	0.8	0.8
NEG	0	0	0	0	0
CINC-2	0.27	0.34	0.29	0.29	0.3
CINC-3	0.05	0.09	0.07	0.05	0.07
CNTF	0.07	0.49	0.66	0.56	0.57
Fractaline	0.04	0.11	0.06	0.08	0.08
GM-CSF	0.15	0.15	0.17	0.15	0.16
IFN-gamma	0.12	0.12	0.14	0.12	0.12
IL1-alpha	0.21	0.2	0.19	0.18	0.18
IL-1bate	0.09	0.08	0.11	0.07	0.08
IL-4	0.21	0.23	0.28	0.2	0.24
IL-6	0.13	0.17	0.2	0.15	0.17
IL-10	0.14	0.17	0.2	0.15	0.17
LIX	0.22	0.37	0.31	0.41	0.36
Leptin	0.04	0.05	0.05	0.04	0.04
MCP-1	0.74	0.81	0.77	0.82	0.8
MIP-3a	0.29	0.43	0.39	0.5	0.44
beta-NGF	0.5	0.45	0.63	0.54	0.54
TIMP-1	0.75	0.74	0.81	0.75	0.76
TNF-alpha	0.16	0.18	0.22	0.15	0.18
VEGF	0.49	0.81	0.58	0.71	0.7

Table 3. RayBio Cytokine Antibody Array 2. Analysis of supernatants from three 72-hour 25ng/ml rrCNTF treated astrocyte cultures and one 72-hour control cytokines of interest shown in red.

RayBio® Cytokine Antibody Arrays - Rat Cytokine Antibody Array System 2					
Normalization (with Background Subtraction)					
	.1%BSA	72 hr rrCNTF a	72 hr rrCNTF b	72 hr rrCNTF c	Average
POS	1	1	1	1	1
NEG	0.01	0	0	0	0
Activin A	0.44	0	0.38	0.41	0.39
Agrin	0.83	0	0.8	0.75	0.77
B7-2/CD86	0.29	0	0.31	0.32	0.31
beta-NGF	0.74	0	0.76	0.78	0.77
CINC-1	0.84	0	0.92	0.79	0.85
CINC-2alpha	0.41	0	0.61	0.41	0.51
CINC-3	0.23	0	0.38	0.17	0.27
CNTF	0.24	0	0.66	0.61	0.63
Fas Ligand	0.66	0	0.67	0.61	0.64
Fractalkine	0.14	0	0.25	0.16	0.21
GM-CSF	0.44	0	0.39	0.37	0.38
ICAM-1	0.3	0	0.3	0.33	0.31
IFN-gamma	0.38	0	0.39	0.41	0.4
IL-1alpha	0.4	0	0.45	0.53	0.49
IL-1beta	0.2	0	0.22	0.21	0.21
IL-1 R6	0.32	0	0.4	0.35	0.37
IL-2	0.51	0	0.55	0.57	0.56
IL-4	0.34	0	0.39	0.38	0.39
IL-6	0.4	0	0.5	0.45	0.48
IL-10	0.36	0	0.43	0.36	0.39
IL-13	0.26	0	0.34	0.22	0.28
Leptin	0.14	0	0.14	0.13	0.13
LIX	0.54	0	0.64	0.42	0.53
L-Selectin	0.32	0	0.28	0.32	0.3
MCP-1	0.86	0	0.83	0.82	0.82
MIP-3alpha	0.53	0	0.71	0.64	0.67
MMP-8	0.1	0	0.12	0.19	0.15
PDGF-AA	0.27	0	0.32	0.21	0.26
Prolactin R	0.3	0	0.36	0.3	0.33
RAGE	0.36	0	0.42	0.35	0.38
Thymus Chemokine-1	0.57	0	0.6	0.55	0.57
TIMP-1	0.89	0	0.96	0.82	0.89
TNF-alpha	0.25	0	0.33	0.22	0.27
VEGF	0.54	0	0.81	0.62	0.71



Table 4. Percent Change in Cytokine Release. Averages from both array 1 and array 2 were calculated from tables 2 and 3 and used in determining overall all percent change in cytokine release. The cytokines of interest were determined by having a minimum percent change of 18%.

Cytokine	Array 1 Control	Array 2 Control	Control Average	Array 1 Treatment Average	Array 2 Treatment Average	Treatment Average	% Δ
<b>CINC-3</b>	0.05	0.23	<b>0.014</b>	0.07	0.27	<b>0.17</b>	<b>21.43%</b>
<b>Fractalkine</b>	0.04	0.14	<b>0.09</b>	0.08	0.21	<b>0.15</b>	<b>66.67%</b>
<b>IL-6</b>	0.13	0.4	<b>0.27</b>	0.17	0.48	<b>0.33</b>	<b>22.22%</b>
<b>LIX</b>	0.22	0.54	<b>0.38</b>	0.36	0.53	<b>0.45</b>	<b>18.42%</b>
<b>MIP-3-α</b>	0.29	0.53	<b>0.41</b>	0.44	0.67	<b>0.56</b>	<b>36.59%</b>
<b>MMP-8</b>		0.1	<b>0.1</b>		0.15	<b>0.15</b>	<b>50.00%</b>
<b>VEGF</b>	0.49	0.54	<b>0.52</b>	0.7	0.71	<b>0.71</b>	<b>36.54%</b>

#### *ELISA-VEGF*

R&D Systems VEGF ELISAs were loaded using 50 µl of supernatant with unknown amounts of protein. A total of 36 samples were analyzed, twelve in each of the following time dependent groups; 24 hours, 48 hours, or 72 hours. All treated cultures (six from each group) received a dosage spike of 25 ng/ml rrCNTF in DMEM and the parallel controls (six of each group) received a 0.1% BSA in PBS spike in DMEM. A non-parametric t-test analysis of the optical densities indicating pg/ml showed no significance (Figure 12).

#### *ELISA- IL-6*

The IL-6 ELISA analysis comprised 27 samples of which each plate well was loaded with 2.0 µg of supernatant. Nine samples were used to analyze the potential release of IL-6 from cultured astrocytes following 24 hours (n = 2),

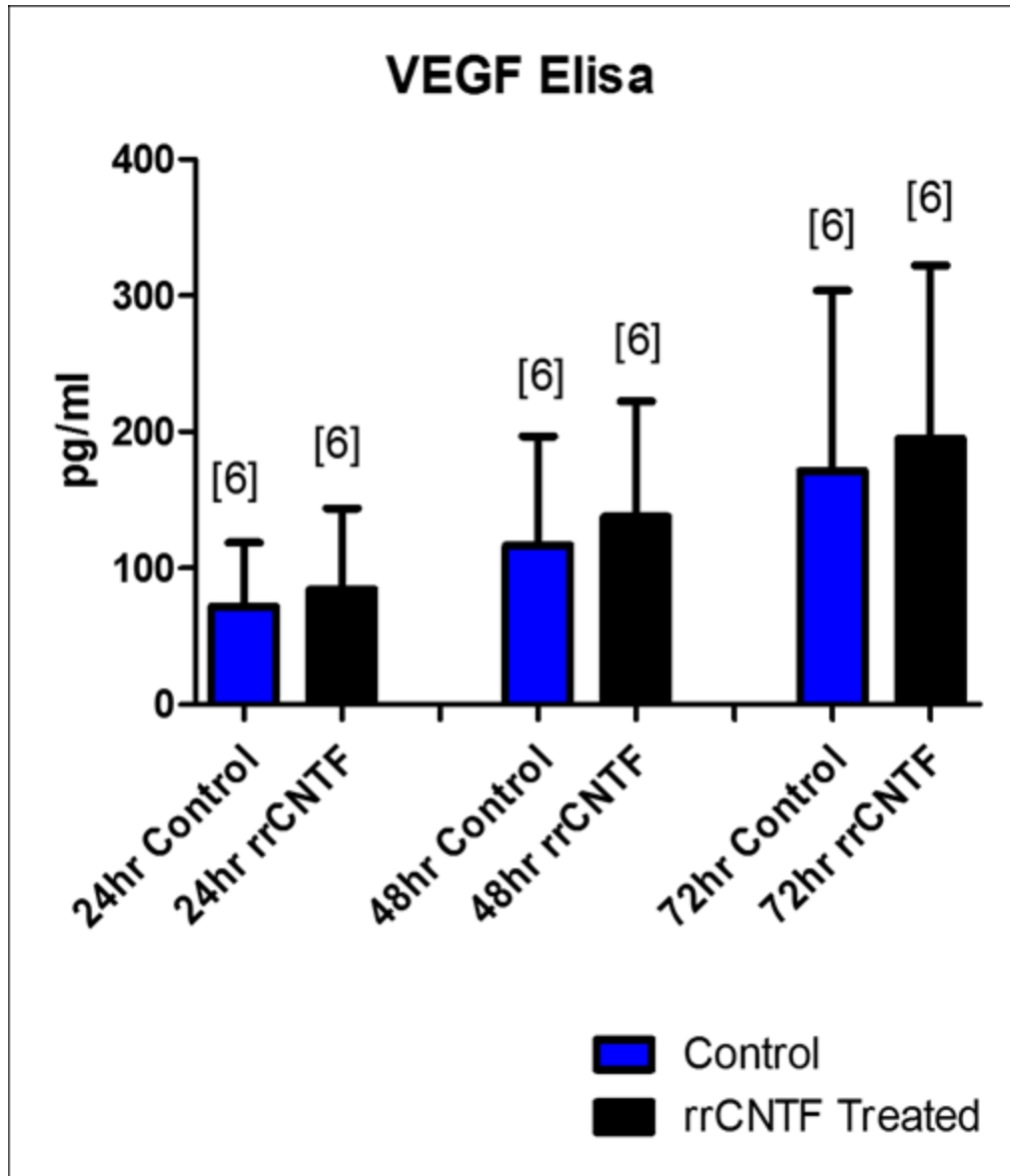


Figure 12. R&D Systems VEGF ELISA. Comparison of VEGF release by astrocytes into the supernatant following a time dependent incubation in 25 ng/ml rrCNTF (black bars) and their parallel controls (blue bars) that received 0.1% BSA in PBS. A non-parametric t-test showed no significance. The error bars are the mean  $\pm$  SD. [n] = number of samples.

48 hours (n = 4), or 72 hours (n = 3) of exposure to a spike of 25 ng/ml rrCNTF in DMEM. Another nine samples were analyzed following either 24 hours (n = 3), 48 hours (n = 3), or 72 hours (n = 3) exposure to a spike of 25 ng/ml reverse sequence CNTF (rsCNTF) in DMEM. The remaining nine samples were controls that received a spike 0.1% BSA in PBS to the DMEM for either 24 hours (n = 4), 48 hours (n = 2), or 72 hours (n = 3). As seen in Figure 13, a one-way ANOVA of the optical densities showed significance only for the 72 hour incubations. The 0.1% BSA in PBS (DMEM; blue bar) showed significance towards both of the treated samples rrCNTF and rsCNTF with p values of 0.0225 and 0.0115 respectively. A two-way ANOVA indicates a very significant column factor with a p value of 0.0021.

#### *ELISA- Fractalkine*

The RayBio Fractalkine ELISA was performed on 20 samples using 2.25 µg of the cytosolic portion from nuclear extraction of cultured astrocytes and supernatant from astrocyte cultures. The cytosolic samples included cultures that were subject to a 24 hour exposure of either a spike of 25 ng/ml rrCNTF into the DMEM (n = 3), a spike of 25 ng/ml rsCNTF into the DMEM (n = 2), or a control spike of 0.1% BSA in PBS added to the DMEM (n = 3). The supernate samples received the same treatments with the all with an [n] of 3 (Figure 14). Analysis of the optical densities showed no significance by one-way ANOVA or t-test.

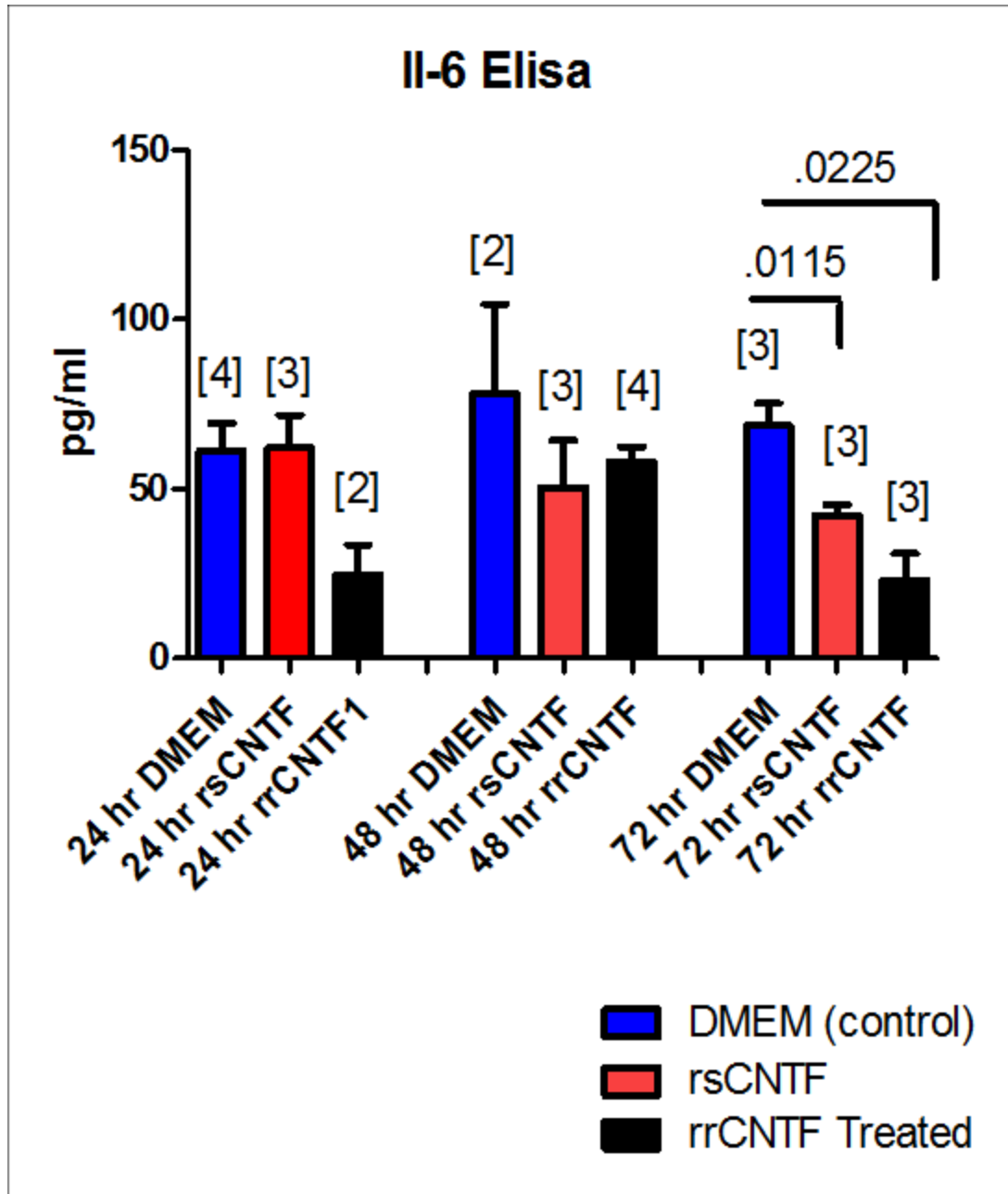


Figure 13. R&D Systems IL-6 ELISA. Comparison of IL-6 release by astrocytes into the supernatant following a time dependent incubation in 25 ng/ml rrCNTF (black bars), 25 ng/ml rsCNTF (red bars), and their parallel controls (DMEM, blue bars) that received 0.1% BSA in PBS. A one-way ANOVA showed significance only at the 72 incubation analysis between the DMEM control and the rsCNTF with a  $p = 0.0115$  and a significance between the DMEM control and the rrCNTF with a  $p = 0.0225$ . A two-way ANOVA showed column factor very significant with a  $p$  value of 0.0021. The error bars are the mean  $\pm$ SD. [n] = number of samples.

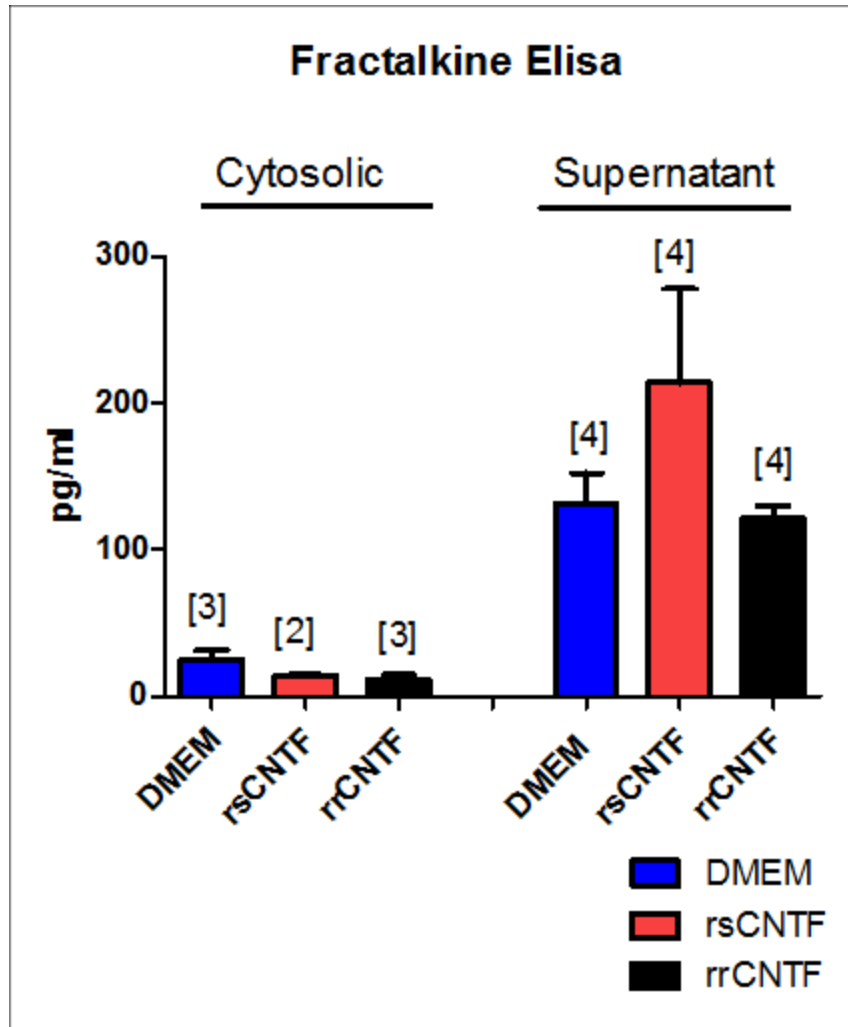


Figure 14. RayBio Fractalkine ELISA. Comparison of Fractalkine release by astrocytes into the supernatant to the cytosolic portion of cultured astrocytes following a time dependent incubation in 25 ng/ml rrCNTF (black bars), 25 ng/ml rsCNTF (red bars), and their parallel controls (DMEM, blue bars) that received 0.1% BSA in PBS. No significance was determined. The error bars are the mean  $\pm$  SD. [n] = number of samples.

### *Elisa-LIX*

The RayBiotech LIX elisa was performed using samples from 24 hour exposure to 25 ng/ml rrCNTF, 25 ng/ml rsCNTF, or 0.1% BSA in PBS. These samples were loaded at 2.25 µg total protein and included both supernatants and cytosolic portions from nuclear extraction. No optical densities were detectable by the microplate reader.

### *PCR*

Gene expression was analysed by of RT<sup>2</sup> PCR. The mRNA was measured in fold increases. The GFAP mRNA was measured and normilized to beta-actin following a time-dependent expose to 25 ng/ml rrCNTF. The parallel non-treated control samples were used as a zero standard base line to observe the changes induced by the rrCNTF exposure. Figure 15 shows the fold increase for 6 hour (n = 4), 12 hour (n = 4), 24 hour (n = 8), and 72 hour (n = 2) exposure times. Analysis showed no statistical signifiance by either a one-way ANOVA or a non-parametric t-test.

SABiosciences RT<sup>2</sup> PCR plates were used to analyse mRNA changes following time dependent exposure to either 25 ng/ml or 100 ng/ml rrCNTF. Four plate kits where utilized; Rat Neurotrophin and Receptors (PARN-031), Rat Signal Signal Transduction Pathway Finder (PARN-014), Rat Chemokines & Receptors (PARN-022), and Rat JAK/STAT Signaling Pathway (PARN-039). The cut off to determine significance in mRNA up-regulation or down-regulation was 3-fold.

## RT<sup>2</sup>PCR Primers

### GFAP mRNA

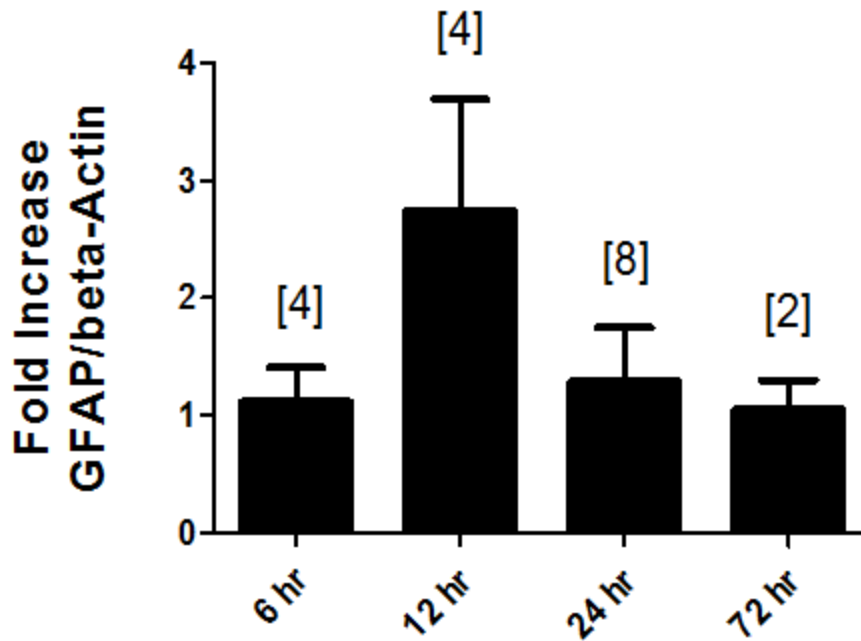


Figure 15. Real-Time Reverse Transcriptase Polymerase Chain Reaction Primers. mRNA fold increases of GFAP following a 6, 12, 24 and 72 hour 25 ng/ml rrCNTF treatment of astrocyte cultures with DMEM timed controls equaling zero. Both a one-way ANOVA and non-parametric t-test analysis demonstrates no statistical significance in GFAP mRNA levels following rrCNTF exposure. The error bars are the mean  $\pm$ SD. [n] = number of samples run in duplicate.

### *Rat Neurotrophin and Receptors*

After 6 hours of exposure to 25 ng/ml rrCNTF only one neurotrophin was seen to meet the set parameters; IL-1 $\beta$  showed a 6.9588 fold increase in mRNA expression (Figure 16). Twelve hour exposure to the same levels of rrCNTF showed a upregulation of 5 neurotrophins and a down regulation of one

## 6 hour Neurotrophins and Receptors (PARN-031)

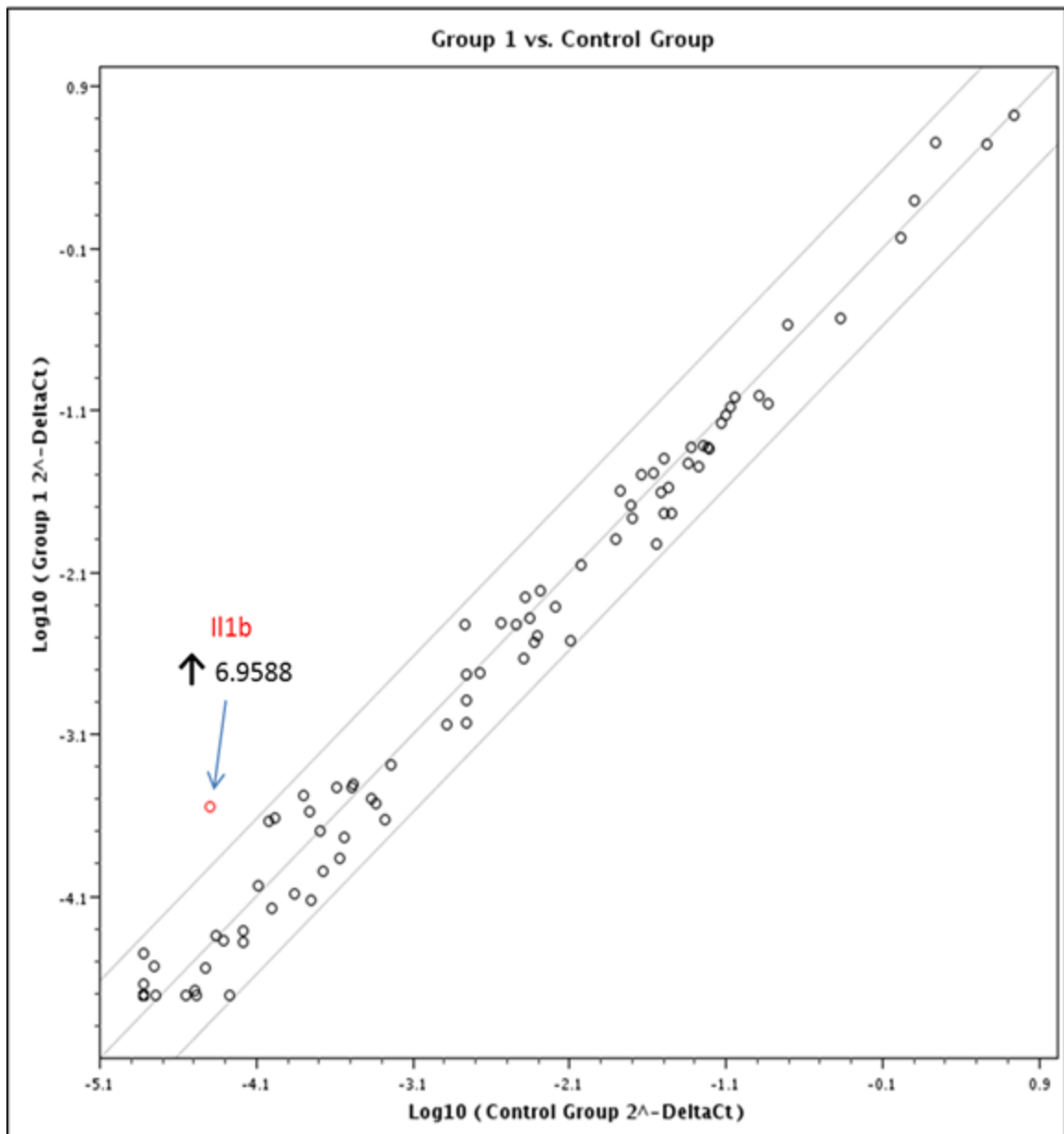


Figure 16. 6 Hour Neurotrophins and Receptors RT<sup>2</sup> PCR. 6 hour exposure to 25 ng/ml rrCNTF. Upregulation of IL-1 $\beta$  mRNA with a 6.9588 fold increase. Fold alteration cut off set at 3.



receptor (Figure 17). Those with fold increase mRNA were Cerebellin 1 precursor (Cbln1; 4.1718), glial cell derived neurotrophic factor (GDNF; 3.4643), interleukin-6 (IL-6 ; 6.6903), transforming growth factor alpha (TGFA; 5.7408) and VGF nerve growth factor inducible (VGF; 4.4184). The down regulated mRNA was of neuropeptide Y receptor Y1 (NPY1R; -4.752).

The 24 hour exposure to 25 ng/ml rrCNTF showed changes in 3 mRNA levels. Increases were noted in artemin (ARTN; 3.993), interleukin-10 (IL-10; 14.8271) (Figure 18). Table 5 shows the comparison between the time points and the fold changes for the Neurotrophins and Receptors RT<sup>2</sup> PCR.

#### *Chemokines and Receptors*

Exposure to 25 ng/ml rrCNTF for six hours resulted in the up-regulation of 12 genes and no down-regulation was noted. Increased mRNA was seen in C-X-C motif chemokine ligand-10 (CXCL-10; 4.7693); C-X-C motif chemokine ligand-11 (CXCL-11; 4.8922), C-C motif chemokine ligand-12 (CCL-12; 3.1066), C-X-C motif chemokine ligand-9 (CXCL-9; 6.8312), C-X-C motif chemokine ligand-13 (CXCL-13; 5.2326), C-C motif chemokine ligand-4 (CCL-4; 8.4304), C-C motif chemokine ligand-5 (CCL-5; 3.0842), C-C motif chemokine ligand-3 (CCL3; 3.0582), platelet factor-4 (PF-4; 5.7743), interleukin 1- $\alpha$  (IL-1 $\alpha$ ; 4.9676), and interleukin-13 (IL-13; 4.324) (Figure 19).

Following 12 hours of exposure, there was an expression change over 3 fold for 7 genes (Figure 20). The three genes that saw an increase in expression were C-C motif chemokine ligand-3 (CCL-3; 3.3708), C-C motif chemokine

## 12 hour Neurotrophins and Receptors (PARN-031)

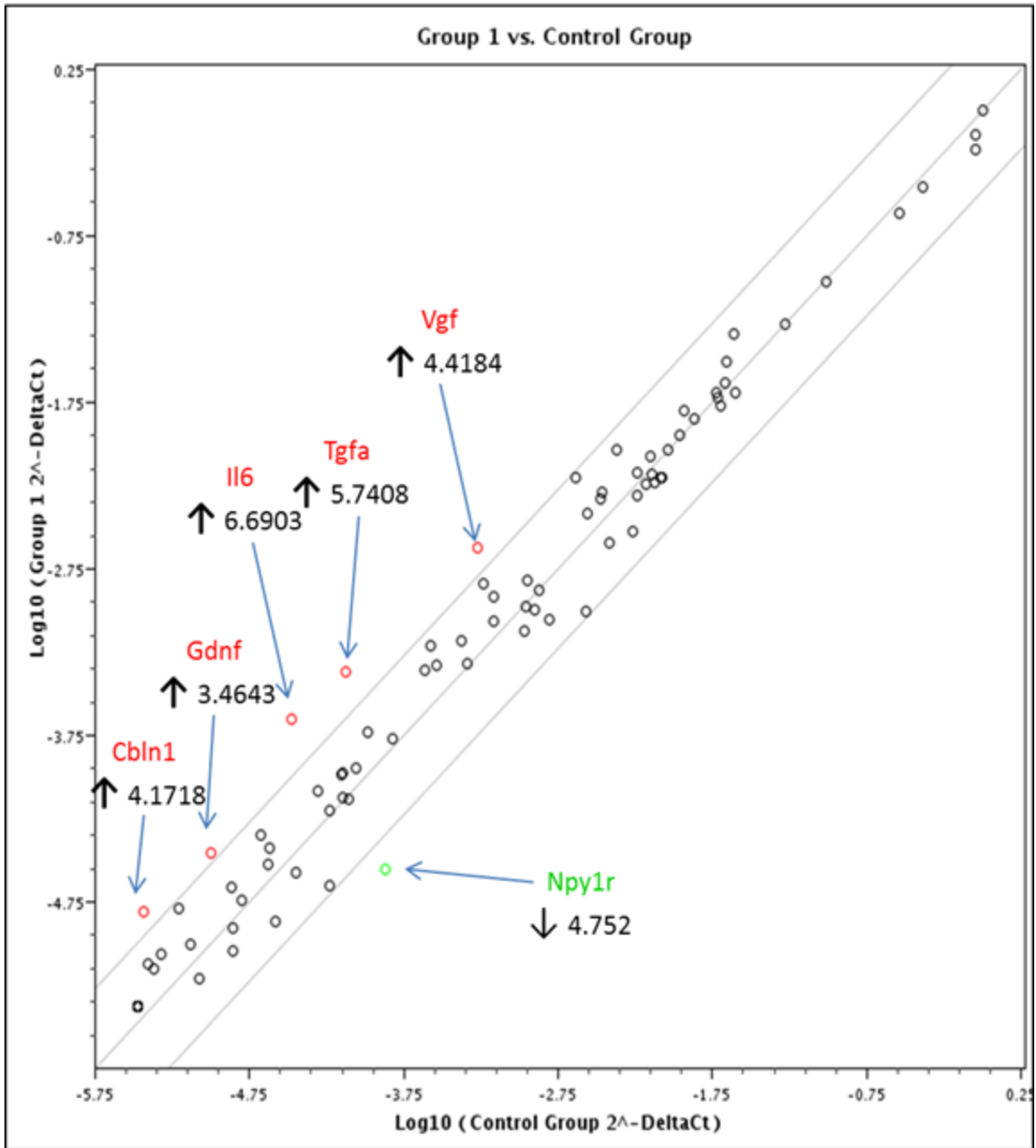


Figure 17. 12 Hour Neurotrophins and Receptors RT<sup>2</sup> PCR. 12 hour exposure to 25 ng/ml rrCNTF. Upregulated factors shown in red. Downregulated factors shown in green. Fold alteration cut off set at 3.

## 24 hr Rat Neurotrophin and Receptors (PARN-031)

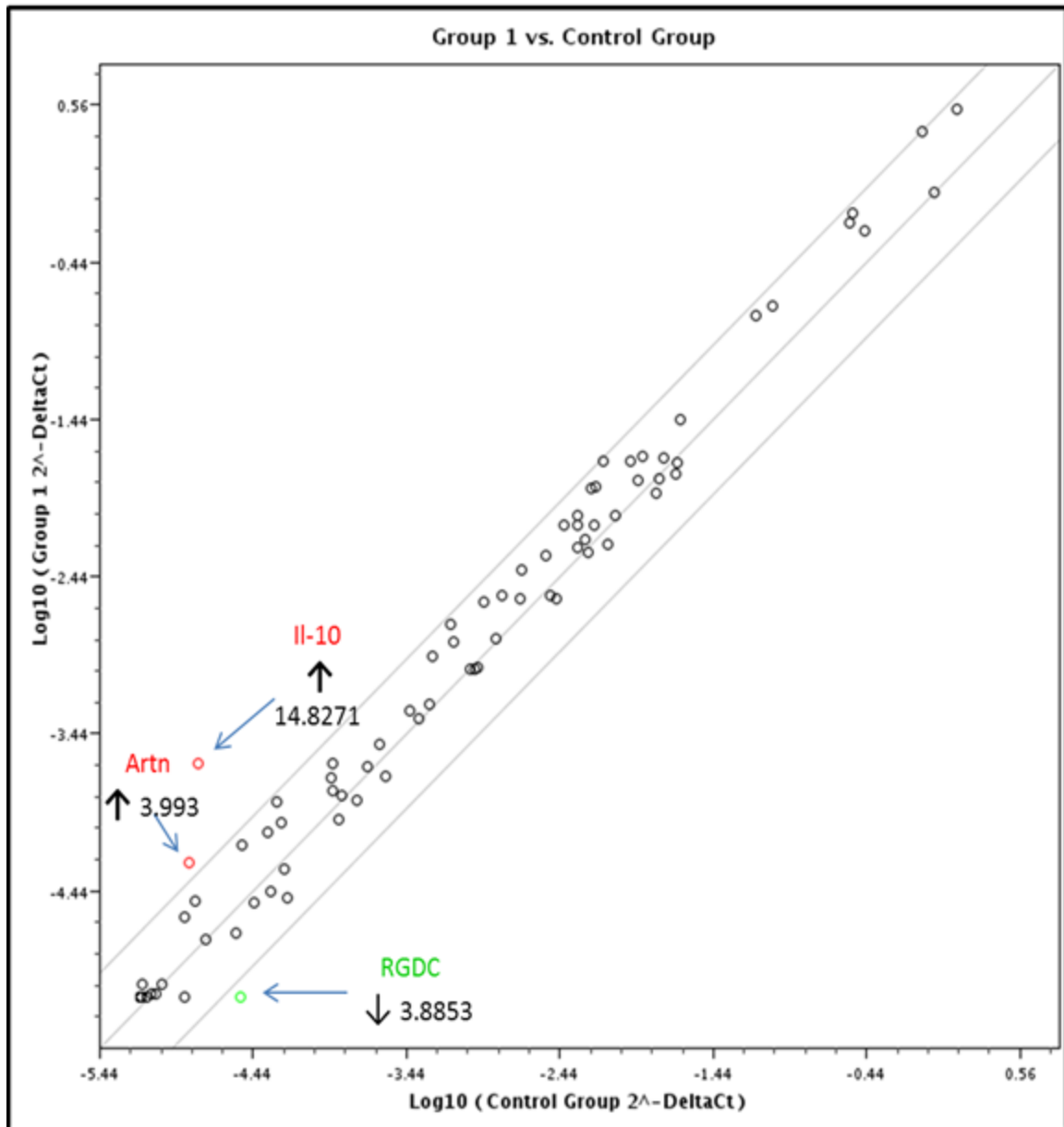


Figure 18. 24 Hour Neurotrophins and Receptors RT<sup>2</sup> PCR. 24-hour exposure to 25 ng/ml rrCNTF. Upregulated factors shown in red. Downregulated factors shown in green. Fold alteration cut off set at 3.

Table 5. Rat Neurotrophin and Receptors RT<sup>2</sup> PCR. Fold increases shown in red. Fold decreases shown in green.

Gene	6 hour	12 hour	24 hour
IL-1 $\beta$ (Interlukin 1 beta)	6.9588		
Vgf (VGF nerve growth factor inducible)		4.4184	
Tgfa (Transforming growth factor alpha)		5.7408	
IL-6 (Interlikin 6)		6.6903	
Gdnf (Glial cell derived neurotrophic factor)		3.4643	
Cbln-1 (Cerebellin 1 precursor )		4.1718	
Npy1r (Neuropeptide Y receptor Y1)		4.752	
IL-10 (interlukin 10)			14.8271
Artn (Artemin)			3.993
RGDC (Rat genomic DNA contamination)			3.8853

ligand-11 (CCL-11; 3.771), and IL-13 (3.3131). The four down-regulated 3 genes were PF-4 (-4.0465), chemokine-like receptor-1 (CMKLR-1; -3.4125), C-C motif chemokine ligand-20 (CCL-20, -3.2557) and chemokine (C-X-C motif) receptor-4 (CXCR-4; -3.0867). After 24 hours of exposure to 100 ng/ml rrCNTF there was no documented gene expression changes with the fold cut off of 3 (Figure 21).

Table 6 shows the comparison between the time points and the fold changes for the Chemokines and Receptors RT<sup>2</sup> PCR.

#### *Jak/STAT Signaling Pathway*

There were a total of nineteen genes that showed an up-regulation for the Jak/STAT Signaling Pathway RT<sup>2</sup> PCR plate after a 6 hour incubation in 25 ng/ml rrCNTF (Figure 22). These nineteen included alpha-2-macroglobulin (A2M; 3.0939), suppressor of cytokine signaling-3 (SOCS-3; 3.1295), upstream transcription factor-1 (USF-1; 3.3338), ISG-15 ubiquitin-like modifier (ISG-15; 4.4753), signal-regulatory protein alpha (SIRPA; 3.1842), SP1 transcription factor (SP-1; 3.2241), high mobility group AT-hook 1 (HMGA-1; 10.6167), guanylate

## 6 hr Chemokines and Receptors (PARN-022)

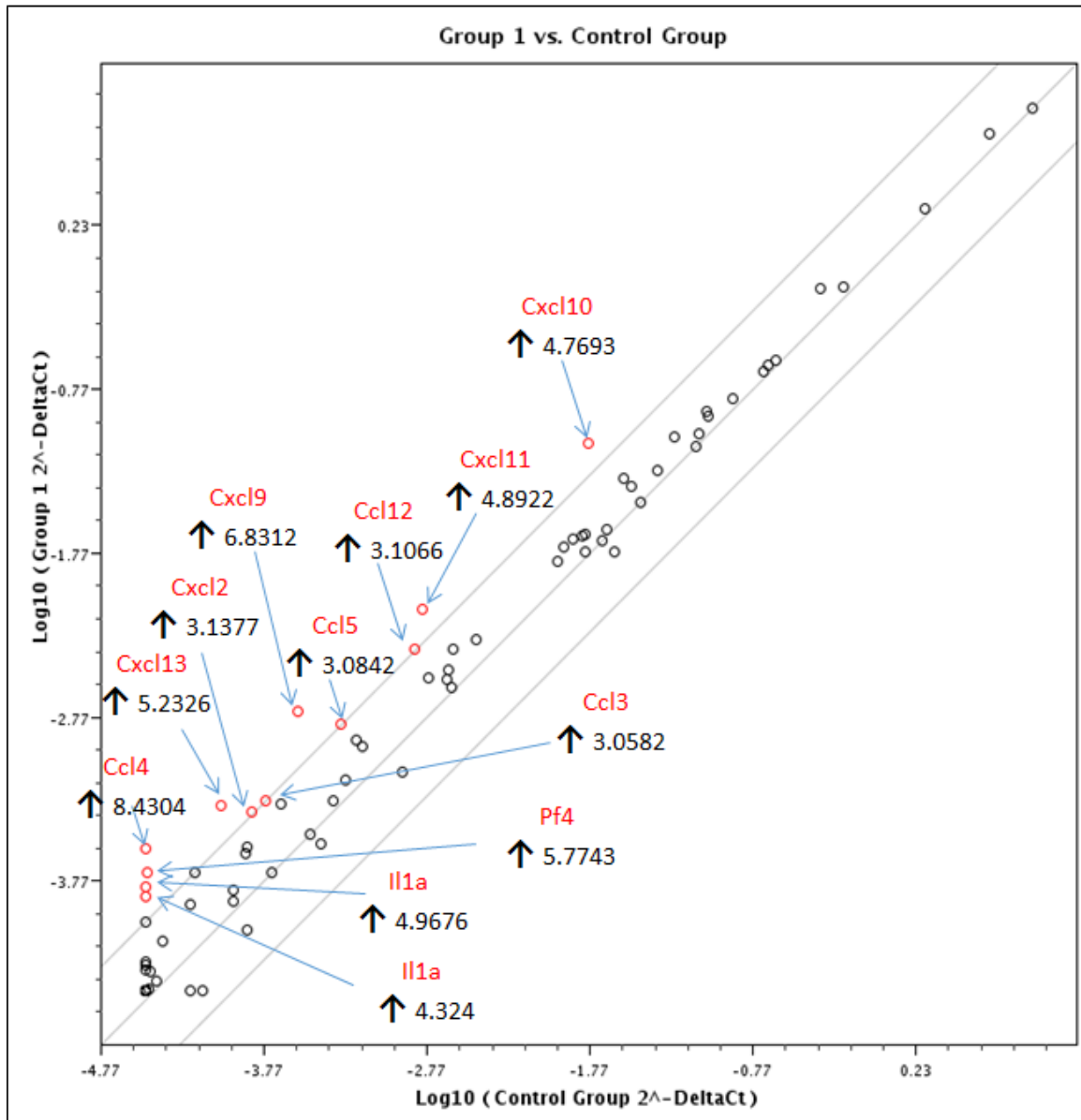


Figure 19. 6 Hour Chemokines and Receptors RT<sup>2</sup> PCR. 6 hour exposure to 25 ng/ml rrCNTF. Upregulated factors shown in red. No downregulated factors. Fold alteration cut off set at 3.

## 12 hour Chemokines and Receptors (PARN-022)

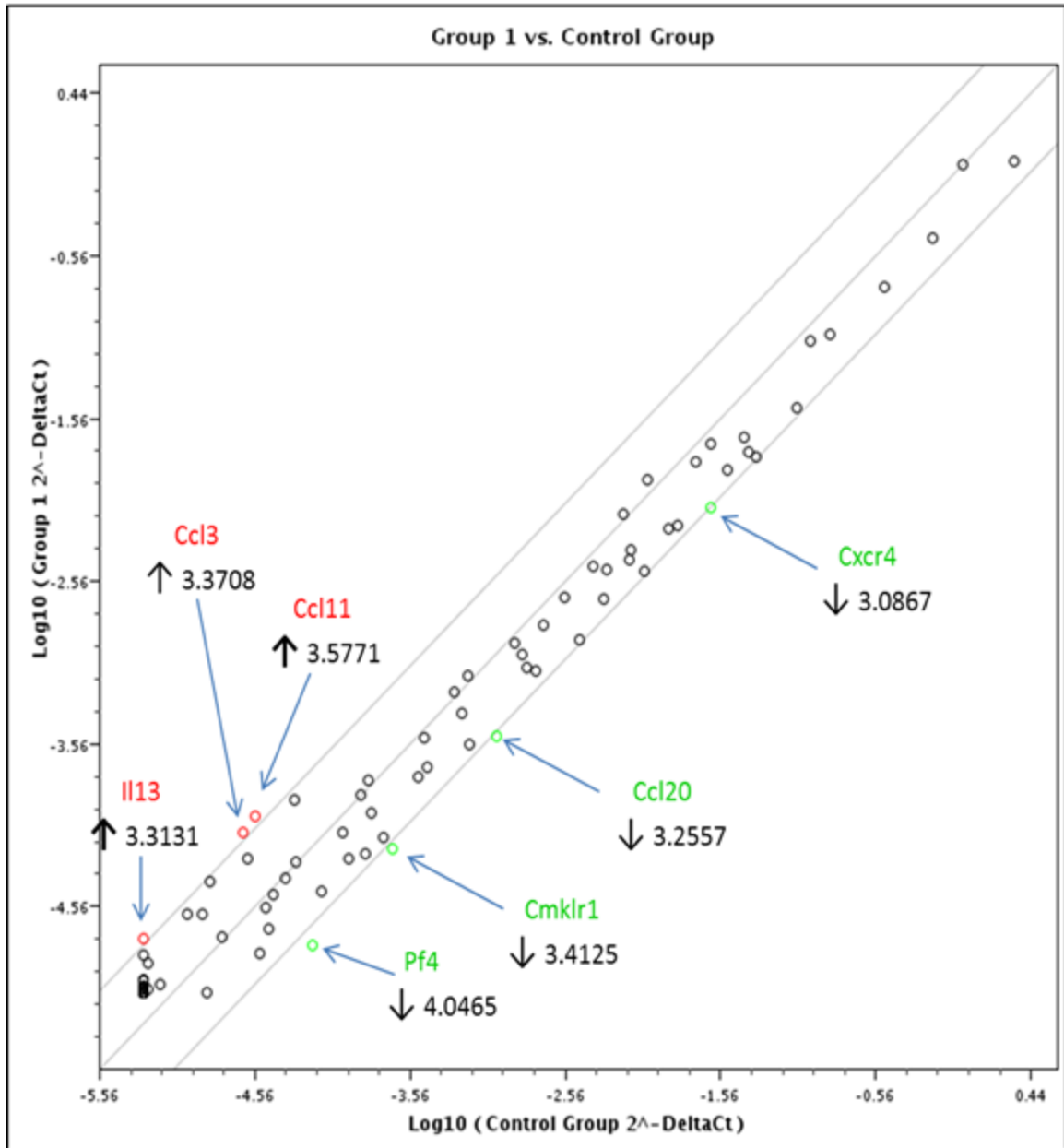


Figure 20. 12 Hour Chemokines and Receptors RT<sup>2</sup> PCR. 12 hour exposure to 25 ng/ml rrCNTF. Upregulated factors shown in red. Downregulated factors shown in green. Fold alteration cut off set at 3.

## 24 hr Rat Chemokines & Receptors (PARN-022)

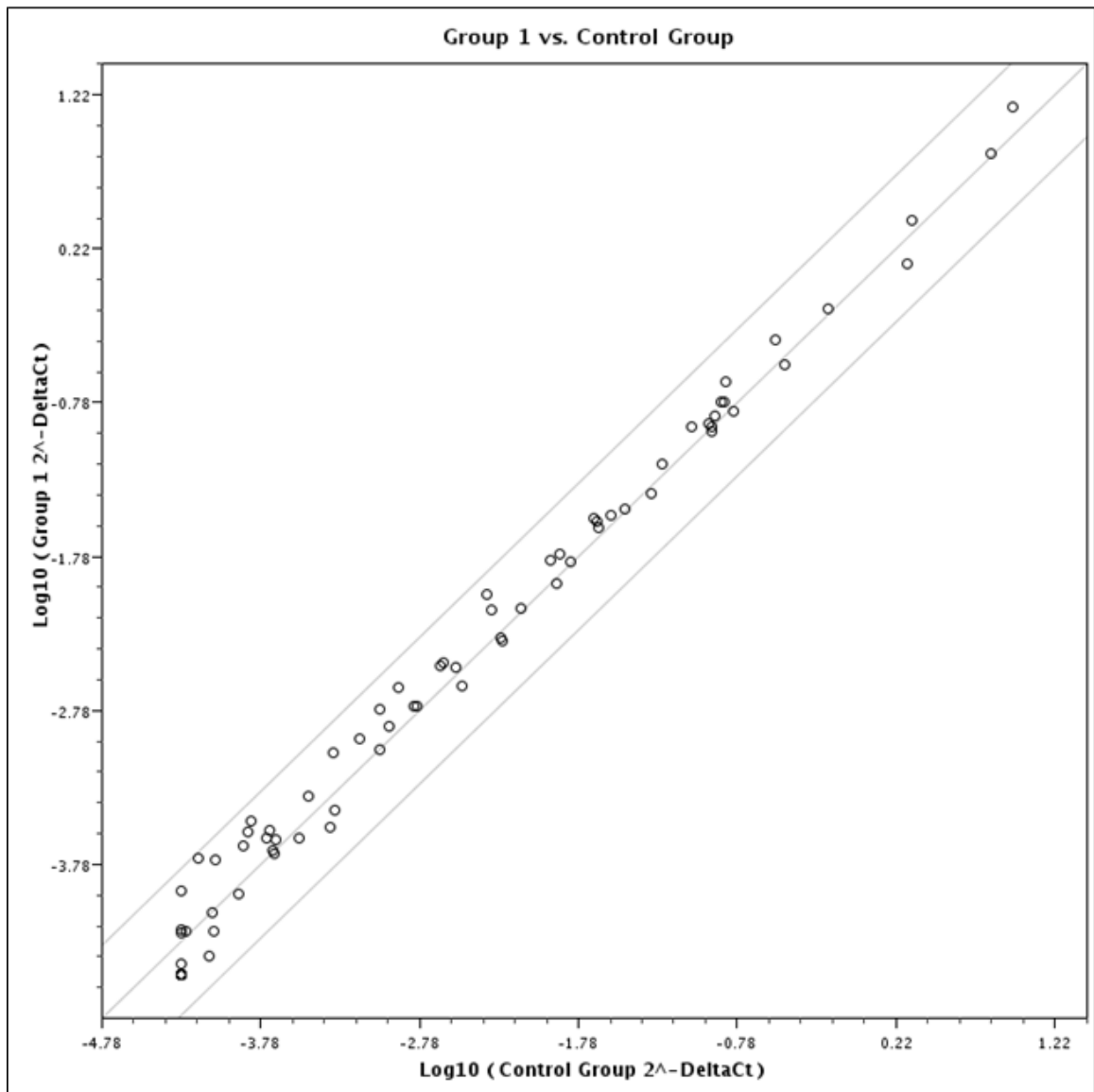


Figure 21. 24 Hour Chemokines and Receptors RT<sup>2</sup> PCR. 24 hour exposure to 100 ng/ml rrCNTF. Fold alteration cut off set at 3.

Table 6. Rate Chemokines and Receptors RT2 PCR Fold Changes. Fold increases shown in red. Fold decreases shown in green.

Gene	6 hour	12 hour	24 hour
Cxcl-10 (C-X-C motif chemokine ligand-10)	4.7693		
Cxcl-11 (C-X-C motif chemokine ligand 11)	4.8922		
Ccl-12 (C-C motif chemokine ligand-12)	3.1066		
Cxcl-9 (C-X-C motif chemokine ligand-9)	6.8312		
Cxcl-13 (C-X-C motif chemokine ligand -13)	5.2326		
Ccl-4 (C-C motif chemokine ligand-4)	8.4304		
Ccl-5 (C-C motif chemokine ligand 5)	3.0842		
Ccl-3 (C-C motif chemokine ligand 3)	3.0582	3.3708	
Pf-4 (Platlet factor -4)	5.7743	4.0465	
IL-1a (interlukin 1 alpha)	4.9676		
IL-13 (Interlukin-13)	4.324	3.3131	
Ccl-11 (C-C motif chemokine ligand 11)		3.771	
Cmklr-1 (Chemokine-like receptor 1)		3.4125	
Ccl-20 (C-C motif chemokine ligand 20)		3.2557	
Cxcr4 (C-X-C motif chemokine receptor 4)		3.0867	

binding protein-1-interferon inducible (Gbp-1; 5.0376), platelet derived growth factor receptor-alpha polypeptide (Pdgfra; 3.0685), CCXL-9 (10.5109), interferon (alpha, beta, and omega) receptor-1 (Ifnar-1; 4.9294), spleen focus forming virus proviral integration oncogene spi-1 (Spi-1; 3.4471), suppressor of cytokine signaling-1 (Socs-1; 5.8105), Janus kinase-3 (Jak-3; 4.2888), colony stimulating factor 1 receptor (Csf1r; 3.5242), erythropoietin receptor (Epor; 3.0516), protein tyrosine phosphate receptor type C (Ptprc; 4.4017), GATA binding protein-3 (Gata-3; 4.1153), and SH2B adaptor binding protein-2 (Sh2b2; 3.5085). No genes were reported to have a down regulation within the test parameters of a 3-fold cut off.



## 6 hour Jak/STAT Signaling Pathway (PARN-039)

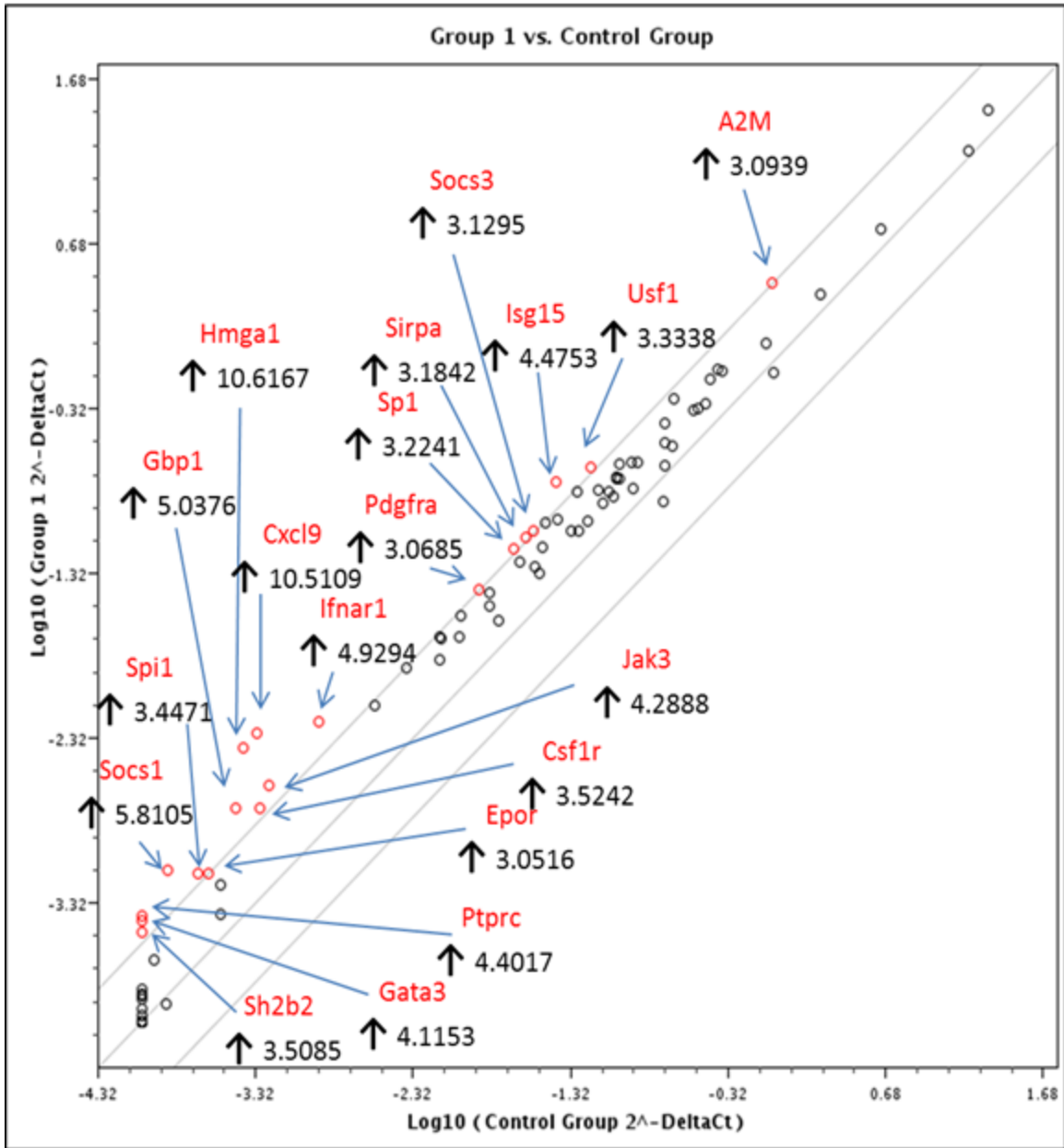


Figure 22. 6 Hour Jak/STAT Signaling Pathway RT<sup>2</sup> PCR. 6 hour exposure to 25 ng/ml rrCNTF. Upregulated factors shown in red. Fold alteration cut off set at 3.

The twelve hour incubation in 25 ng/ml rrCNTF analysis using the Jak/STAT signaling pathway RT<sup>2</sup> PCR plate showed no gene expression changes with the test parameters of a 3-fold cut off (Figure 23). Using the Signal Transduction Pathway Finder RT<sup>2</sup> PCR (Figure 24), the 24 hour incubation resulted in expression changes for 7 genes. Only one gene showed an up-regulation in expression; C-C motif chemokine ligand-20 (CCL-20; 4.8775). The six genes that displayed a down regulation were Jun-B proto-oncogene (Junb; -3.0441), nuclear factor of kappa light polypeptide gene enhancer in B-cells (Nfkb; -5.3454), myelocytomatosis oncogene (Myc; -4.9734), interleukin 4 receptor alpha (IL-4ra; -3.1791), bone morphogenetic protein-2 (Bmp-2; -3.3723), and t cell specific transcription factor-7 (Tcf-7; -3.8404). Table 7 shows the comparison between the 6 hour and 12 hour Jak/STAT Signaling Pathway RT<sup>2</sup> PCR and the 24 hour Signal Transduction Pathway Finder RT<sup>2</sup> PCR.

Specific Aim III: Determine if Response is a Result of CNTF Activation of the JAK2/STAT3 Pathway by Examining if the Inhibition of JAK2/STAT3 will Alter the CNTF Induced Functional Outcome

#### *Inhibition Testing-AG490*

Cell viability was tested using XTT assay in 96 well plates. Each treatment was run in triplicate. Media only wells and wells without treatment were used as controls. Graphs are designed with the Y-axis being percent survivability and the X-axis being time passed since treatment. Cell viability readings were taken every two hours up to 12 hours. (Figure 25 A) shows the cell viability following 5  $\mu$ M AG490 (blue), 10  $\mu$ M AG490 (red), 25  $\mu$ M AG490 (green), 50  $\mu$ M AG490 (purple), and 100  $\mu$ M AG490 (teal). Figure 25 B) displays the viability following

## 12 hour Jak/STAT Signaling Pathway (PARN-039)

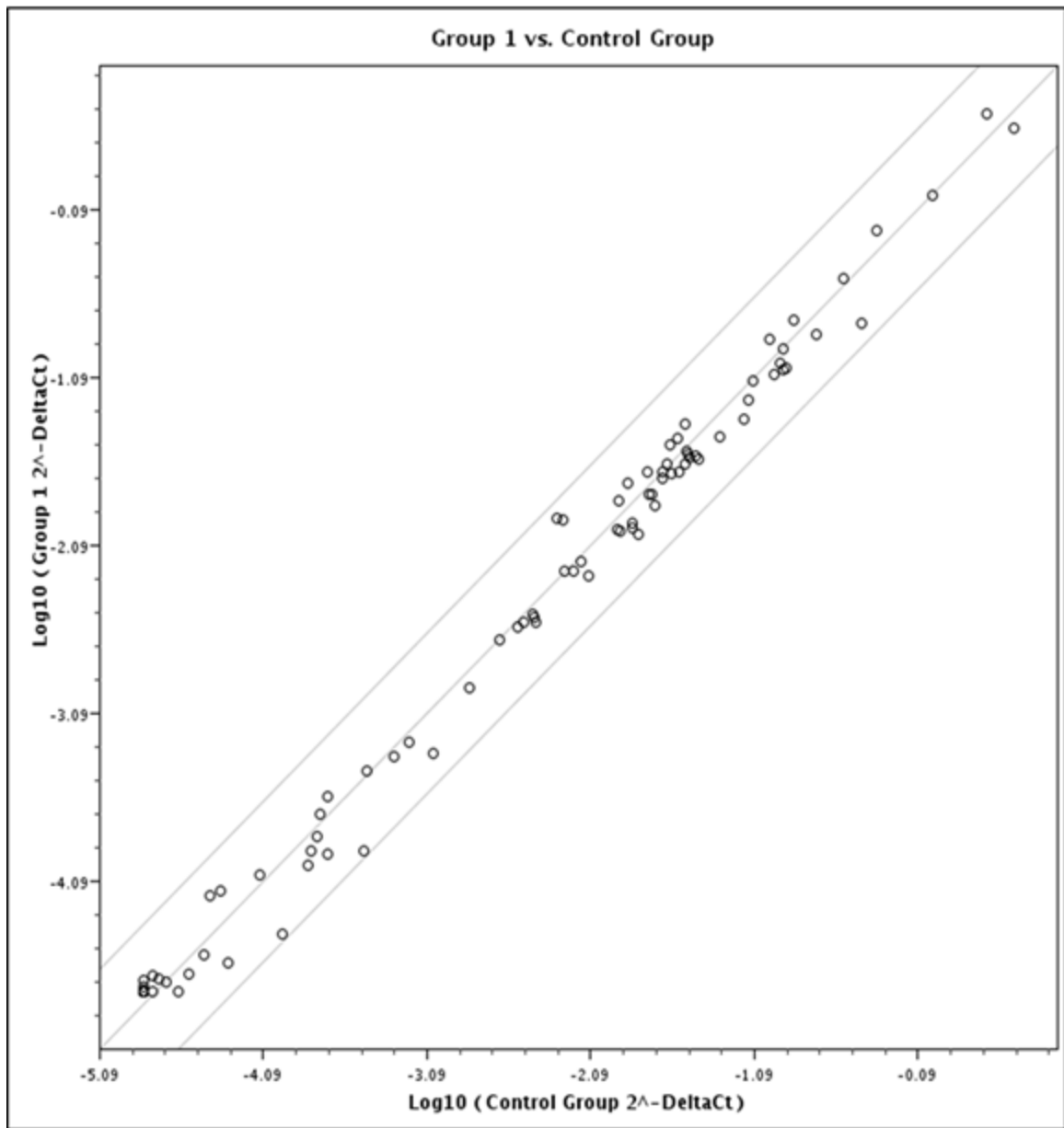


Figure 23. 12 Hour Jak/STAT Signaling Pathway RT2 PCR. 12 hour exposure to 25 ng/ml rrCNTF. Fold alteration cut off set at 3.

## 24 hr Signal Transduction Pathway Finder (PARN-014)

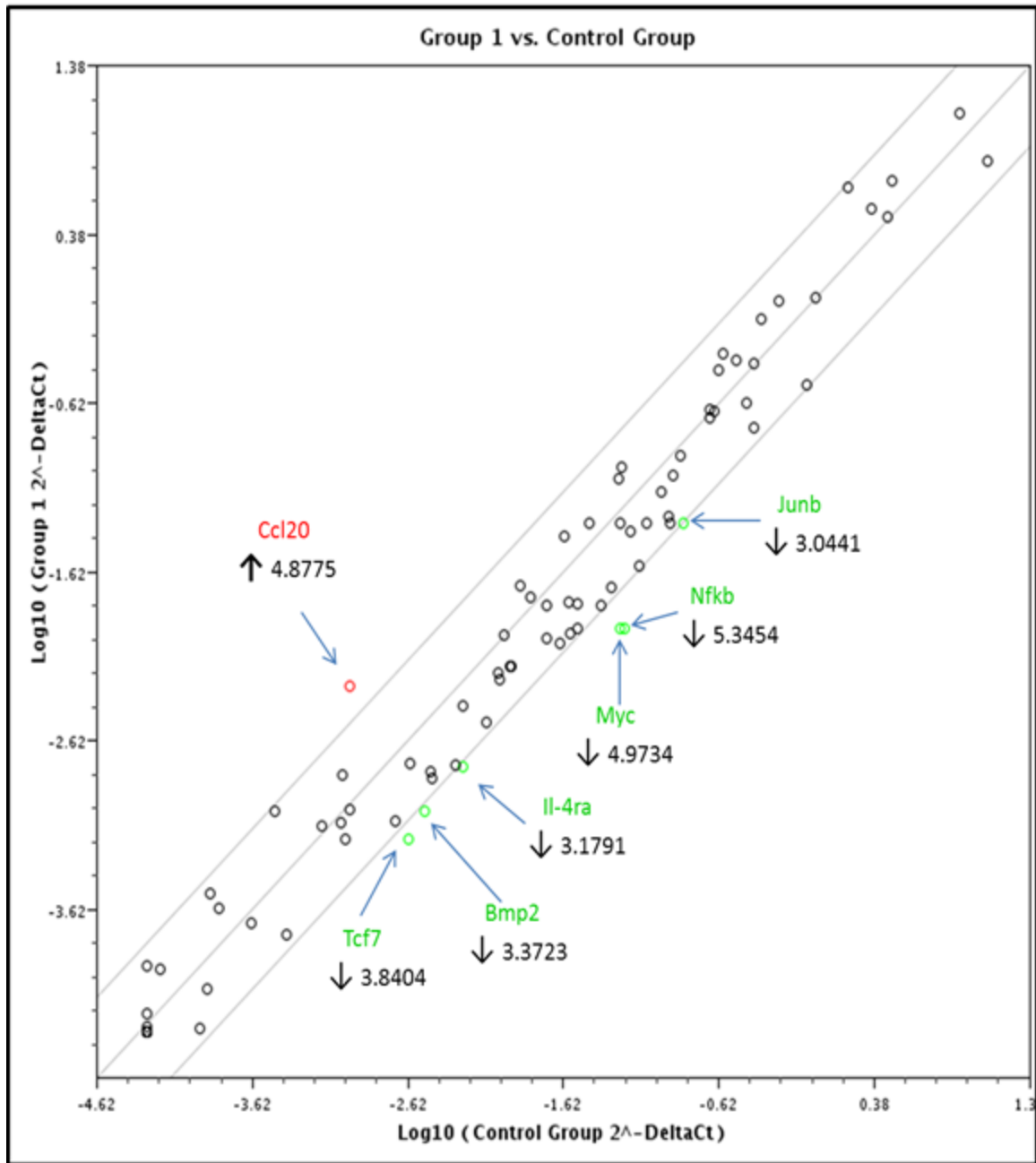
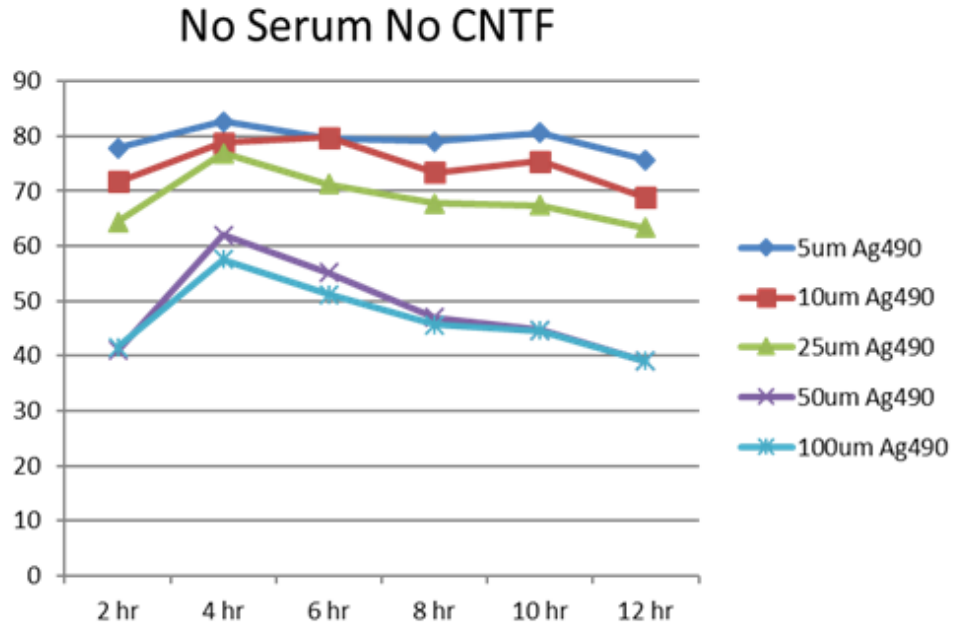


Figure 24. 24 Hour Signal Transduction Pathway Finder RT<sup>2</sup> PCR. 24 hour exposure to 25 ng/ml rrCNTF. Upregulated factors shown in red. Downregulated factors shown in green. Fold alteration cut off set at 3.

Table 7. 6 and 12 Hour Jak/STAT Signaling Pathway RT<sup>2</sup> PCR and the 24 Hour Signal Transduction Pathway Finder RT<sup>2</sup> PCR Fold Changes. Fold increases shown in red. Fold decreases shown in green.

Gene	6 hr	12 hr	24 hr
Ccl-20 (C-C motif chemokine ligand 20)			4.8875
Bmp-2 (Bone morphogenetic protein 2)			3.33723
IL-4ra (Interlukin 4 receptor alpha)			3.1791
Junb (Jun B proto-oncogene)			3.0441
Myc (Myelocytomatosis oncogene)			4.9734
Nfkb-1 (Nuclear factor of kappa light polypeptide gene enhancer in B-cells 1)			5.3454
Tcf-7 (Transcription factor 7, T-cell specific)			3.8404
A2M (Alpha-2-macroglobulin)	3.0939		
Socs (Suppressor of cytokine signaling-3)	3.1295		
Usf (Upstream transcription factor-1)	3.3338		
Isg-15 (ISG-15 ubiquitin-like modifier )	4.4753		
Sirpa (Signal-regulatory protein alpha)	3.1842		
Sp-1 (SP1 transcription factor)	3.2241		
Hmga-1 (High mobility group AT-hook 1)	10.6167		
Gbp-1 (guanylate binding protein-1-interferon inducible)	5.0376		
Pdgfra (platelet derived growth factor receptor-alpha polypeptide)	3.0685		
Ccxl-9 (C-X-C motif chemokine ligand-9)	10.5109		
Ifnar-1 (interferon-alpha-beta-omega-receptor-1)	4.9294		
Spi-1 (spleen focus forming virus proviral inteegration oncogene spi-1)	3.4471		
Socs-1 (suppressor of cytokine signaling-1)	5.8105		
Jak-3 (Janus kinase-3)	4.2888		
Csf-1r (Colony stimulating factor 1 receptor)	3.5242		
Epor (erythropoietin receptor)	3.0516		
Ptprc (Protein tyrosine phosphate teceptor type C)	4.4017		
Gata-3 (GATA binding protein-3)	4.1153		
Sh2b2 (SH2B adaptor binding protein-2)	3.5085		

A.



B.

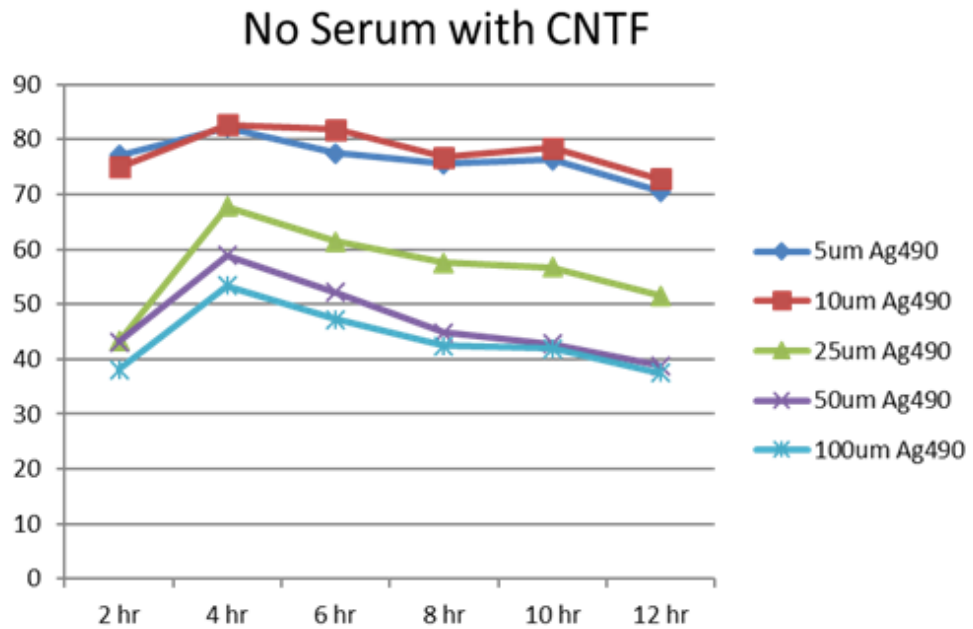


Figure 25. XTT Cell Viability Dosage Inhibition with AG490.  
A) Cell viability from 2 to 12 hours following 5 dosages of AG490.  
B) Cell viability from 2-12 hours following 5 dosages of AG490 plus 25 ng/ml rrCNTF. X-axis time passed.  
Y-axis percent survivability.

5  $\mu$ M AG490 plus 25 ng/ml rrCNTF (blue), 10  $\mu$ M AG490 plus 25 ng/ml rrCNTF (red), 25  $\mu$ M AG490 plus 25 ng/ml rrCNTF (green), 50  $\mu$ M Ag490 plus 25 ng/ml rrCNTF (purple), and 100  $\mu$ M AG490 plus 25 ng/ml rrCNTF (teal). Cell viability was highest at 4 hours for all treatment conditions. Cell exposure to 50  $\mu$ M/ml AG490 and higher resulted in highest cell death with and without rrCNTF. Western blot analysis was performed on both nuclear extraction portions following treatments as listed in the prior paragraph. The blot was stained for pSTAT3 tyr 705 and normalized using tSTAT3 (Figure 26). The nuclear portion is shown with black bars and the cytosolic portion in white. Controls included no treatment and rrCNTF only each with a sample number of 2. All AG490 dilution samples had an (n) of 1 and all AG490 dilutions plus 25 ng/ml rrCNTF had 2 samples each. Statistical analysis shows no significant decrease between the CNTF only samples, the AG490 only samples, or the CNTF plus AG490 samples.

#### *Inhibition Testing-Cucurbitacin*

Cell viability was tested using XTT assay in 96 well plates. Each treatment was run in with a n of 8. Media only wells and wells without treatment were used as controls. Graphs are designed with the Y-axis being percent survivability and the X-axis being time passed since treatment. Readings were taken every two hours up till 12 hours. Figure 27 A) shows the cell viability in DMEM with 10% FBS with the following treatments 25 ng/ml rrCNTF (blue), 10nM/ml cucurbitacin (red), and 25 ng/ml rrCNTF plus 10 mM/ml cucurbitacin (green). Figure 28 B)

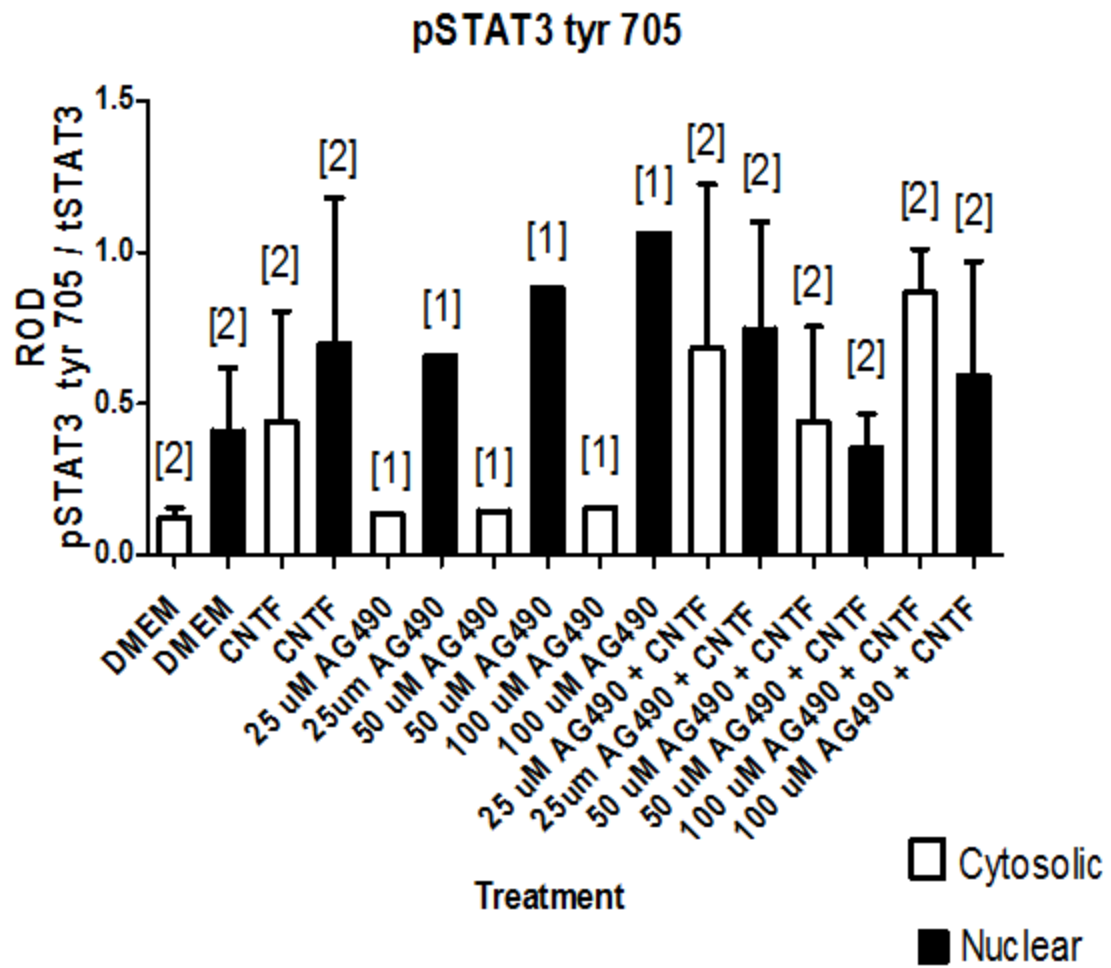


Figure 26. Nuclear Extraction Western Blot Analysis of pSTAT3 tyr 705 Translocation Following Dosage Inhibition with AG490. Astrocyte nuclear extraction (black) and cytosolic extraction (white) comparison. Ratio of optical density normalized with tSTAT3. The error bars are the mean  $\pm$  SD. [n] = number of experimental samples.



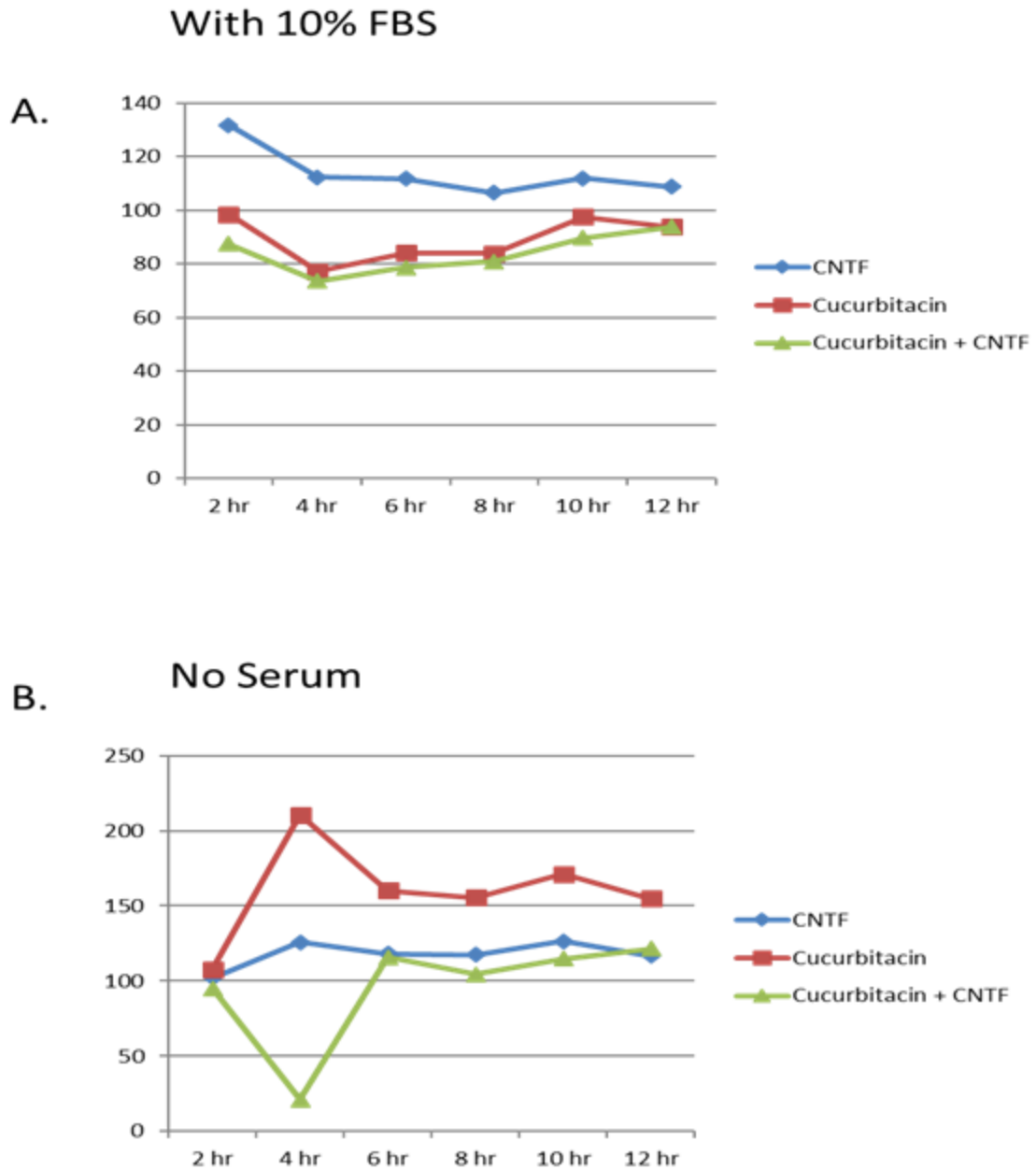


Figure 27. XTT Cell Viability Dosage Inhibition with Cucurbitacin.  
 A) Cell viability in DMEM with 10% FBS from 2 to 12 hours following 25 ng/ml rrCNTF exposure (blue), 10 mM/ml curcubitacin (red) or 25 ng/ml rrCNTF plus 10 mM/ml curcubitacin.  
 B) Cell viability in DMEM without FBS from 2 to 12 hours following 25 ng/ml rrCNTF exposure (blue), 10 mM/ml curcubitacin (red) or 25 ng/ml rrCNTF plus 10 mM/ml curcubitacin.  
 X-axis time passed. Y-axis percent survivability reading

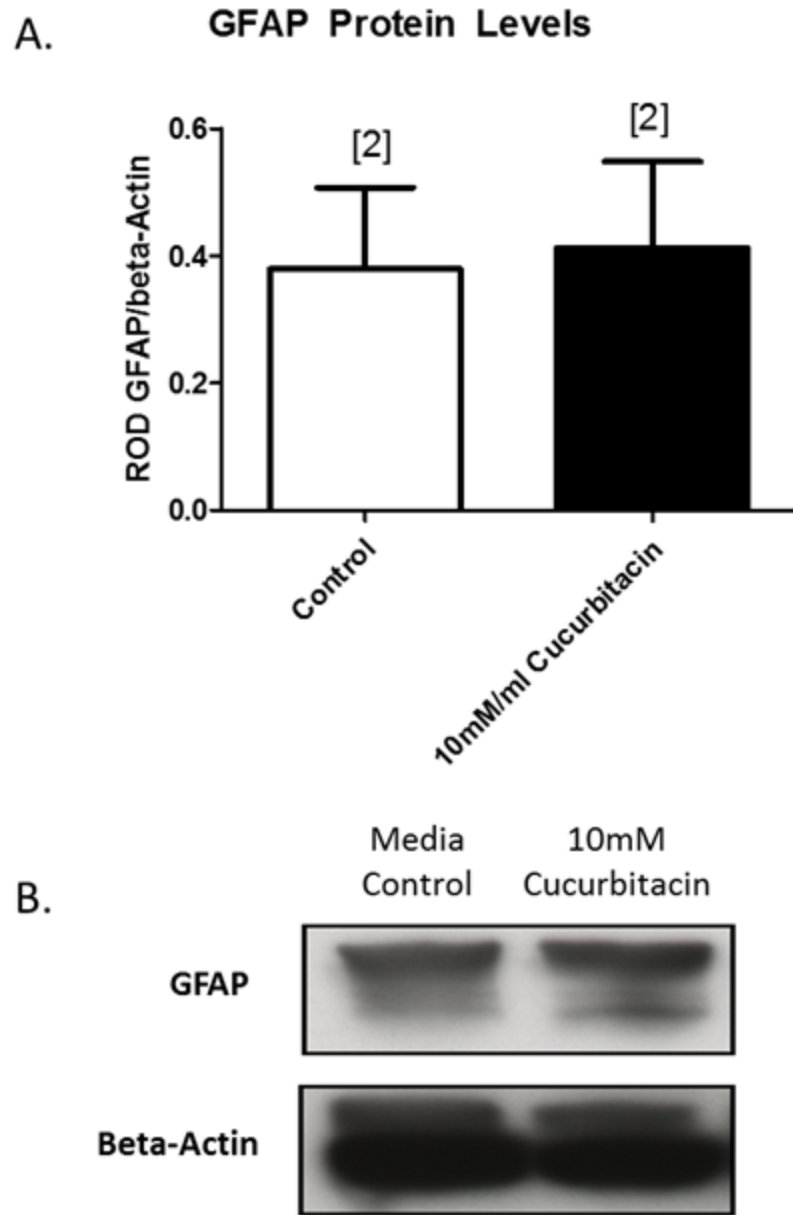


Figure 28. GFAP Protein Western Blot Analysis. 1 hour exposure to 10 mM/ml curcubitacin.  
 A) ration of optical density analysis of control sample (n=2; white) and treated sample (n=2; black). Ration of optical density normalized with  $\beta$ -actin.  
 B) Western blot showing protein expression.  
 The error bars are the mean  $\pm$  SD. [n] = number of experimental samples.

displays the viability in DMEM without FBS with the same treatments as figure A. Cell viability was highest in cultures that received FBS.

Western blot analysis was performed on total protein from astrocyte tissue homogenates following treatment a 1 hour exposure to 10 mM/ml cucurbitacin. The blot was stained for GFAP and normalized using  $\beta$ -actin (Figure 27). The control is shown in white (n=2) and the treated sample (n=2) in black. Statistical analysis shows no significant change in GFAP protein expression.

The translocation of pSTAT3 tyr 705 following cucurbitacin treatment was analyzed using nuclear extraction Western blots. The blot was stained for pSTAT3 tyr 705 and normalized using tSTAT3 (Figure 29). The nuclear portion is shown with black bars and the cytosolic portion in white. Controls included no treatment, rrCNTF only, and cucurbitacin only. Each sample was run in triplicate. Treated samples were exposed to 10 mM/ml cucurbitacin for 1 hour. Samples receiving 25 ng/ml rrCNTF were spike treated for 30 minutes following the completion of the 1 hour cucurbitacin incubation. Figure 28 A shows the ratio of optical density of the samples with a one-way ANOVA significance between the CNTF cytosolic and nuclear extraction ( $p = 0.0061$ ). Figure B is the Western blot showing the protein expression for pSTAT3 and the normalizing protein tSTAT3.

A. Nuclear Translocation of pSTAT3 tyr 705

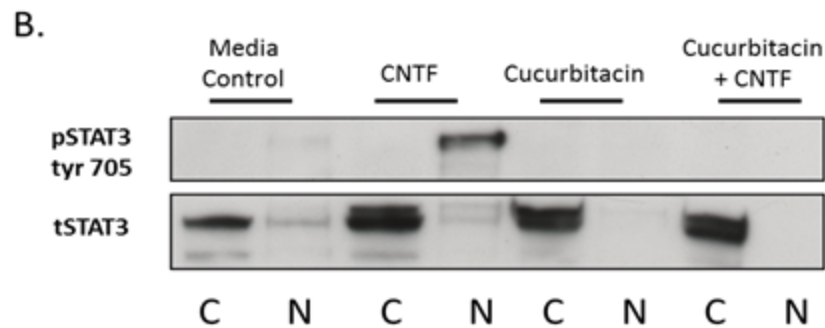
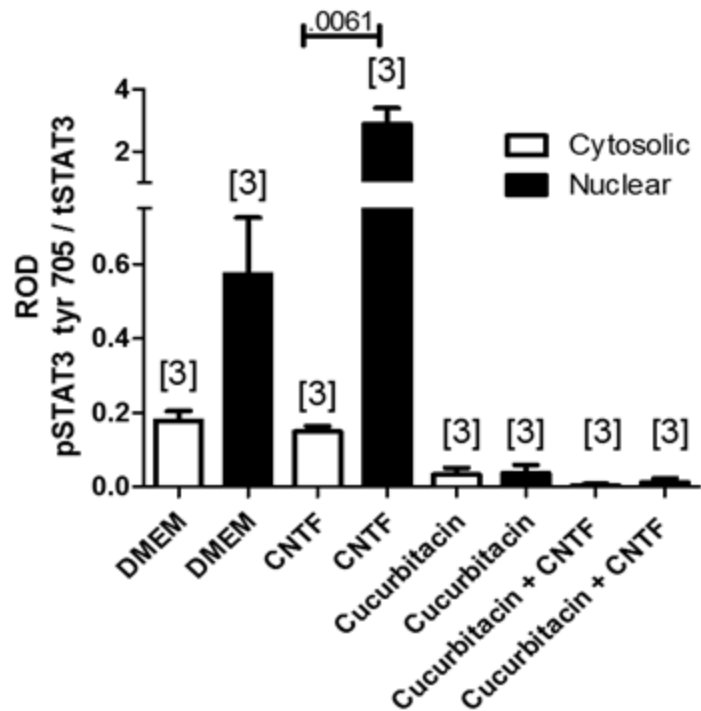


Figure 29. Cucurbitacin Inhibition of pSTAT3 tyr 705. Inhibition with Cucurbitacin for 1 hour followed by 30 minute spike of rrCNTF. Astrocyte nuclear extraction (black) and cytosolic extraction (white) comparison.

A) ROD analysis of control extractions (n = 3), 25 ng/ml rrCNTF extractions (n = 3), 10 mM/ml cucurbitacin (n = 3), and 25 ng/ml rrCNTF plus 10 mM/ml cucurbitacin (n = 3) extractions. One-way ANOVA indicates significance between CNTF nuclear and cytosolic extractions (p = 0.0061). Samples normalized with tSTAT3

B) Western blot showing protein expression for pSTAT3 tyr 705 and tSTAT3.

The error bars are the mean  $\pm$  SD. [n] = number of experimental samples

Specific Aim IV: Determine if the Functional Response Promotes  
Survival and Sprouting of Neurons Utilizing the  
Hypothalamic Explants Cultures

*Paraventricular Nucleus Oxytocinergic Neuron Counts*

The functional response of astrocytes to CNTF was examined using the application of astrocyte conditioned media (ACM) to the hypothalamic explants cultures. Treatments included control ACM (n = 15), 25 ng/ml rrCNTF exposure (n = 19), 50  $\mu$ M AG490 (n = 22), 25 ng/ml rrCNTF plus 50  $\mu$ M AG490 (n = 18), 10  $\mu$ M cucurbitacin (n = 16), and 25 ng/ml rrCNTF plus 10  $\mu$ M cucurbitacin (n = 20). Figure 29 shows the oxytocinergic cell counts (Y-axis) within the PVN. Using a one-way ANOVA there was significance between the control ACM and the rrCNTF ( $p \leq 0.01$ ), between the CNTF plus AG490 ( $p \leq 0.01$ ), and between the CNTF and CNTF plus cucurbitacin ( $p \leq 0.001$ ) (Figure 30).

*Supraoptic Nucleus Oxytocinergic Neuron Counts*

The functional response of astrocytes to CNTF was examined using the application of astrocyte conditioned media (ACM) to the hypothalamic explants cultures. Treatments included control ACM (n = 15), 25 ng/ml rrCNTF exposure (n = 19), 50  $\mu$ M AG490 (n = 22), 25 ng/ml rrCNTF plus 50  $\mu$ M AG490 (n = 18), 10  $\mu$ M cucurbitacin (n = 16), and 25 ng/ml rrCNTF plus 10  $\mu$ M cucurbitacin (n = 20). Figure 30 shows the oxytocinergic cell counts (Y-axis) within the SON. Using a one-way ANOVA there was significance between the control ACM and the rrCNTF ( $p \leq 0.05$ ), between the AG490 and CNTF plus AG490 ( $p \leq 0.01$ ),

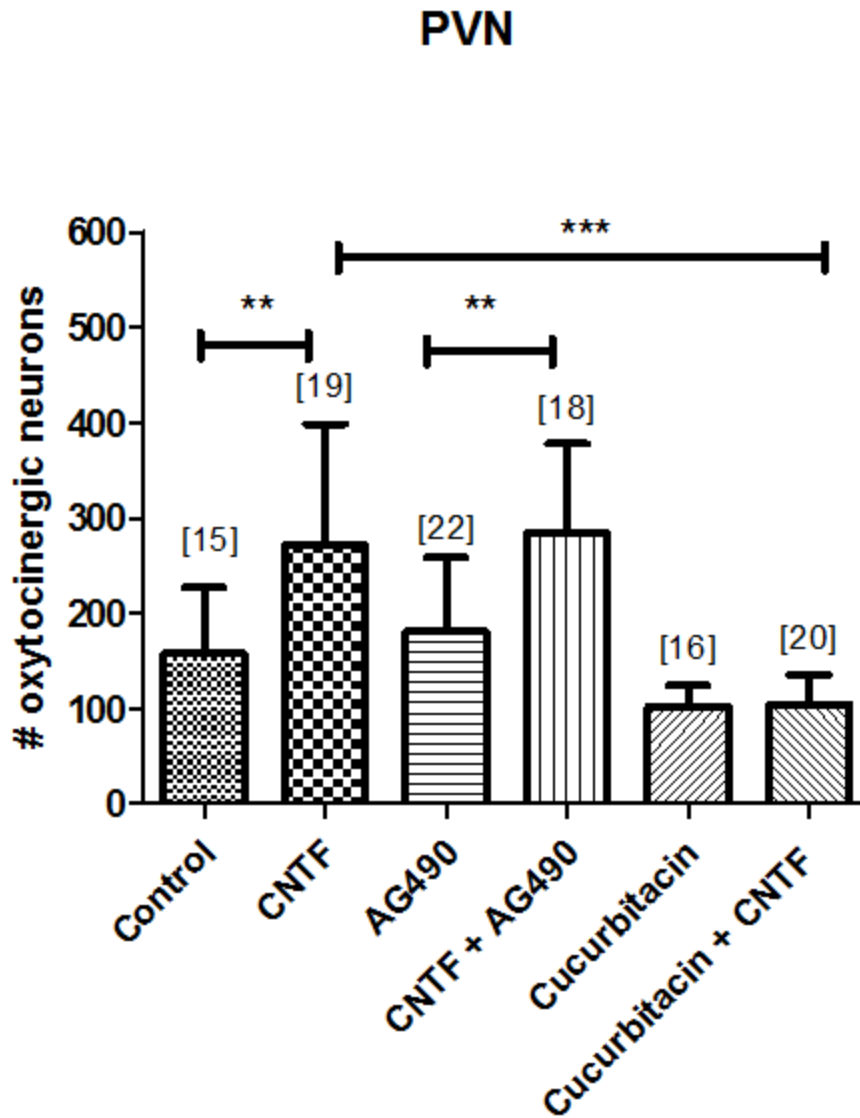


Figure 30. Paraventricular Nucleus Oxytocinergic Neuron Counts. Immunohistochemical neuronal cell counts demonstrates that astrocytes produce neuroprotective factors in response to exogenous CNTF. CNTF treated astrocytes ACM promoted the survival of OT neurons ( $p \leq 0.01$ ) as did the application of CNTF plus AG490 ACM ( $p \leq 0.01$ ). The astrocytes intracellular pathway involved can be inhibited by cucurbitacin and showed a significant decrease in OT neuron survival ( $p \leq 0.001$ ). Y-axis OT neuron cell count. The error bars are the mean  $\pm$  SD. [n] = number of experimental samples.

between the CNTF and CNTF plus cucurbitacin ( $p \leq 0.01$ ), between the control ACM and the cucurbitacin ( $p \leq 0.01$ ), and between the control ACM and the cucurbitacin plus CNTF ( $p \leq 0.01$ ) (Figure 31).

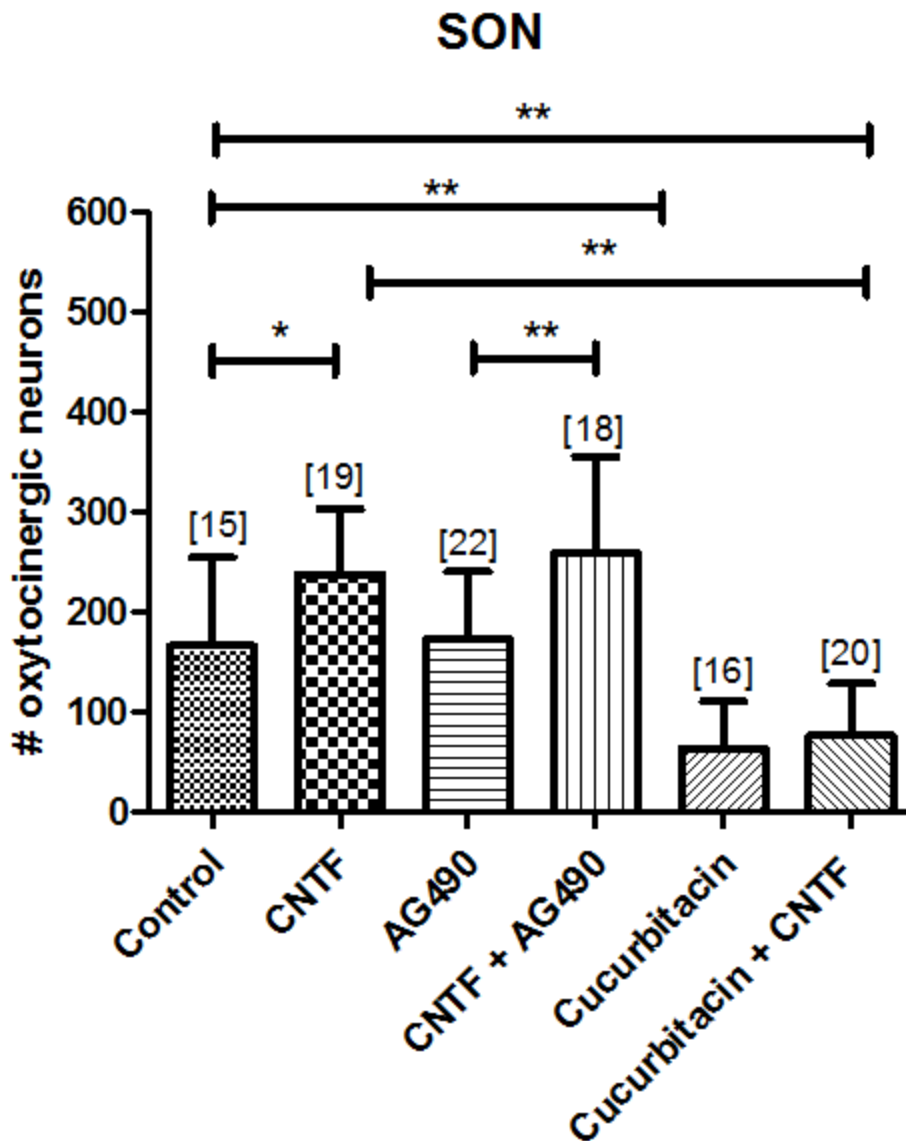


Figure 31. Supraoptic Nucleus Oxytocinergic Neuron Counts. Immunohistochemical neuronal cell counts demonstrates that astrocytes produce neuroprotective factors in response to exogenous CNTF. CNTF treated astrocytes' ACM promoted the survival of OT neurons compared to control ( $p \leq 0.05$ ) as did the application of CNTF plus AG490 ACM compared to just AG490 ( $p \leq 0.01$ ). The astrocytes intracellular pathway involved can be inhibited by cucurbitacin and showed a significant decrease in OT neuron survival ( $p \leq 0.01$ ). Y-axis OT neuron cell count. The error bars are the mean  $\pm$  SD. [n] = number of experimental samples.



## CHAPTER IV

### DISCUSSION

The results of the this study demonstrate the activation of primary cortical rat astrocyte cultures by the application of exogenous rrCNTF. First, this activation was confirmed by comparison of GFAP upregulation following exposure and the confirmation that primary cortical rat astrocytes maintain the tripartite CNTF receptor complex. Then it was determined that this activation produces a cascade effect through the JAK/STAT3 pathway by means of phosphorylation of STAT3 tyrosine 705. This cascade effect influences genes expression by either upregulation or down-regulation. This changed expression of possible neuroprotective factors was tested by means of applying astrocyte conditioned media to hypothalamic organotypic explant cultures. Our data suggest that CNTF potentiates survival and sprouting of axotomized magnocellular neurons through activation of astrocyte-specific signal transduction pathways leading to increased expression levels of factors which mediate the neuronal response.

## Specific Aim I: Determine if CNTF Activates the JAK/STAT Pathway in Astrocytes

### *rrCNTF Infused SON*

The cannula placement and pump-outflow was determined for each cannula based on the reports of Adam Sudbeck. It was determined that the cannula was inserted to the proper position at an occurrence of 75% by immunohistochemical analysis. The out-flow rate was calculated at 0.94  $\mu$ l per hour over the 72 hours the mini-osmotic pump was in place. We observed an increase in the immunoreactivity of GFAP in the astrocytes within the SON and the brain parenchyma surrounding the cannula tip. This immunoreactivity was confirmed via western blot analysis of GFAP levels within the rrCNTF infused SON, aCSF infused SON, and the corresponding contralateral SON (Figure 4). Our data is in agreement with data published by Seidel et al. (2015) and Park et al. (2000) that increase levels of CNTF, from exogenous application or naturally, results in increased levels of GFAP protein within the proximal astrocytes. This data established that these samples could be used as a positive control for comparison with the primary rat cortical astrocyte cultures.

### *Primary Astrocyte Cultures*

The primary rat cortical astrocyte cell cultures were visually assessed throughout the purification process. This visual assessment would look for abnormalities within the media, the confluency of the cells, and overall appearance of the astrocytes. Any abnormalities would classify a culture as

contaminated and result in its disposal. Cultures that were deemed visually normal were used for further experiments.

Once cells had reached the desired visual confluency of 70-80% they were analyzed for purity and cell type identification. The identification of astrocytes was verified by fluorescent immunocytochemistry staining for the GFAP protein which is localized to the astrocyte cytosol. Purity was assessed by fluorescent immunocytochemistry staining for microglial cells with OX-42 or Tomato Lectin. Microglial cells were never observed following the second purification of the cell cultures and according to McCarthy and De Vellis (1980), the layered stratification seen prior to the first pass provides a complete removal of oligodendrocytes in the purification and splitting process inhibiting the reappearance of the cell type. This immunocytochemical analysis demonstrated that the cultures had a purity level of  $\geq 98\%$  primary astrocytes.

In order for CNTF to activate its signaling pathways, it must first bind to the receptor complex. It has been shown that the gp130 and LIFR- $\beta$  components are necessary for CNTF signaling and mediate the intracellular signaling response to the binding of CNTF to CNTFR- $\alpha$  (Davis, Aldrich, Stahl, et al., 1993; Davis et al., 1991; Ip, McClain, et al., 1993). Askvig et al. (2012) demonstrated that all three components to the tripartite CNTF receptor complex are found colocalized on the astrocytes of the intact SON. Additionally, it has been shown that LIFR-  $\beta$  is not present on the vasopressinergic magnocellular neurons of the SON (Askvig et al., 2013). This presumable absence of a crucial component to CNTF induced activation suggests that the observed CNTF effect of

magnocellular neuron survival and sprouting is due to an autocrine signaling mechanism via the astrocytes.

The necessity of all three receptor components to potentiate the noted effects made it crucial to demonstrate that the cultured primary astrocytes retain all the components. Figure 6 A-C showed via fluorescent staining that the expression of CNTFR- $\alpha$  is present. The western blot visualization (Figure 6 D) showed that LIFR- $\beta$  and gp130 are also present in the cultured astrocytes. The levels of gp130 appear to be much lower than LIFR- $\beta$  in comparison to the SON tissue homogenate control. One reason for this discrepancy is that the tissue control is a heterogeneous mixture of cells incorporating both astrocytes and the magnocellular neurons. As previously stated, LIFR- $\beta$  is localized to the astrocytes of the SON and not the neurons whereas the gp130 component is found on both of these cells. Therefore the tissue homogenate control would have an expectedly larger ratio of gp130 to LIFR- $\beta$  in comparison to the two astrocyte samples. Regardless of the lower astrocytic gp130 levels, the receptor component was still present allowing for proper binding of CNTF. These lower levels overall may lead to decreased activity levels of CNTF activated astrocytes. The possible decreased activity may result in lower levels of STAT activity.

The binding of CNTF to its receptor complex, and subsequent activation of the astrocytes is seen via the activation of multiple pathways. The focus of this study was the Jak/STAT pathway. The Jak2/STAT3 pathway has been demonstrated by Askvig et al. (2013) to be present in the SON that the inhibition of this pathway abolishes the pro-survival response elicited by CNTF. To ensure

the ability of the cultured astrocytes to be activated following exposure to exogenous CNTF, the translocation of pSTAT tyr 705 was observed by fluorescent immunocytochemical staining (Figure 8) and western blot analysis (Figures 9 and 10) of the nuclear extraction components. The fluorescent immunocytochemical staining at five time points (10, 20, 30, 60, and 90 minutes) showed that not only are the cultured primary astrocytes able to be activated following exogenous CNTF exposure, but that this activation is a relatively quick and transient activation with the translocation of pSTAT tyr 705 from the cytosol to the nucleus within the first 10 minutes of exposure

#### *Summary of Specific Aim I*

From this information we were able to confirm that not only are the primary rat cortical astrocyte cultures  $\geq 98\%$  pure cultures, but that they react to CNTF in manners similar to astrocytes found in vivo within the SON. These cultured astrocytes maintained the presence of all three components of the CNTF receptor complex; CNTFR- $\alpha$ , gp-130, and LIFR- $\beta$ . The cultured cells became activated in response to exogenous rrCNTF as seen by elevated levels of GFAP. The Jak/STAT pathway was activated in as little as ten minutes as noted by the presence of phosphorylated STAT3 tyrosine 705 in immunocytochemical staining and the translocation of pSTAT3 tyr 705 from the cytosol of the astrocyte to the nucleus as analyzed by western blot.

Specific Aim II: Determine the functional response of astrocytes to CNTF

The magnocellular neuronal cells of the SON and PVN have demonstrated enhanced survival numbers following CNTF exposure.

Additionally, the exposure has been shown to have an influence on axonal sprouting. Our lab has evidence suggesting CNTF potentiates a collateral sprouting response following unilateral lesion (Askvig, Leiphon, et al., 2012; Watt et al., 2006). Furthermore, our lab has also demonstrated that CNTF promotes magnocellular neuron process outgrowth in hypothalamic organotypic cultures (Askvig & Watt, 2015). Moreover, our lab has determined that astrocytes are the source of CNTF within the supraoptic nucleus (Watt et al., 2006). Following the release of CNTF from astrocytes, CNTF is presumed to evoke a response via an autocrine signaling mechanism on the very cells that released it. The question that we are addressing is regarding the possible functional response supplied by cultured astrocytes following CNTF stimulation that may potentially lead to the observed pro-survival and sprouting effects seen both in vivo and in the organotypic cultures.

#### *Cytokine Release Analysis*

The central nervous system environment is highly influenced by the resident astrocytes. These glial cells are responsible for many aspects of keeping the CNS in a homeostatic environment. One of the many ways astrocytes influence their environment is through the release of cytokines. In order to determine the cytokine production and release of cultured astrocyte following exogenous rrCNTF exposure, of the supernatant was analyzed using a membrane array. The comparison of 34 cytokines using the RayBio Cytokine Arrays 1 and 2 showed an increase in release of multiple cytokines. Of the cytokines that exhibited an increased release four were chosen to study further;

fractalkine, IL-6, VEGF, and LIX. These cytokines were further observed via ELISA and compared at several exposure time points to either rrCNTF, rsCNTF, or a no treatment control.

### *Fractalkine*

Fractalkine, also known as CXCL1, has been shown to induce migration and cell activation of microglial cells. Additionally, this cytokine is known to help in the support and survival of developing neurons (Arnoux & Audinat, 2015). The membrane arrays analysis of fractalkine showed a 66.67% increase in release over the control supernatant following rrCNTF exposure. This increase is a 1.836-fold change. Upon further quantitative exploration using the RayBio Fractalkine ELISA kit, no significant increase was detected in either the supernatant or the cytosolic portion of the treated cultured cells compared to the control.

Intracellularly, fractalkine was also observed using the Rat Chemokines and Receptors RT<sup>2</sup> PCR kit from SABiosciences. This examination of RNA for fractalkine showed an 18% increase or a 1.18-fold increase over the control values. Unfortunately, this fold increase did not fall within our parameters of a 3-fold increase for significance.

The reason for the discrepancies seen in the cellular release is unknown. Originally there was the possibility that the phenol red dye in the DMEM supernatant was affecting the ELISA outcome. This factor was removed by using phenol red free DMEM and no significant changes were observed. Another potential concern was the possibility of the supernatant being oversaturated. The

supernatant is a soup composing of the media components as well as of the substances released from cultured cells. This potential oversaturation might prevent adequate sampling and analysis when attempting to observe one component among the many. This possible issue was tackled through a Slide-A-Lyzer Dialysis Cassettes (Thermo Scientific, Rockford, IL) with a 7 kDA molecular weight cut off. Even with the trouble shooting performed, the ELISAs were unable to replicate the increase in fractalkine release seen using the membrane arrays.

### *IL-6*

IL-6 became a cytokine of interest because it is a known pro-anti-inflammatory cytokine that is believed to promote survival of cholinergic neurons, induce synthesis of nerve growth factor, aid in the regulation of synaptic functions (Gruol, 2015), and is known to assist astrocytes during the vasculogenesis phase of development. Additionally, CNTF is a member of the IL-6 cytokine family with the shared gp130 receptor (Patterson, 1992). And the expectation the IL-6 would be a potential neuroprotective and axonal sprouting factor has been documented by Leibinger et al. (2013).

Our analysis showed a combined increase of 22.22% on the RayBio Membrane Arrays 1 and 2, equivalent to a 1.24-fold increase. Quantitative analysis of IL-6 release into the supernatant by the cultured astrocytes using the R&D Systems ELISA did show significance at the 72-hour time point using a one-way ANOVA between the control and treated samples with a p value of 0.0225. A two-way ANOVA indicated a very significant column factor of  $p = 0.0021$ .



Unfortunately, this significance was with a higher quantity of IL-6 release in the control supernatant over either of the treated samples. At the RNA level, the Neurotrophins and Receptors RT<sup>2</sup> PCR analysis of IL-6 showed a down regulation. Here we observed a -1.01-fold decrease equivalent to a -3.23% change.

Similar to that of fractalkine, the reasons for the discrepancies is unknown. A possible solution would be to increase the number of (n) for each of the tests. Increasing the number of samples may help bring the different experimental data sets closer together. Additionally, the ELISAs and cytokine membrane arrays observed cytokine release following 72 hours of rrCNTF exposure and the RT<sup>2</sup> PCR only went to 24 hours. It is possible that an increased RNA change would be seen at a later time point.

### *VEGF*

VEGF acts on endothelial cells by increasing permeability, inducing angiogenesis, migration, but most importantly by inhibiting apoptosis (Saito et al., 2011). Interestingly, a European study of 1000 amyotrophic lateral sclerosis patients exhibited a reduced VEGF plasma level (Lambrechts et al., 2003). Additionally the application of VEGF to organotypic cultures has shown an increased survival of dopaminergic neurons (W. F. Silverman, Krum, Mani, & Rosenstein, 1999). These finding point towards VEGF having neuroprotective potential within our system.

The release of VEGF by cultured astrocytes presented a 36.54% increase, or a 1.386-fold increase, after a 72 hour rrCNTF incubation when analyzing the

cytokine membrane arrays. Quantitative analysis of VEGF using the R&D Systems ELISA showed a different outcome. No significance was observed between the rrCNTF treated cultures' and the control cultures' supernatants. Furthermore, the RT<sup>2</sup> PCR Signal transduction Pathwayfinder analysis showed a 121% decrease in RNA equivalent to a -2.22-fold reduction.

VEGF's production by astrocytes is known to decrease following the vacuolization of the CNS (Sofroniew & Vinters, 2010). However, it could be hypothesized that following traumatic brain injury, one would see increased levels of VEGF during the repair and formation of blood vessels within the CNS. Similar to IL-6, the RT<sup>2</sup> PCR only looked at 6, 12 and 24-hour time points. It is possible that the increase in RNA production happens at a later time point, or that the astrocyte needs an outside stimulus in addition to CNTF for the production of VEGF.

### *LIX*

According to the cytokine membrane array, the chemokine LIX, also known as CXCL5, showed an 18.4% increase in cellular release. This is equivalent to a 1.24 fold increase following a 72 hour exogenous exposure to CNTF. The ELISA was not able to detect any optical density, and the RT<sup>2</sup> PCR Chemokines and Receptors showed a -23.98%, or 1.24 fold down regulation in gene expression. This chemokine, which acts as a neutrophil chemoattractant, currently has no published data regarding its release from astrocytes in response to CNTF and very little is known about its role in the CNS.

### *Summary of Specific Aim II*

The tested cytokines (IL-6, fractalkine, VEGF, and LIX), all showed variances between the RayBio Cytokine Membrane Arrays and the quantitative RayBio and R&D Systems ELISAs for expression and release. The SaBiosciences RT<sup>2</sup> PCRs indicated that there are changes in RNA expression, although these changes did not fall within our set 3-fold parameter and some indicated a down regulation. However, even though there was little to no consistency between the data sets, these cytokines may still have a potential neuroprotective effect. An additional data point of 72 hours should be established with the RT<sup>2</sup> PCR for a better time comparison. Additionally, these cytokines could be individually administered exogenously to MCN cell cultures or to the hypothalamic explant cultures to test the possibility of pro-survival factors associated with each of the cytokines.

Specific Aim III: Determine if Response is a Result of CNTF Activation of the JAK2/STAT3 Pathway by Examining if the Inhibition of JAK2/STAT3 will Alter the CNTF Induced Functional Outcome

It has been demonstrated that the neurotrophin CNTF functions through the activation of multiple pathways (Alonzi et al., 2001; Askvig & Watt, 2015; Dolcet et al., 2001). The pathway of interest in this study was the Jak2/STAT3 pathway which had previously been shown to be necessary in the CNTF-mediated survival of the MCN (Askvig, Lo, et al., 2012; Askvig et al., 2013). This was demonstrated by decreased neuronal survival following the use of two inhibitors; AG490, a Jak2 inhibitor, and cucurbitacin a STAT3 inhibitor.

## AG490

The Jak2 inhibitor AG490 is a proven inhibitor preventing the prosurvival effects of CNTF within the intact SON (Askvig, Lo, et al., 2012). Prior to the application of AG490 to the cultured cells for testing the inhibitory affects, the proper dosage was determined by cell viability. Cell viability was the highest after 4 hours of incubation in AG490 and dosages of 50  $\mu$ M and higher had a roughly 20% decrease in cell survival regardless of CNTF exposure (Figure 26). However, even with the higher dosages of 50  $\mu$ M and 100  $\mu$ M we saw a survival rate between 40-50% over the twelve-hour testing period allowing for us to use the same dosage of 50  $\mu$ M used by Askvig et.al. (2013) in our inhibition experiments. Following the AG490 exposure, the translocation of pSTAT3 tyr 705 from the astrocyte cytosol to the nucleus was still observed The translocation seen within the inhibited cultures was equivalent to those that did not receive AG490. This observation indicates that the inhibition of Jak2 via AG490 either did not occur or that the cultured astrocytes were utilizing another pathway. With the translocation of pSTAT3 tyr 705 to the nucleus, it is expected that the astrocytes would still be able to produce its neuroprotective effects in response to activation by CNTF. The binding of CNTF to its receptor has the ability to potentiate an activity via the phosphorylation of any member of the Jak-Tyk family (Stahl et al., 1994; Stahl et al., 1995). Additionally, Stahl et al. (1995) indicated that in their unpublished data, the phosphorylation of STAT3 is a constant but that the activation of different Jak subunits is cell dependent. This is a possible explanation for the discrepancy seen between the inhibition documented within

the explant cultures and the inability of AG490 to inhibit the CNTF induced activation of the cultured astrocytes. Being the explant cultures are an intact cellular brain model, it is possible that the exposure to AG490 played an inhibitory role within a different cell resulting in the decreased neuronal survival seen. Conversely, it is possible that being the cultured astrocytes are a cortical culture and not just astrocytes cultured from the hypothalamic neurosecretory system, that different populations of astrocytes respond differently to the exposure of CNTF by eliciting either Jak 1 or Tyk2.

#### *Cucurbitacin*

Cucurbitacin, a known STAT3 inhibitor, has been demonstrated by our lab to prevent the pro-survival effects initiated by CNTF in organotypic cultures (Askvig et al., 2013; Askvig & Watt, 2015). Similar to AG490, cell viability was tested for this inhibitor to ensure that prolonged exposure did not induce detrimental cellular death. Figure 27 illustrates that the cell viability is highest for cells exposed to FBS and CNTF while in the presence of cucurbitacin over a 12-hour time frame starting. A majority of the readings indicate a cell viability higher than 100% when compared to the controls. This could be a result of several factors. One possible factor is that astrocytes proliferate at a high rate, especially when exposed to stress (Sofroniew & Vinters, 2010). The introduction of CNTF and/or cucurbitacin may potentially increase the proliferation rate of the cultured astrocytes. Regardless of the readings, we were able to determine that cucurbitacin does not have an apoptotic effect on the cultured astrocytes at the given dosage.

The examination of cucurbitacin's inhibition effect on the cultured astrocytes was tested by observing the translocation of pSTAT3 tyr 705 from the cytosol to the nucleus. It is expected that the inhibition of STAT by cucurbitacin would prevent the translocation event from occurring. The nuclear extraction analysis showed the expected results as can be seen in Figure 29. By preventing the translocation of pSTAT3 tyr 705 to the nucleus, it can be deduced that the activation of the astrocyte by CNTF is being prevented. This inhibitory effect would theoretically prevent the cultured astrocyte from producing any probable neuroprotective substances in response to the CNTF that has been documented *in vivo* and in the hypothalamic explant cultures. This arresting of the CNTF activation pathway would undoubtedly result in magnocellular neuron loss.

Specific Aim IV: Determine if the Functional Response Promotes  
Survival and Sprouting of Neurons Utilizing the  
Hypothalamic Explants Cultures

*Astrocyte Conditioned Media Application*

The organotypic hypothalamic explant cultures provides a model that is very comparable to experimentation *in vivo*. This model provides an exceedingly effective means of observing the OT and VP neurons found within the MNS (Askvig, Lo, et al., 2012; House, Thomas, Kusano, & Gainer, 1998). Our lab has previously shown that the exogenous application of CNTF to the explant cultures results in a significant oxytocinergic neuron survival rate. Additionally, Askvig et al. (2012, 2015) showed that multiple pathways are activated by CNTF through the inhibition of those pathways in these cultures.

The application of treated astrocyte conditioned media to the organotypic hypothalamic explant cultures displayed significant neuroprotective effects. ACM from astrocytes treated with exogenous CNTF displayed a significant rate of OT neuron survival when compared to ACM from non-treated cultures. This effect attests that CNTF stimulates cultured astrocytes and initiates an increased production and expression of factors that result in a prosurvival neuronal response.

The addition of an AG490 inhibition treatment to the astrocyte cultures did not diminish the prosurvival effects seen with CNTF (Figures 30 and 31). This corresponds to the previous discussion indicating that the inhibition of Jak2 by AG490 in astrocyte cultures does not prevent the phosphorylation and translocation of STAT3 tyr 705 to the nucleus. With the translocation of pSTAT3 tyr 705, we are still seeing an activation of the cultured astrocyte and the upregulation of prosurvival factors as displayed by the application of the ACM to the explant cultures. This was the expected outcome following the translocation study, and confirmed that the inhibition of Jak2 within cultured astrocytes does not arrest the CNTF signaling pathway. As previously mentioned, this is in contrast to the explant inhibition studies which applied the inhibitor AG490 directly to the explant cultures mediating a decreased survival of the OT neurons. Again, this could be due to CNTF activating another member of the Jak-Tyk family within the cultured cortical astrocytes.

The inhibition of STAT3 in the astrocyte cultures with cucurbitacin produced a drastic and significant decrease in OT neuron survival following the

ACM application (Figures 30 and 31). The addition of cucurbitacin resulted in lower neuron survival compared to all other treatments, including the control ACM. Unlike the other treatments, the addition of CNTF following a 1 hour incubation in the presence of the inhibitor did not result in a statistically significant increase in neuron survival within either the PVN or the SON. This data brings to light that the translocation of pSTAT tyr 705 is absolutely necessary for the activation of cultured astrocytes by CNTF to potentiate survival of axotomized magnocellular neurons.

### Summary

The present study demonstrated that CNTF potentiates survival of axotomized magnocellular neurons through activation of astrocyte-specific signal transduction pathways leading to increased expression levels of factors which mediate the neuronal response. In order for this to occur, it was necessary to demonstrate the activation of the Jak/STAT pathway within the cultured astrocytes by first proving that the tripartite receptor complex is maintained and expressed in the primary rat cortical astrocyte cultures.

Activation of the Jak/STAT pathway by exogenous CNTF in astrocytes was shown by the translocation of phosphorylated STAT3 tyrosine 705 from the cytosol to the cell nucleus. The translocation of STAT initiates a functional response within the astrocytes. This functional response is seen in the expression changes of an undetermined amount of cytokines, chemokines, receptors, and neurotransmitters among other possible factors. Some potentially increased factors include VEGF, IL-6, LIX, and fractalkine.



The inhibition of Jak2 by AG490 does not diminish the activation of cultured astrocytes by CNTF, as shown by the nuclear extraction analysis displaying that pSTAT3 tyr was still translocating. This was further demonstrated in the OT neuron counts of both the PVN and SON from the explant cultures. Conversely, the inhibition of STAT3 via cucurbitacin did prevent the translocation of pSTAT3 tyr 705. This inhibition was shown to significantly arrest the CNTF induced release of neuronal pro-survival affects within the explant cultures.

This study demonstrates that astrocytes are an essential component to the CNTF story. Further experiments to expand on this study would be designed to better understand what neuronal pro-survival factors are being released by the astrocytes in response to CNTF. Our current VEGF, LIX, IL-6 and fractalkine data is inconsistent. As previously mentioned, it would be worthwhile to divulge further into these cytokines by looking at additional time points and doing qPCR. A continuation study could utilize a Digi west which analyzes over 1000 potential proteins by using only 1 mg of sample. This experimentation could be utilized on a condensed supernatant as well as the cytosolic nuclear extraction. This analysis, albeit broad, is more qualitative than the cytokine membrane arrays and would potentially assist in honing in on potential neuroprotective factors produced by the astrocytes. Additionally, further exploration of the low level of gp130 expression on the cultured astrocytes would be necessary to determine if the in vitro expression affects the overall outcome. As noted by the RT<sup>2</sup> PCR data, numerous genes have a minimum of a three-fold expression change and the ACM application to explant cultures proves that astrocytes are reacting to CNTF

in a manner that promotes oxytocin magnocellular neuron survival. Among these genes is the explanation for the astrocytes ability to potentiate the survival of magnocellular neurons.

## REFERENCES

- Adler, R., Landa, K. B., Manthorpe, M., & Varon, S. (1979). Cholinergic neurotrophic factors: intraocular distribution of trophic activity for ciliary neurons. *Science*, *204*(4400), 1434-1436.
- Alonso, G., & Assenmacher, I. (1981). Radioautographic studies on the neurohypophysial projections of the supraoptic and paraventricular nuclei in the rat. *Cell Tissue Res*, *219*(3), 525-534.
- Alonzi, T., Middleton, G., Wyatt, S., Buchman, V., Betz, U. A., Muller, W., . . . Davies, A. M. (2001). Role of STAT3 and PI 3-kinase/Akt in mediating the survival actions of cytokines on sensory neurons. *Mol Cell Neurosci*, *18*(3), 270-282. doi:10.1006/mcne.2001.1018
- Alvarez-Buylla, R., Livett, B. G., Uttenthal, L. O., Hope, D. B., & Milton, S. H. (1973). Immunochemical evidence for the transport of neurophysin in the hypothalamo-neurohypophysial system of the dog. *Z Zellforsch Mikrosk Anat*, *137*(4), 435-450.
- Antunes, J. L., Carmel, P. W., & Zimmerman, E. A. (1977). Projections from the paraventricular nucleus to the zona externa of the median eminence of the rhesus monkey: an immunohistochemical study. *Brain Res*, *137*(1), 1-10.
- Arakawa, Y., Sendtner, M., & Thoenen, H. (1990). Survival effect of ciliary neurotrophic factor (CNTF) on chick embryonic motoneurons in culture: comparison with other neurotrophic factors and cytokines. *J Neurosci*, *10*(11), 3507-3515.
- Arnoux, I., & Audinat, E. (2015). Fractalkine Signaling and Microglia Functions in the Developing Brain. *Neural Plast*, *2015*, 689404. doi:10.1155/2015/689404
- Arthur, F. E., Shivers, R. R., & Bowman, P. D. (1987). Astrocyte-mediated induction of tight junctions in brain capillary endothelium: an efficient in vitro model. *Brain Res*, *433*(1), 155-159.

- Askvig, J. M., Leiphon, L. J., & Watt, J. A. (2012). Neuronal activity and axonal sprouting differentially regulate CNTF and CNTF receptor complex in the rat supraoptic nucleus. *Exp Neurol*, *233*(1), 243-252. doi:10.1016/j.expneurol.2011.10.009
- Askvig, J. M., Lo, D. Y., Sudbeck, A. W., Behm, K. E., Leiphon, L. J., & Watt, J. A. (2012). Inhibition of the Jak-STAT pathway prevents CNTF-mediated survival of axotomized oxytocinergic magnocellular neurons in organotypic cultures of the rat supraoptic nucleus. *Exp Neurol*. doi:10.1016/j.expneurol.2012.10.023
- Askvig, J. M., Lo, D. Y., Sudbeck, A. W., Behm, K. E., Leiphon, L. J., & Watt, J. A. (2013). Inhibition of the Jak-STAT pathway prevents CNTF-mediated survival of axotomized oxytocinergic magnocellular neurons in organotypic cultures of the rat supraoptic nucleus. *Exp Neurol*, *240*, 75-87. doi:10.1016/j.expneurol.2012.10.023
- Askvig, J. M., & Watt, J. A. (2015). The MAPK and PI3K pathways mediate CNTF-induced neuronal survival and process outgrowth in hypothalamic organotypic cultures. *J Cell Commun Signal*, *9*(3), 217-231. doi:10.1007/s12079-015-0268-8
- Ayoub, A. E., & Salm, A. K. (2003). Increased morphological diversity of microglia in the activated hypothalamic supraoptic nucleus. *J Neurosci*, *23*(21), 7759-7766.
- Barbin, G., Manthorpe, M., & Varon, S. (1984). Purification of the chick eye ciliary neuronotrophic factor. *J Neurochem*, *43*(5), 1468-1478.
- Bazan, J. F. (1991). Neuropoietic cytokines in the hematopoietic fold. *Neuron*, *7*(2), 197-208.
- Bernal, G. M., & Peterson, D. A. (2011). Phenotypic and gene expression modification with normal brain aging in GFAP-positive astrocytes and neural stem cells. *Aging Cell*, *10*(3), 466-482. doi:10.1111/j.1474-9726.2011.00694.x
- Bodian, D., & Maren, T. H. (1951). The effect of neuro- and adenohipophysectomy on retrograde degeneration in hypothalamic nuclei of the rat. *J Comp Neurol*, *94*(3), 485-511.
- Bonfanti, L., Poulain, D. A., & Theodosis, D. T. (1993). Radial glia-like cells in the supraoptic nucleus of the adult rat. *J Neuroendocrinol*, *5*(1), 1-5.

- Bonni, A., Frank, D. A., Schindler, C., & Greenberg, M. E. (1993). Characterization of a pathway for ciliary neurotrophic factor signaling to the nucleus. *Science*, *262*(5139), 1575-1579.
- Bourque, C. W., Oliet, S. H., & Richard, D. (1994). Osmoreceptors, osmoreception, and osmoregulation. *Front Neuroendocrinol*, *15*(3), 231-274. doi:10.1006/frne.1994.1010
- Bush, T. G., Puvanachandra, N., Horner, C. H., Polito, A., Ostenfeld, T., Svendsen, C. N., . . . Sofroniew, M. V. (1999). Leukocyte infiltration, neuronal degeneration, and neurite outgrowth after ablation of scar-forming, reactive astrocytes in adult transgenic mice. *Neuron*, *23*(2), 297-308.
- Bushong, E. A., Martone, M. E., Jones, Y. Z., & Ellisman, M. H. (2002). Protoplasmic astrocytes in CA1 stratum radiatum occupy separate anatomical domains. *J Neurosci*, *22*(1), 183-192.
- Carter, C. S. (1998). Neuroendocrine perspectives on social attachment and love. *Psychoneuroendocrinology*, *23*(8), 779-818.
- Christopherson, K. S., Ullian, E. M., Stokes, C. C., Mallowney, C. E., Hell, J. W., Agah, A., . . . Barres, B. A. (2005). Thrombospondins are astrocyte-secreted proteins that promote CNS synaptogenesis. *Cell*, *120*(3), 421-433. doi:10.1016/j.cell.2004.12.020
- Cross, B. A., Dyball, R. E., Dyer, R. G., Jones, C. W., Lincoln, D. W., Morris, J. F., & Pickering, B. T. (1975). Endocrine neurons. *Recent Prog Horm Res*, *31*, 243-294.
- Dani, J. W., & Smith, S. J. (1995). The triggering of astrocytic calcium waves by NMDA-induced neuronal activation. *Ciba Found Symp*, *188*, 195-205; discussion 205-199.
- Davis, S., Aldrich, T. H., Ip, N. Y., Stahl, N., Scherer, S., Farruggella, T., . . . et al. (1993). Released form of CNTF receptor alpha component as a soluble mediator of CNTF responses. *Science*, *259*(5102), 1736-1739.
- Davis, S., Aldrich, T. H., Stahl, N., Pan, L., Taga, T., Kishimoto, T., . . . Yancopoulos, G. D. (1993). LIFR beta and gp130 as heterodimerizing signal transducers of the tripartite CNTF receptor. *Science*, *260*(5115), 1805-1808.

- Davis, S., Aldrich, T. H., Valenzuela, D. M., Wong, V. V., Furth, M. E., Squinto, S. P., & Yancopoulos, G. D. (1991). The receptor for ciliary neurotrophic factor. *Science*, *253*(5015), 59-63.
- Dobrea, G. M., Unnerstall, J. R., & Rao, M. S. (1992). The expression of CNTF message and immunoreactivity in the central and peripheral nervous system of the rat. *Brain Res Dev Brain Res*, *66*(2), 209-219.
- Dolcet, X., Soler, R. M., Gould, T. W., Egea, J., Oppenheim, R. W., & Comella, J. X. (2001). Cytokines promote motoneuron survival through the Janus kinase-dependent activation of the phosphatidylinositol 3-kinase pathway. *Mol Cell Neurosci*, *18*(6), 619-631. doi:10.1006/mcne.2001.1058
- Dunn, F. L., Brennan, T. J., Nelson, A. E., & Robertson, G. L. (1973). The role of blood osmolality and volume in regulating vasopressin secretion in the rat. *J Clin Invest*, *52*(12), 3212-3219. doi:10.1172/JCI107521
- Ebendal, T., Olson, L., Seiger, A., & Hedlund, K. O. (1980). Nerve growth factors in the rat iris. *Nature*, *286*(5768), 25-28.
- Eddleston, M., & Mucke, L. (1993). Molecular profile of reactive astrocytes--implications for their role in neurologic disease. *Neuroscience*, *54*(1), 15-36.
- Escartin, C., Pierre, K., Colin, A., Brouillet, E., Delzescaux, T., Guillermier, M., . . . Bonvento, G. (2007). Activation of astrocytes by CNTF induces metabolic plasticity and increases resistance to metabolic insults. *J Neurosci*, *27*(27), 7094-7104. doi:10.1523/JNEUROSCI.0174-07.2007
- Falke, N. (1991). Modulation of oxytocin and vasopressin release at the level of the neurohypophysis. *Prog Neurobiol*, *36*(6), 465-484.
- Faulkner, J. R., Herrmann, J. E., Woo, M. J., Tansey, K. E., Doan, N. B., & Sofroniew, M. V. (2004). Reactive astrocytes protect tissue and preserve function after spinal cord injury. *J Neurosci*, *24*(9), 2143-2155. doi:10.1523/JNEUROSCI.3547-03.2004
- Fee, D., Grzybicki, D., Dobbs, M., Ihyer, S., Clotfelter, J., Macvilay, S., . . . Fabry, Z. (2000). Interleukin 6 promotes vasculogenesis of murine brain microvessel endothelial cells. *Cytokine*, *12*(6), 655-665. doi:10.1006/cyto.1999.0599
- Felten, D. L., & Cashner, K. A. (1979). Cytoarchitecture of the supraoptic nucleus. A Golgi study. *Neuroendocrinology*, *29*(4), 221-230.

- Fitch, M. T., & Silver, J. (2008). CNS injury, glial scars, and inflammation: Inhibitory extracellular matrices and regeneration failure. *Exp Neurol*, 209(2), 294-301. doi:10.1016/j.expneurol.2007.05.014
- Flament-Durand, J. (1980). The hypothalamus: anatomy and functions. *Acta Psychiatr Belg*, 80(4), 364-375.
- Frank, D. A., & Greenberg, M. E. (1996). Signal transduction pathways activated by ciliary neurotrophic factor and related cytokines. *Perspect Dev Neurobiol*, 4(1), 3-18.
- Friedman, B., Scherer, S. S., Rudge, J. S., Helgren, M., Morrissey, D., McClain, J., . . . et al. (1992). Regulation of ciliary neurotrophic factor expression in myelin-related Schwann cells in vivo. *Neuron*, 9(2), 295-305.
- Garcia-Segura, L. M., & Melcangi, R. C. (2006). Steroids and glial cell function. *Glia*, 54(6), 485-498. doi:10.1002/glia.20404
- Gariano, R. F. (2003). Cellular mechanisms in retinal vascular development. *Prog Retin Eye Res*, 22(3), 295-306.
- Gearing, D. P., Ziegler, S. F., Comeau, M. R., Friend, D., Thoma, B., Cosman, D., . . . Mosley, B. (1994). Proliferative responses and binding properties of hematopoietic cells transfected with low-affinity receptors for leukemia inhibitory factor, oncostatin M, and ciliary neurotrophic factor. *Proc Natl Acad Sci U S A*, 91(3), 1119-1123.
- Gerwins, P., Skoldenberg, E., & Claesson-Welsh, L. (2000). Function of fibroblast growth factors and vascular endothelial growth factors and their receptors in angiogenesis. *Crit Rev Oncol Hematol*, 34(3), 185-194.
- Gomori, G. (1939). A differential stain for cell types in the pancreatic islets. *Am J Pathol*, 15(4), 497-499 492.
- Gomori, G. (1941). Observations with differential stains on human islets of langerhans. *Am J Pathol*, 17(3), 395-406 393.
- Gomori, G. (1950). Aldehyde-fuchsin: a new stain for elastic tissue. *Am J Clin Pathol*, 20(7), 665-666.
- Gordon, G. R., Mulligan, S. J., & MacVicar, B. A. (2007). Astrocyte control of the cerebrovasculature. *Glia*, 55(12), 1214-1221. doi:10.1002/glia.20543

- Gruol, D. L. (2015). IL-6 regulation of synaptic function in the CNS. *Neuropharmacology*, 96(Pt A), 42-54.  
doi:10.1016/j.neuropharm.2014.10.023
- Haas, C., Neuhuber, B., Yamagami, T., Rao, M., & Fischer, I. (2012). Phenotypic analysis of astrocytes derived from glial restricted precursors and their impact on axon regeneration. *Exp Neurol*, 233(2), 717-732.  
doi:10.1016/j.expneurol.2011.11.002
- Halassa, M. M., Fellin, T., & Haydon, P. G. (2007). The tripartite synapse: roles for gliotransmission in health and disease. *Trends Mol Med*, 13(2), 54-63.  
doi:10.1016/j.molmed.2006.12.005
- Harris, G. W. (1947). The innervation and actions of the neuro-hypophysis; an investigation using the method of remote-control stimulation. *Philos Trans R Soc Lond B Biol Sci*, 232(590), 385-441.
- Harris, G. W. (1948). Hypothalamus and pituitary gland with special reference to the posterior pituitary and labour. *Br Med J*, 1(4546), 339-342.
- Hatton, G. I. (1983). Some well-kept hypothalamic secrets disclosed. *Fed Proc*, 42(12), 2869-2874.
- Hatton, G. I. (1986). Plasticity in the hypothalamic magnocellular neurosecretory system. *Fed Proc*, 45(9), 2328-2333.
- Hatton, G. I. (1988). Pituicytes, glia and control of terminal secretion. *J Exp Biol*, 139, 67-79.
- Helfand, S. L., Riopelle, R. J., & Wessells, N. K. (1978). Non-equivalence of conditioned medium and nerve growth factor for sympathetic, parasympathetic, and sensory neurons. *Exp Cell Res*, 113(1), 39-45.
- Helfand, S. L., Smith, G. A., & Wessells, N. K. (1976). Survival and development in culture of dissociated parasympathetic neurons from ciliary ganglia. *Dev Biol*, 50(2), 541-547.
- Hernandez, V. S., Vazquez-Juarez, E., Marquez, M. M., Jauregui-Huerta, F., Barrio, R. A., & Zhang, L. (2015). Extra-neurohypophyseal axonal projections from individual vasopressin-containing magnocellular neurons in rat hypothalamus. *Front Neuroanat*, 9, 130.  
doi:10.3389/fnana.2015.00130



- Hibi, M., Nakajima, K., & Hirano, T. (1996). IL-6 cytokine family and signal transduction: a model of the cytokine system. *J Mol Med (Berl)*, *74*(1), 1-12.
- Hirano, T., Matsuda, T., & Nakajima, K. (1994). Signal transduction through gp130 that is shared among the receptors for the interleukin 6 related cytokine subfamily. *Stem Cells*, *12*(3), 262-277. doi:10.1002/stem.5530120303
- Hou-Yu, A., Lamme, A. T., Zimmerman, E. A., & Silverman, A. J. (1986). Comparative distribution of vasopressin and oxytocin neurons in the rat brain using a double-label procedure. *Neuroendocrinology*, *44*(2), 235-246.
- House, S. B., Li, C., Yue, C., & Gainer, H. (2009). Effects of ciliary neurotrophic factor and leukemia inhibiting factor on oxytocin and vasopressin magnocellular neuron survival in rat and mouse hypothalamic organotypic cultures. *J Neurosci Methods*, *178*(1), 128-133. doi:10.1016/j.jneumeth.2008.12.004
- House, S. B., Thomas, A., Kusano, K., & Gainer, H. (1998). Stationary organotypic cultures of oxytocin and vasopressin magnocellular neurones from rat and mouse hypothalamus. *J Neuroendocrinol*, *10*(11), 849-861.
- Hudgins, S. N., & Levison, S. W. (1998). Ciliary neurotrophic factor stimulates astroglial hypertrophy in vivo and in vitro. *Exp Neurol*, *150*(2), 171-182. doi:10.1006/exnr.1997.6735
- Hughes, S. M., Lillien, L. E., Raff, M. C., Rohrer, H., & Sendtner, M. (1988). Ciliary neurotrophic factor induces type-2 astrocyte differentiation in culture. *Nature*, *335*(6185), 70-73. doi:10.1038/335070a0
- Iadecola, C., & Nedergaard, M. (2007). Glial regulation of the cerebral microvasculature. *Nat Neurosci*, *10*(11), 1369-1376. doi:10.1038/nn2003
- Ip, N. Y., Li, Y. P., van de Stadt, I., Panayotatos, N., Alderson, R. F., & Lindsay, R. M. (1991). Ciliary neurotrophic factor enhances neuronal survival in embryonic rat hippocampal cultures. *J Neurosci*, *11*(10), 3124-3134.
- Ip, N. Y., McClain, J., Barrezueta, N. X., Aldrich, T. H., Pan, L., Li, Y., . . . Yancopoulos, G. D. (1993). The alpha component of the CNTF receptor is required for signaling and defines potential CNTF targets in the adult and during development. *Neuron*, *10*(1), 89-102.

- Ip, N. Y., Nye, S. H., Boulton, T. G., Davis, S., Taga, T., Li, Y., . . . et al. (1992). CNTF and LIF act on neuronal cells via shared signaling pathways that involve the IL-6 signal transducing receptor component gp130. *Cell*, *69*(7), 1121-1132.
- Ip, N. Y., Wiegand, S. J., Morse, J., & Rudge, J. S. (1993). Injury-induced regulation of ciliary neurotrophic factor mRNA in the adult rat brain. *Eur J Neurosci*, *5*(1), 25-33.
- Ip, N. Y., & Yancopoulos, G. D. (1992). Ciliary neurotrophic factor and its receptor complex. *Prog Growth Factor Res*, *4*(2), 139-155.
- Ip, N. Y., & Yancopoulos, G. D. (1996). The neurotrophins and CNTF: two families of collaborative neurotrophic factors. *Annu Rev Neurosci*, *19*, 491-515. doi:10.1146/annurev.ne.19.030196.002423
- Ju, G., Liu, S., & Tao, J. (1986). Projections from the hypothalamus and its adjacent areas to the posterior pituitary in the rat. *Neuroscience*, *19*(3), 803-828.
- Justicia, C., Gabriel, C., & Planas, A. M. (2000). Activation of the JAK/STAT pathway following transient focal cerebral ischemia: signaling through Jak1 and Stat3 in astrocytes. *Glia*, *30*(3), 253-270.
- Kahn, M. A., Ellison, J. A., Speight, G. J., & de Vellis, J. (1995). CNTF regulation of astrogliosis and the activation of microglia in the developing rat central nervous system. *Brain Res*, *685*(1-2), 55-67.
- Kalimo, H. (1975). Ultrastructural studies on the hypothalamic neurosecretory neurons of the rat. III. Paraventricular and supraoptic neurons during lactation and dehydration. *Cell Tissue Res*, *163*(2), 151-168.
- Kamiguchi, H., Yoshida, K., Sagoh, M., Sasaki, H., Inaba, M., Wakamoto, H., . . . Toya, S. (1995). Release of ciliary neurotrophic factor from cultured astrocytes and its modulation by cytokines. *Neurochem Res*, *20*(10), 1187-1193.
- Kang, S. S., Keasey, M. P., Cai, J., & Hagg, T. (2012). Loss of neuron-astroglial interaction rapidly induces protective CNTF expression after stroke in mice. *J Neurosci*, *32*(27), 9277-9287. doi:10.1523/JNEUROSCI.1746-12.2012
- Kato, A. C., & Lindsay, R. M. (1994). Overlapping and additive effects of neurotrophins and CNTF on cultured human spinal cord neurons. *Exp Neurol*, *130*(2), 196-201. doi:10.1006/exnr.1994.1198

- Kimelberg, H. K. (2010). Functions of mature mammalian astrocytes: a current view. *Neuroscientist*, 16(1), 79-106. doi:10.1177/1073858409342593
- Koehler, R. C., Roman, R. J., & Harder, D. R. (2009). Astrocytes and the regulation of cerebral blood flow. *Trends Neurosci*, 32(3), 160-169. doi:10.1016/j.tins.2008.11.005
- Kruger, T. H., Haake, P., Chereath, D., Knapp, W., Janssen, O. E., Exton, M. S., . . . Hartmann, U. (2003). Specificity of the neuroendocrine response to orgasm during sexual arousal in men. *J Endocrinol*, 177(1), 57-64.
- Lam, A., Fuller, F., Miller, J., Kloss, J., Manthorpe, M., Varon, S., & Cordell, B. (1991). Sequence and structural organization of the human gene encoding ciliary neurotrophic factor. *Gene*, 102(2), 271-276.
- Lambrechts, D., Storkebaum, E., Morimoto, M., Del-Favero, J., Desmet, F., Marklund, S. L., . . . Carmeliet, P. (2003). VEGF is a modifier of amyotrophic lateral sclerosis in mice and humans and protects motoneurons against ischemic death. *Nat Genet*, 34(4), 383-394. doi:10.1038/ng1211
- Laterra, J., Guerin, C., & Goldstein, G. W. (1990). Astrocytes induce neural microvascular endothelial cells to form capillary-like structures in vitro. *J Cell Physiol*, 144(2), 204-215. doi:10.1002/jcp.1041440205
- Lee, M. Y., Deller, T., Kirsch, M., Frotscher, M., & Hofmann, H. D. (1997). Differential regulation of ciliary neurotrophic factor (CNTF) and CNTF receptor alpha expression in astrocytes and neurons of the fascia dentata after entorhinal cortex lesion. *J Neurosci*, 17(3), 1137-1146.
- Leibinger, M., Muller, A., Gobrecht, P., Diekmann, H., Andreadaki, A., & Fischer, D. (2013). Interleukin-6 contributes to CNS axon regeneration upon inflammatory stimulation. *Cell Death Dis*, 4, e609. doi:10.1038/cddis.2013.126
- Leng, G., Caquineau, C., & Sabatier, N. (2005). Regulation of oxytocin secretion. *Vitam Horm*, 71, 27-58. doi:10.1016/S0083-6729(05)71002-5
- Leranth, C., Zaborszky, L., Marton, J., & Palkovits, M. (1975). Quantitative studies on the supraoptic nucleus in the rat. I. Synaptic organization. *Exp Brain Res*, 22(5), 509-523.
- Levison, S. W., Ducceschi, M. H., Young, G. M., & Wood, T. L. (1996). Acute exposure to CNTF in vivo induces multiple components of reactive gliosis. *Exp Neurol*, 141(2), 256-268. doi:10.1006/exnr.1996.0160

- Levison, S. W., Hudgins, S. N., & Crawford, J. L. (1998). Ciliary neurotrophic factor stimulates nuclear hypertrophy and increases the GFAP content of cultured astrocytes. *Brain Res*, 803(1-2), 189-193.
- Liesi, P., Dahl, D., & Vaehri, A. (1983). Laminin is produced by early rat astrocytes in primary culture. *J Cell Biol*, 96(3), 920-924.
- Lillien, L. E., Sendtner, M., & Raff, M. C. (1990). Extracellular matrix-associated molecules collaborate with ciliary neurotrophic factor to induce type-2 astrocyte development. *J Cell Biol*, 111(2), 635-644.
- Lillien, L. E., Sendtner, M., Rohrer, H., Hughes, S. M., & Raff, M. C. (1988). Type-2 astrocyte development in rat brain cultures is initiated by a CNTF-like protein produced by type-1 astrocytes. *Neuron*, 1(6), 485-494.
- Lin, L. F., Mismer, D., Lile, J. D., Armes, L. G., Butler, E. T., 3rd, Vannice, J. L., & Collins, F. (1989). Purification, cloning, and expression of ciliary neurotrophic factor (CNTF). *Science*, 246(4933), 1023-1025.
- Liu, K. D., Gaffen, S. L., & Goldsmith, M. A. (1998). JAK/STAT signaling by cytokine receptors. *Curr Opin Immunol*, 10(3), 271-278.
- Magavi, S., Friedmann, D., Banks, G., Stolfi, A., & Lois, C. (2012). Coincident generation of pyramidal neurons and protoplasmic astrocytes in neocortical columns. *J Neurosci*, 32(14), 4762-4772. doi:10.1523/JNEUROSCI.3560-11.2012
- Manthorpe, M., Barbin, G., & Varon, S. (1982). Isoelectric focusing of the chick eye ciliary neurotrophic factor. *J Neurosci Res*, 8(2-3), 233-239. doi:10.1002/jnr.490080213
- Manthorpe, M., Skaper, S. D., Williams, L. R., & Varon, S. (1986). Purification of adult rat sciatic nerve ciliary neurotrophic factor. *Brain Res*, 367(1-2), 282-286.
- Markakis, E. A., Palmer, T. D., Randolph-Moore, L., Rakic, P., & Gage, F. H. (2004). Novel neuronal phenotypes from neural progenitor cells. *J Neurosci*, 24(12), 2886-2897. doi:10.1523/JNEUROSCI.4161-03.2004
- McCarthy, K. D., & de Vellis, J. (1980). Preparation of separate astroglial and oligodendroglial cell cultures from rat cerebral tissue. *J Cell Biol*, 85(3), 890-902.

- McDonald, N. Q., Panayotatos, N., & Hendrickson, W. A. (1995). Crystal structure of dimeric human ciliary neurotrophic factor determined by MAD phasing. *EMBO J*, *14*(12), 2689-2699.
- Miller, R. H., & Raff, M. C. (1984). Fibrous and protoplasmic astrocytes are biochemically and developmentally distinct. *J Neurosci*, *4*(2), 585-592.
- Miyata, S., & Hatton, G. I. (2002). Activity-related, dynamic neuron-glia interactions in the hypothalamo-neurohypophysial system. *Microsc Res Tech*, *56*(2), 143-157. doi:10.1002/jemt.10012
- Montmayeur, J. P., & Borrelli, E. (1994). Targeting of G alpha i2 to the Golgi by alternative spliced carboxyl-terminal region. *Science*, *263*(5143), 95-98.
- Nag, S. (2011). Morphology and properties of astrocytes. *Methods Mol Biol*, *686*, 69-100. doi:10.1007/978-1-60761-938-3\_3
- Nedergaard, M., Ransom, B., & Goldman, S. A. (2003). New roles for astrocytes: redefining the functional architecture of the brain. *Trends Neurosci*, *26*(10), 523-530. doi:10.1016/j.tins.2003.08.008
- Neugebauer, K. M., Tomaselli, K. J., Lilien, J., & Reichardt, L. F. (1988). N-cadherin, NCAM, and integrins promote retinal neurite outgrowth on astrocytes in vitro. *J Cell Biol*, *107*(3), 1177-1187.
- Neumann, I., Russell, J. A., & Landgraf, R. (1993). Oxytocin and vasopressin release within the supraoptic and paraventricular nuclei of pregnant, parturient and lactating rats: a microdialysis study. *Neuroscience*, *53*(1), 65-75.
- Nordmann, J. J. (1977). Ultrastructural morphometry of the rat neurohypophysis. *J Anat*, *123*(Pt 1), 213-218.
- Oberheim, N. A., Wang, X., Goldman, S., & Nedergaard, M. (2006). Astrocytic complexity distinguishes the human brain. *Trends Neurosci*, *29*(10), 547-553. doi:10.1016/j.tins.2006.08.004
- Olivecrona, H. (1957). Paraventricular nucleus and pituitary gland. *Acta Physiol Scand Suppl*, *40*(136), 1-178.
- Panayotatos, N., Radziejewska, E., Acheson, A., Somogyi, R., Thadani, A., Hendrickson, W. A., & McDonald, N. Q. (1995). Localization of functional receptor epitopes on the structure of ciliary neurotrophic factor indicates a conserved, function-related epitope topography among helical cytokines. *J Biol Chem*, *270*(23), 14007-14014.

- Park, C. K., Ju, W. K., Hofmann, H. D., Kirsch, M., Ki Kang, J., Chun, M. H., & Lee, M. Y. (2000). Differential regulation of ciliary neurotrophic factor and its receptor in the rat hippocampus following transient global ischemia. *Brain Res*, 861(2), 345-353.
- Patterson, P. H. (1992). The emerging neuropoietic cytokine family: first CDF/LIF, CNTF and IL-6; next ONC, MGF, GCSF? *Curr Opin Neurobiol*, 2(1), 94-97.
- Pedersen, C. A., & Boccia, M. L. (2006). Vasopressin interactions with oxytocin in the control of female sexual behavior. *Neuroscience*, 139(3), 843-851. doi:10.1016/j.neuroscience.2006.01.002
- Pfeiffer-Guglielmi, B., Fleckenstein, B., Jung, G., & Hamprecht, B. (2003). Immunocytochemical localization of glycogen phosphorylase isozymes in rat nervous tissues by using isozyme-specific antibodies. *J Neurochem*, 85(1), 73-81.
- Phelps, C. H. (1972). Barbiturate-induced glycogen accumulation in brain. An electron microscopic study. *Brain Res*, 39(1), 225-234.
- Poulain, D. A., & Wakerley, J. B. (1982). Electrophysiology of hypothalamic magnocellular neurones secreting oxytocin and vasopressin. *Neuroscience*, 7(4), 773-808.
- Prevot, V., Croix, D., Bouret, S., Dutoit, S., Tramu, G., Stefano, G. B., & Beauvillain, J. C. (1999). Definitive evidence for the existence of morphological plasticity in the external zone of the median eminence during the rat estrous cycle: implication of neuro-glio-endothelial interactions in gonadotropin-releasing hormone release. *Neuroscience*, 94(3), 809-819.
- Price, J., & Hynes, R. O. (1985). Astrocytes in culture synthesize and secrete a variant form of fibronectin. *J Neurosci*, 5(8), 2205-2211.
- Raub, T. J., Kuentzel, S. L., & Sawada, G. A. (1992). Permeability of bovine brain microvessel endothelial cells in vitro: barrier tightening by a factor released from astrogloma cells. *Exp Cell Res*, 199(2), 330-340.
- Rhodes, C. H., Morrell, J. I., & Pfaff, D. W. (1981). Immunohistochemical analysis of magnocellular elements in rat hypothalamus: distribution and numbers of cells containing neurophysin, oxytocin, and vasopressin. *J Comp Neurol*, 198(1), 45-64. doi:10.1002/cne.901980106

- Richardson, P. M. (1994). Ciliary neurotrophic factor: a review. *Pharmacol Ther*, 63(2), 187-198.
- Robertshaw, D. (1989). Central and peripheral osmoreceptors. *Acta Physiol Scand Suppl*, 583, 151-156.
- Rosso, L., & Mienville, J. M. (2009). Pituicyte modulation of neurohormone output. *Glia*, 57(3), 235-243. doi:10.1002/glia.20760
- Rudge, J. S., Alderson, R. F., Pasnikowski, E., McClain, J., Ip, N. Y., & Lindsay, R. M. (1992). Expression of Ciliary Neurotrophic Factor and the Neurotrophins-Nerve Growth Factor, Brain-Derived Neurotrophic Factor and Neurotrophin 3-in Cultured Rat Hippocampal Astrocytes. *Eur J Neurosci*, 4(6), 459-471.
- Rudge, J. S., Li, Y., Pasnikowski, E. M., Mattsson, K., Pan, L., Yancopoulos, G. D., . . . Ip, N. Y. (1994). Neurotrophic factor receptors and their signal transduction capabilities in rat astrocytes. *Eur J Neurosci*, 6(5), 693-705.
- Rusnak, M., House, S. B., Arima, H., & Gainer, H. (2002). Ciliary neurotrophic factor increases the survival of magnocellular vasopressin and oxytocin neurons in rat supraoptic nucleus in organotypic cultures. *Microsc Res Tech*, 56(2), 101-112. doi:10.1002/jemt.10015
- Rusnak, M., House, S. B., & Gainer, H. (2003). Long-term effects of ciliary neurotrophic factor on the survival of vasopressin magnocellular neurones in the rat supraoptic nucleus in vitro. *J Neuroendocrinol*, 15(10), 933-939.
- Russell, J. A., & Leng, G. (1998). Sex, parturition and motherhood without oxytocin? *J Endocrinol*, 157(3), 343-359.
- Saito, T., Shibasaki, K., Kurachi, M., Puentes, S., Mikuni, M., & Ishizaki, Y. (2011). Cerebral capillary endothelial cells are covered by the VEGF-expressing foot processes of astrocytes. *Neurosci Lett*, 497(2), 116-121. doi:10.1016/j.neulet.2011.04.043
- Salm, A. K., Hatton, G. I., & Nilaver, G. (1982). Immunoreactive glial fibrillary acidic protein in pituicytes of the rat neurohypophysis. *Brain Res*, 236(2), 471-476.
- Salm, A. K., & Hawrylak, N. (2004). Glial limitans elasticity subjacent to the supraoptic nucleus. *J Neuroendocrinol*, 16(8), 661-668. doi:10.1111/j.1365-2826.2004.01219.x

- Sarafian, T. A., Montes, C., Imura, T., Qi, J., Coppola, G., Geschwind, D. H., & Sofroniew, M. V. (2010). Disruption of astrocyte STAT3 signaling decreases mitochondrial function and increases oxidative stress in vitro. *PLoS One*, 5(3), e9532. doi:10.1371/journal.pone.0009532
- Sawchenko, P. E., & Swanson, L. W. (1981). A method for tracing biochemically defined pathways in the central nervous system using combined fluorescence retrograde transport and immunohistochemical techniques. *Brain Res*, 210(1-2), 31-51.
- Sawchenko, P. E., & Swanson, L. W. (1983). The organization and biochemical specificity of afferent projections to the paraventricular and supraoptic nuclei. *Prog Brain Res*, 60, 19-29. doi:10.1016/S0079-6123(08)64371-X
- Seghezzi, G., Patel, S., Ren, C. J., Gualandris, A., Pintucci, G., Robbins, E. S., . . . Mignatti, P. (1998). Fibroblast growth factor-2 (FGF-2) induces vascular endothelial growth factor (VEGF) expression in the endothelial cells of forming capillaries: an autocrine mechanism contributing to angiogenesis. *J Cell Biol*, 141(7), 1659-1673.
- Seidel, J. L., Faideau, M., Aiba, I., Pannasch, U., Escartin, C., Rouach, N., . . . Shuttleworth, C. W. (2015). Ciliary neurotrophic factor (CNTF) activation of astrocytes decreases spreading depolarization susceptibility and increases potassium clearance. *Glia*, 63(1), 91-103. doi:10.1002/glia.22735
- Sendtner, M., Carroll, P., Holtmann, B., Hughes, R. A., & Thoenen, H. (1994). Ciliary neurotrophic factor. *J Neurobiol*, 25(11), 1436-1453. doi:10.1002/neu.480251110
- Sendtner, M., Kreutzberg, G. W., & Thoenen, H. (1990). Ciliary neurotrophic factor prevents the degeneration of motor neurons after axotomy. *Nature*, 345(6274), 440-441. doi:10.1038/345440a0
- Seniuk, N. A., Henderson, J. T., Tatton, W. G., & Roder, J. C. (1994). Increased CNTF gene expression in process-bearing astrocytes following injury is augmented by R(-)-deprenyl. *J Neurosci Res*, 37(2), 278-286. doi:10.1002/jnr.490370213
- Silverman, A. J., & Zimmerman, E. A. (1983). Magnocellular neurosecretory system. *Annu Rev Neurosci*, 6, 357-380. doi:10.1146/annurev.ne.06.030183.002041



- Silverman, W. F., Krum, J. M., Mani, N., & Rosenstein, J. M. (1999). Vascular, glial and neuronal effects of vascular endothelial growth factor in mesencephalic explant cultures. *Neuroscience*, *90*(4), 1529-1541.
- Sladek, C. D., Fisher, K. Y., Sidorowicz, H. E., & Mathiasen, J. R. (1995). Osmotic stimulation of vasopressin mRNA content in the supraoptic nucleus requires synaptic activation. *Am J Physiol*, *268*(4 Pt 2), R1034-1039.
- Snow, D. M., Lemmon, V., Carrino, D. A., Caplan, A. I., & Silver, J. (1990). Sulfated proteoglycans in astroglial barriers inhibit neurite outgrowth in vitro. *Exp Neurol*, *109*(1), 111-130.
- Sofroniew, M. V. (2005). Reactive astrocytes in neural repair and protection. *Neuroscientist*, *11*(5), 400-407. doi:10.1177/1073858405278321
- Sofroniew, M. V. (2009). Molecular dissection of reactive astrogliosis and glial scar formation. *Trends Neurosci*, *32*(12), 638-647. doi:10.1016/j.tins.2009.08.002
- Sofroniew, M. V., & Glasmann, W. (1981). Golgi-like immunoperoxidase staining of hypothalamic magnocellular neurons that contain vasopressin, oxytocin or neurophysin in the rat. *Neuroscience*, *6*(4), 619-643.
- Sofroniew, M. V., & Vinters, H. V. (2010). Astrocytes: biology and pathology. *Acta Neuropathol*, *119*(1), 7-35. doi:10.1007/s00401-009-0619-8
- Somjen, G. G. (1988). Nervenkitz: notes on the history of the concept of neuroglia. *Glia*, *1*(1), 2-9. doi:10.1002/glia.440010103
- Stahl, N., Boulton, T. G., Farruggella, T., Ip, N. Y., Davis, S., Witthuhn, B. A., . . . et al. (1994). Association and activation of Jak-Tyk kinases by CNTF-LIF-OSM-IL-6 beta receptor components. *Science*, *263*(5143), 92-95.
- Stahl, N., Davis, S., Wong, V., Taga, T., Kishimoto, T., Ip, N. Y., & Yancopoulos, G. D. (1993). Cross-linking identifies leukemia inhibitory factor-binding protein as a ciliary neurotrophic factor receptor component. *J Biol Chem*, *268*(11), 7628-7631.
- Stahl, N., Farruggella, T. J., Boulton, T. G., Zhong, Z., Darnell, J. E., Jr., & Yancopoulos, G. D. (1995). Choice of STATs and other substrates specified by modular tyrosine-based motifs in cytokine receptors. *Science*, *267*(5202), 1349-1353.

- Stahl, N., & Yancopoulos, G. D. (1994). The tripartite CNTF receptor complex: activation and signaling involves components shared with other cytokines. *J Neurobiol*, *25*(11), 1454-1466. doi:10.1002/neu.480251111
- Stellwagen, D., & Malenka, R. C. (2006). Synaptic scaling mediated by glial TNF- $\alpha$ . *Nature*, *440*(7087), 1054-1059. doi:10.1038/nature04671
- Stockli, K. A., Lillien, L. E., Naher-Noe, M., Breitfeld, G., Hughes, R. A., Raff, M. C., . . . Sendtner, M. (1991). Regional distribution, developmental changes, and cellular localization of CNTF-mRNA and protein in the rat brain. *J Cell Biol*, *115*(2), 447-459.
- Stockli, K. A., Lottspeich, F., Sendtner, M., Masiakowski, P., Carroll, P., Gotz, R., . . . Thoenen, H. (1989). Molecular cloning, expression and regional distribution of rat ciliary neurotrophic factor. *Nature*, *342*(6252), 920-923. doi:10.1038/342920a0
- Suh, S. W., Bergher, J. P., Anderson, C. M., Treadway, J. L., Fosgerau, K., & Swanson, R. A. (2007). Astrocyte glycogen sustains neuronal activity during hypoglycemia: studies with the glycogen phosphorylase inhibitor CP-316,819 ([R-R\*,S\*]-5-chloro-N-[2-hydroxy-3-(methoxymethylamino)-3-oxo-1-(phenylmethyl)pro pyl]-1H-indole-2-carboxamide). *J Pharmacol Exp Ther*, *321*(1), 45-50. doi:10.1124/jpet.106.115550
- Summy-Long, J. Y., Hu, S., Long, A., & Phillips, T. M. (2008). Interleukin-1 $\beta$  release in the supraoptic nucleus area during osmotic stimulation requires neural function. *J Neuroendocrinol*, *20*(11), 1224-1232. doi:10.1111/j.1365-2826.2008.01783.x
- Sun, D., Lye-Barthel, M., Masland, R. H., & Jakobs, T. C. (2010). Structural remodeling of fibrous astrocytes after axonal injury. *J Neurosci*, *30*(42), 14008-14019. doi:10.1523/JNEUROSCI.3605-10.2010
- Sun, H., Benardais, K., Stanslowsky, N., Thau-Habermann, N., Hensel, N., Huang, D., . . . Petri, S. (2013). Therapeutic potential of mesenchymal stromal cells and MSC conditioned medium in Amyotrophic Lateral Sclerosis (ALS)--in vitro evidence from primary motor neuron cultures, NSC-34 cells, astrocytes and microglia. *PLoS One*, *8*(9), e72926. doi:10.1371/journal.pone.0072926
- Swanson, L. W., & Kuypers, H. G. (1980). The paraventricular nucleus of the hypothalamus: cytoarchitectonic subdivisions and organization of projections to the pituitary, dorsal vagal complex, and spinal cord as demonstrated by retrograde fluorescence double-labeling methods. *J Comp Neurol*, *194*(3), 555-570. doi:10.1002/cne.901940306

- Swanson, L. W., & Sawchenko, P. E. (1983). Hypothalamic integration: organization of the paraventricular and supraoptic nuclei. *Annu Rev Neurosci*, 6, 269-324. doi:10.1146/annurev.ne.06.030183.001413
- Vaca, K., & Wendt, E. (1992). Divergent effects of astroglial and microglial secretions on neuron growth and survival. *Exp Neurol*, 118(1), 62-72.
- van den Pol, A. N. (1982). The magnocellular and parvocellular paraventricular nucleus of rat: intrinsic organization. *J Comp Neurol*, 206(4), 317-345. doi:10.1002/cne.902060402
- Varon, S., Manthorpe, M., & Adler, R. (1979). Cholinergic neuronotrophic factors: I. Survival, neurite outgrowth and choline acetyltransferase activity in monolayer cultures from chick embryo ciliary ganglia. *Brain Res*, 173(1), 29-45.
- Vutskits, L., Bartanusz, V., Schulz, M. F., & Kiss, J. Z. (1998). Magnocellular vasopressinergic neurons in explant cultures are rescued from cell death by ciliary neurotrophic factor and leukemia inhibiting factor. *Neuroscience*, 87(3), 571-582.
- Watt, J. A., Bone, S., Pressler, M., Cranston, H. J., & Paden, C. M. (2006). Ciliary neurotrophic factor is expressed in the magnocellular neurosecretory system of the rat in vivo: evidence for injury- and activity-induced upregulation. *Exp Neurol*, 197(1), 206-214. doi:10.1016/j.expneurol.2005.09.009
- Watt, J. A., & Hobbs, N. K. (2000). Interleukin-1beta immunoreactivity in identified neurons of the rat magnocellular neurosecretory system: evidence for activity-dependent release. *J Neurosci Res*, 60(4), 478-489. doi:10.1002/(SICI)1097-4547(20000515)60:4<478::AID-JNR6>3.0.CO;2-R
- Watt, J. A., Moffet, C. W., Zhou, X., Short, S., Herman, J. P., & Paden, C. M. (1999). Central peptidergic neurons are hyperactive during collateral sprouting and inhibition of activity suppresses sprouting. *J Neurosci*, 19(5), 1586-1598.
- Watt, J. A., & Paden, C. M. (1991). Compensatory sprouting of uninjured magnocellular neurosecretory axons in the rat neural lobe following unilateral hypothalamic lesion. *Exp Neurol*, 111(1), 9-24.
- Weiss, M. L., & Hatton, G. I. (1990a). Collateral input to the paraventricular and supraoptic nuclei in rat. I. Afferents from the subfornical organ and the anteroventral third ventricle region. *Brain Res Bull*, 24(2), 231-238.

- Weiss, M. L., & Hatton, G. I. (1990b). Collateral input to the paraventricular and supraoptic nuclei in rat. II. Afferents from the ventral lateral medulla and nucleus tractus solitarius. *Brain Res Bull*, 25(4), 561-567.
- Wiese, S., Karus, M., & Faissner, A. (2012). Astrocytes as a source for extracellular matrix molecules and cytokines. *Front Pharmacol*, 3, 120. doi:10.3389/fphar.2012.00120
- Wilhelmsson, U., Bushong, E. A., Price, D. L., Smarr, B. L., Phung, V., Terada, M., . . . Pekny, M. (2006). Redefining the concept of reactive astrocytes as cells that remain within their unique domains upon reaction to injury. *Proc Natl Acad Sci U S A*, 103(46), 17513-17518. doi:10.1073/pnas.0602841103
- Wilks, A. F., Harpur, A. G., Kurban, R. R., Ralph, S. J., Zurcher, G., & Ziemiecki, A. (1991). Two novel protein-tyrosine kinases, each with a second phosphotransferase-related catalytic domain, define a new class of protein kinase. *Mol Cell Biol*, 11(4), 2057-2065.
- Winter, C. G., Saotome, Y., Levison, S. W., & Hirsh, D. (1995). A role for ciliary neurotrophic factor as an inducer of reactive gliosis, the glial response to central nervous system injury. *Proc Natl Acad Sci U S A*, 92(13), 5865-5869.
- Wishingrad, M. A., Koshlukova, S., & Halvorsen, S. W. (1997). Ciliary neurotrophic factor stimulates the phosphorylation of two forms of STAT3 in chick ciliary ganglion neurons. *J Biol Chem*, 272(32), 19752-19757.
- Zhang, B., Glasgow, E., Murase, T., Verbalis, J. G., & Gainer, H. (2001). Chronic hypoosmolality induces a selective decrease in magnocellular neurone soma and nuclear size in the rat hypothalamic supraoptic nucleus. *J Neuroendocrinol*, 13(1), 29-36.
- Zhang, C., & Harder, D. R. (2002). Cerebral capillary endothelial cell mitogenesis and morphogenesis induced by astrocytic epoxyeicosatrienoic Acid. *Stroke*, 33(12), 2957-2964.